Fall 10-31-1997

Fractionally sampled decorrelating detectors for time-varying rayleigh fading CDMA channels

Huaping Liu
New Jersey Institute of Technology

Copyright Warning & Restrictions

The copyright law of the United States (Title 17, United States Code) governs the making of photocopies or other reproductions of copyrighted material.

Under certain conditions specified in the law, libraries and archives are authorized to furnish a photocopy or other reproduction. One of these specified conditions is that the photocopy or reproduction is not to be "used for any purpose other than private study, scholarship, or research." If a, user makes a request for, or later uses, a photocopy or reproduction for purposes in excess of "fair use" that user may be liable for copyright infringement,

This institution reserves the right to refuse to accept a copying order if, in its judgment, fulfillment of the order would involve violation of copyright law.

Please Note: The author retains the copyright while the New Jersey Institute of Technology reserves the right to distribute this thesis or dissertation

Printing note: If you do not wish to print this page, then select "Pages from: first page # to: last page #" on the print dialog screen

ABSTRACT

FRACTIONALLY SAMPLED DECORRELATING DETECTORS FOR TIME-VARYING RAYLEIGH FADING CDMA CHANNELS

by
Huaping Liu

In this dissertation, we propose novel decorrelating multiuser detectors in DS-CDMA time-varying frequency-nonselective and frequency-selective fading channels and analyze their performance. We address the common shortcomings of existing multiuser detectors in a mobile environment, such as detector complexity and the error floor. An analytical approach is employed almost exclusively and Monte Carlo simulation is used to confirm the theoretical results. Practical channel models, such as Jakes' and Markovian, are adopted in the numerical examples.

The proposed detectors are of the decorrelating type and utilize fractional sampling to simultaneously achieve two goals: (1) the novel realization of a decorrelator with lower computational complexity and shorter processing latency; and (2) the significant reduction of the probability of error floor associated with time-varying fading.

The analysis of the impact of imperfect power control on IS-95 multiple access interference is carried out first and the ineffectiveness of IS-95 power control in a mobile radio environment is demonstrated. Fractionally-spaced bit-by-bit decorrelator structures for the frequency-nonselective and frequency-selective channels are then proposed. The matrix singularity problem associated with decorrelation is also addressed, and its solution is suggested.

A decorrelating receiver employing differentially coherent detection for an asynchronous CDMA, frequency-nonselective time-varying Rayleigh fading channel is proposed. A maximum likelihood detection principle is applied at the fractionally-spaced decorrelator output, resulting in a significantly reduced error floor. For

coherent detection, a novel single-stage and two-stage decision feedback (DF) maximum *a posteriori* (MAP) channel estimator is proposed. These estimators are applicable to a channel with an arbitrary spaced-time correlation function.

The fractionally-spaced decorrelating detector is then modified and extended to a frequency-selective time-varying fading channel, and is shown to be capable of simultaneously eliminating MAI, ISI, and path cross-correlation interference. The implicit equivalent frequency diversity is exploited through multipath combining, and the effective time diversity is achieved by fractional sampling for significant performance improvement.

The significance of the outcome of this research is in the design of new lower complexity multiuser detectors that do not exhibit the usual deficiencies and limitations associated with a time-varying fading and multipath CDMA mobile environment.

FRACTIONALLY SAMPLED DECORRELATING DETECTORS FOR TIME-VARYING RAYLEIGH FADING CDMA CHANNELS

by
Huaping Liu

A Dissertation
Submitted to the Faculty of
New Jersey Institute of Technology
in Partial Fulfillment of the Requirements for the Degree of
Doctor of Philosophy in Electrical Engineering

Department of Electrical and Computer Engineering

October 1997

APPROVAL PAGE

FRACTIONALLY SAMPLED DECORRELATING DETECTORS FOR TIME-VARYING RAYLEIGH FADING CDMA CHANNELS

Huaping Liu

Dr. Zoran Siveski, Dissertation Advisor — Date
Assistant Professor of Electrical and Computer Engineering, NJIT

Dr. Nirwan Ansari, Committee Member — Date
Professor of Electrical and Computer Engineering, NJIT

Dr. Joseph Frank, Committee Member — Date
Associate Professor of Electrical and Computer Engineering, NJIT

Dr. Denis Blackmore, Committee Member — Date
Professor of Mathematics, NJIT

Dr. Justin Chuang, Committee Member — Date
Principal Technical Staff Member, AT&T Research

BIOGRAPHICAL SKETCH

Author: Huaping Liu

Degree: Doctor of Philosophy

Date: October 1997

Undergraduate and Graduate Education:

- Doctor of Philosophy in Electrical Engineering,
  New Jersey Institute of Technology, Newark, NJ, October 1997
- Master of Science in Electrical Engineering,
  Nanjing University of Posts and Telecommunications, Nanjing, P.R. China, April 1990
- Bachelor of Science in Electrical Engineering,
  Nanjing University of Posts and Telecommunications, Nanjing, P.R. China, July 1987

Major: Electrical Engineering

Presentations and Publications:

H. Liu and Z. Siveski, "Differentially coherent CDMA multiuser detector for Rayleigh fading channels," *Proc. of the 30th Annual Conference on Information Sciences and Systems*, pp. 86–89, Princeton, NJ, Mar. 1996.

H. Liu and Z. Siveski, "Differentially coherent decorrelating detector for CDMA single-path time-varying Rayleigh fading channels," *under revision for publication in IEEE Trans. on Communications*, Aug. 1996.

H. Liu and Z. Siveski, "Fractionally sampled decorrelator for CDMA Rayleigh fading channels," *Electronics Letters*, vol. 33, no. 9, pp. 741–742, Apr. 1997.

H. Liu and Z. Siveski, "A method of calculating transmitted power of mobiles in sectored cellular CDMA reverse link with imperfect power control," *Proc. of the 31st Annual Conference on Information Sciences and Systems*, pp. 299–302, John Hopkins University, Baltimore, MD, Mar. 1997.

H. Liu, Z. Siveski, and N. Ansari, "Coherent decorrelating detector with imperfect channel estimates for CDMA Rayleigh fading channels," *Proc. of ICC'97*, pp. 600–604, Montreal, Canada, June 1997.

To my parents,
and to Xiaoyong Tang and Zijie Liu

ACKNOWLEDGMENT

I would like to express my sincere gratitude to Dr. Zoran Siveski who very competently guided and advised me in my Ph.D. research. He has always provided me with valuable ideas, comments and materials. I especially appreciated his good-natured guidance, both academically and personally. His constant support has benefited me during all phases of my Ph.D. career, from writing papers and dissertation to seeking employment. I gained greatly from our daily working together.

I am also indebted to Dr. Nirwan Ansari whose academic and nonacademic assistance, and whose encouragement and confidence have been invaluable to me through the years. My interactions with him were extremely fulfilling.

Special thanks go to Dr. Justin Chuang for his gentle and thoughtful discussions to improve the quality of my dissertation. I am extremely thankful to Dr. Danis Blackmore for his useful suggestions and detailed corrections of the English in my dissertation. I also want to thank Dr. Joseph Frank for serving on my Ph.D. committee.

It was a great pleasure having an opportunity to work with so many friends. Among them are David Chen, Gary Wang and others, more than I can name. Their diligence and daily presence made my time at NJIT especially fulfilling. Lisa Fitton provided a lot of help in my daily life in the lab, and was always ready to make prompt corrections of English grammar. To all of them, I express my sincere thanks.

My deepest gratitude is expressed to my wife for her support, endurance and understanding of the many months I had time only for one devotion — writing papers and this dissertation. I would also like to mention my son who came into my life and made my life happier and more lively. Above all, my mother and father have given me so much, that I could never pay it back in my life time. I dedicate this dissertation to them.

TABLE OF CONTENTS

TABLE OF CONTENTS
(Continued)

TABLE OF CONTENTS
(Continued)

LIST OF FIGURES

LIST OF FIGURES
(Continued)

LIST OF FIGURES
(Continued)

Figure **Page**

CHAPTER 1

INTRODUCTION

1.1 Overview

Wireless communications systems and services allow people or machines to communicate at any time, anywhere making users free of time and location restriction in communicating with one another. In wired communications systems, data can be in principle transmitted without limit in throughput, because we can always install more physical media, such as fiber optic, cable etc., into the existing communications systems. However, we don't have the same means of increasing the data throughput in wireless communications systems due to the finite spectrum allocation. The rapidly expanding number of subscribers to the wireless services triggered great research effort in order to increase spectral efficiency in wireless communications systems. Quality of data transmission in a wireless channel is often affected by a myriad of reasons such as self-generated interference, shadowing effect, multipath and time-varying fading of the channel etc. System design in such a detrimental environment becomes more challenging.

The radio spectrum is a limited and scarce resource, so the challenge is to increase the number of users that can access the system simultaneously with a guaranteed data communication quality at affordable system complexity, and hence optimize the multiple users communication network capabilities. Design of such a system, unlike the wired one, is not only in maximizing the link capacity limited by Gaussian noise and the available bandwidth. Instead, the interference generated by the system itself due to the necessity for spectrum reuse becomes the major concern. In order to increase the supportable number of users per Hz per unit area for a given radio propagation condition and a specific data transmission quality, the system is always cellularized and very often sectored. Theoretically, we can always shrink the size of a cell (or sector) and increase the number of users per Hz per unit area without

bound. Practically, infinitely shrunk cell size increases the whole system complexity and is not realizable, so the solution to this challenge is to design new systems or implement new features in the existing systems in order to maximize simultaneously supportable users/Hz/unit area.

At present, multiple access in cellular radio systems is achieved by three schemes or combinations thereof: frequency-division multiple access (FDMA), time-division multiple access (TDMA) and more than one type of code-division multiple access (CDMA) [1]. The majority of the existing wireless networks is still based on analog technology FDMA, i.e., channelization is achieved by separating each user's signal in the frequency domain. Conversion to digital technologies like TDMA and CDMA is taking place rapidly. European digital wireless standard GSM and the north American digital wireless standards IS-54 and IS-95 are being deployed world wide.

While in academia CDMA technology has long been recognized as a leading candidate for digital wireless systems, industry-wide acknowledgement of CDMA was received relatively recently. The present CDMA system uses a spread spectrum technique and is being developed according to north American standard IS-95. Spread spectrum techniques were originally used in military communications for anti-jamming [53]. Because of the signal's wideband nature, it is perceived as a noise-like time signal to the receiver of narrowband signals. CDMA fully utilizes this property of spread spectrum communications techniques and possesses many other favorable characteristics, such as its inherent immunity against interference [15] [39], performance enhancement by using RAKE type of receivers in a multipath environment which is typical for mobile communication scenarios, soft capacity and soft handoff [13], etc. Although digital multiple access schemes like TDMA can be designed to be more robust to interference than their analog counterparts, they still

[1]We will concentrate on direct sequence spread spectrum CDMA (DS-SS CDMA), and as widely used in the literature, refer to it as CDMA.

need sufficient distance (usually measured by a frequency reuse factor) between cells using the same frequency to make the co-channel interference small enough for good communication quality. The only exception is the CDMA cellular system, which trades bandwidth for processing gain and tolerates a higher co-channel interference by spreading the information signal over a wide bandwidth and de-spreading at the receiver, leaving only a relatively small portion of the power of undesired signals to fall into the desired signal frequency band, and thus making the design of systems with frequency reuse factor equal to one feasible. In theory, if perfect orthogonality can be achieved for all active users in the system, co-channel interference can be eliminated completely. Advantages of CDMA over FDMA and TDMA in mobile communications are also discussed in [25].

Despite a lot of promising features of CDMA systems, we are still facing many challenges in achieving its full potential. The major impediment in the present CDMA system is the near-far problem.

1.2 Conventional Detection for CDMA System

The conventional single-user CDMA detector consists of a bank of matched filters each matched to the signature waveform of a user. The detector treats each user's signal separately with other users' signals considered as interference. The desired user's signal is detected by using the inherent interference suppression capability of the CDMA system quantified by processing gain. This can be easily elucidated by two-user's antipodal signals transmitted in a channel assumed for simplicity to be synchronous. The received baseband signals in the i^{th} bit interval [2] for both user 1 and user 2 can be written in vector form as

$$\boldsymbol{x} = \begin{bmatrix} x_1 \\ x_2 \end{bmatrix} = \begin{bmatrix} \sqrt{a_1}c_1b_1 + \rho\sqrt{a_2}c_2b_2 + n_1 \\ \sqrt{a_2}c_2b_2 + \rho\sqrt{a_1}c_1b_1 + n_2 \end{bmatrix} = \boldsymbol{PACb} + \boldsymbol{n}, \tag{1.1}$$

[2] For simplicity, we will omit index i whenever possible.

where

$$\boldsymbol{P} = \begin{bmatrix} 1 & \rho \\ \rho & 1 \end{bmatrix}, \ \boldsymbol{A} = \begin{bmatrix} \sqrt{a_1} & 0 \\ 0 & \sqrt{a_2} \end{bmatrix}, \ \boldsymbol{C} = \begin{bmatrix} c_1 & 0 \\ 0 & c_2 \end{bmatrix}, \ \boldsymbol{b} = \begin{bmatrix} b_1 \\ b_2 \end{bmatrix} \text{ and } \boldsymbol{n} = \begin{bmatrix} n_1 \\ n_2 \end{bmatrix}$$

stand for the cross-correlation matrix between user 1 and user 2's normalized signature waveforms, signal amplitudes, normalized channel coefficients [3], information bits and AWGN for user 1 and user 2 respectively.

In the conventional CDMA detector, the information bit of user 1 is detected as:

$$\widehat{b}_1 = \text{sgn}(x_1).$$

This detector is optimum in the sense that it minimizes the probability of error in a single-user channel corrupted by additive white Gaussian noise [68], or when user 1 and 2's codes are orthogonal to each other. From this simple two-user example, we have the following conclusions on the conventional CDMA system:

- the CDMA system capacity is essentially interference limited, as one more user joins the system, other users experience more interference
- near-far problem is the major shortcoming of the conventional CDMA system, even when ρ is very small, if $a_2 \gg a_1$, detection of b_1 is impossible
- tight power control and design of codes possessing smaller cross-correlation properties are major remedies for near-far problem

As it will be shown later, the present CDMA system capacity is very sensitive to imperfect power control. While the slow long-term attenuation variations such as shadowing effects can be compensated for effectively by power control, the short-term attenuation variation when signals are experiencing fast fading is hard to compensate for even with the closed-loop power control. For mobile communications, the channel

[3]Channel is assumed constant over one bit interval for deriving the discrete-time channel model.

is essentially time-varying; the fading rapidity of which is proportionally related to the channel Doppler spread. Tight power control makes the system complex, and still can not remedy its near-far problem in the fast fading channel. Multiuser detection is a possible solution for a higher capacity and better communication quality CDMA system in such an environment because of its superior interference suppression ability and the near-far resistant nature.

1.3 Multiuser Detection for CDMA System

Multiuser detection makes use of partial or full available information of multiple-access interference (MAI) to perform joint detection of all or a subset of users simultaneously. MAI is not treated as noise as in the conventional detector, but as useful information to assist detecting the desired user's information. For many of the proposed multiuser detectors, the information needed about MAI includes users' relative delays in an asynchronous channel, cross correlation among each user's spreading code, and possibly interference users' energy for some multiuser detectors. The major achievement of multiuser detection is its exemption of power control because of its near-far resistant nature and increased capacity due to the elimination/mitigation of the MAI effect. In some cases, as in cellular systems, however, the capacity increase may be not tremendous, but certainly not trivial [13].

1.3.1 Optimal Detector

The optimal multiuser detector in asynchronous multiple-access Gaussian channel was developed in [67]. Its extension to frequency nonselective and frequency selective Rayleigh fading channel were described in [88] and [85], respectively. It is a maximum-likelihood sequence detector that uses full knowledge of the signature waveforms, relative delays and the fading channel coefficients of each user to detect the transmitted information vector of all users. The optimal multiuser detector

is near-far resistant and as expected has excellent performance in both Gaussian and Rayleigh fading channels. It was also shown that the detector performance is almost invariant to fading rapidity [88]. However the optimal multiuser detector has prohibitive complexity; rendering the actual implementation of such a detector infeasible for a system with usually a relatively big user population.

1.3.2 Suboptimal Detectors

Multiuser detection is mainly aimed for the CDMA reverse link [13]. CDMA system capacity is rarely forward link limited since the base station is rarely power limited, unlike the mobile station which requires low power radiation and light weight. Increasing the reverse link capacity by applying multiuser detection at the base station while keeping the required mobile station maximum transmitted power constant will usually improve the overall system capacity. However, the increase of the reverse link capacity far beyond that of the forward link through very complicated receiver design is not suggested since the forward link eventually limits the overall system capacity in this case. Therefore, low complexity multiuser detectors design that maintain the detector's near-far resistant nature and a certain degree of capacity improvement is crucial.

Suboptimal detector designs are aimed to meet such a requirement at the expense of inferior performance in comparison to the optimal detector. Design of suboptimal multiuser detectors is essentially in finding a tradeoff between complexity and performance.

Decorrelating type of detectors are examples of such suboptimal multiuser detectors. Decorrelator used in a synchronous and an asynchronous Gaussian multiple-access channel was developed in [47] and [48], respectively. The basic idea of the decorrelator is easy to understand if the received signal in (1.1) is taken as an example. If $\boldsymbol{x}$ is multiplied by $\boldsymbol{P}^{-1}$, multiple access interference is eliminated

completely at the expense of increasing the background noise at the decorrelator output. From the implementation point of view, this procedure of matrix inversion and multiplication is just a proper linear combination of the sampled received signals of all users after matched filters. In the asynchronous channel, when an infinite processing length of received data is assumed, the decorrelator is a linear K-input K-output filter [48], and achieves optimal near-far resistance. Following the work in [47] and [48], the decorrelating structure was extended or used in a number of other multiuser detectors for different communication scenarios. Decorrelating detector performance analysis in a single path Rayleigh fading channel was carried out in [88]. Symbol by symbol coherent detection using the decorrelator was carried out in [87] [93] in which the fading channel coefficients are estimated by using a Kalman filter prior to coherent detection. An error floor [4] was observed when estimation error caused by channel fluctuation was taken into consideration, and the floor at the decorrelator output was shown to be the same as that of a single user transmission. In a synchronous frequency selective channel, the multipath decorrelating detector (MDD) with the maximum-ratio combining is presented in [90] in which decorrelation of all users' individual signal paths is performed first, followed by a whitening filter and the maximal ratio combiner (MRC). The asynchronous MDD is analyzed in [84] in which the asynchronous multipath channel is transformed into an equivalent synchronous system where the data sequence is transmitted from $N \times K \times L$ users, where N is the sequence length, K is the number of active asynchronous users and L is the number of resolvable multiple paths for each user. An infinite horizon decorrelator results in a KL-input KL-output linear time-invariant, but non-causal filter with a known transfer function [48]. Windows truncation [76] by taking a block of bits is necessary for practically realizing the infinite horizon decorrelator at the expense of introducing edge effects due to the asynchronous nature of the

[4] Irreducible probability of error which can not be lowered by increasing the transmitted signal power.

transmission. The edge effect can be neglectable for a long block, however, a long block means that a bigger matrix needs to be inverted. One remedy to the edge effect is to insert a zero bit in the end of each block. Again, we need somehow to tradeoff between matrix size and data transmission efficiency. A quasi-synchronous CDMA (QS-CDMA) channel is defined in [19], where a Q-chip QS-CDMA is defined as that in which the maximum relative delays of each user is small than Q chips. The edge effect problem in the windowed decorrelator can be relaxed for such a system. Another bit-by-bit decorrelator was proposed in [28] for such a QS-CDMA channel, in which only a portion of the desired user's bit containing no inter-symbol multiple access interference is used for decorrelation and for performing data detection. The processing interval is taken from the beginning of the bit of the user with the longest relative delay plus the delay spread of that user due to channel time-dispersion, to the end of the bit of the user with the least relative delay, resulting in a portion of each user's energy being discarded in performing detection. This detector will work for a relatively small relative delays of multiuser and channel delay spread, so it is very restricted in application. In [52], a decorrelator is also used in a single user frequency selective Rayleigh fading multipath channel to cancel intersymbol interference (ISI) and interference caused by non-zero path cross-correlation before the RAKE combining. Another multipath combining decorrelating detector structure called a RAKE-based decorrelating detector (RDD) [22] [37] [5] performs multipath combining first, followed by a decorrelation based on the cross-correlation of users' combined signals. It was found that the performance of RDD is uniformly better than that of the MDD with respect to the desired user's signal to noise ratio [22] assuming perfect channel estimates. Moreover, the RDD requires the multipath fading channel parameters of all users and its performance deteriorates rapidly when both the desired and interferer's channel exhibit mismatch. A differential coherent

[5]The detector in [37] is for a synchronous multiple access channel, although it is termed "uplink".

version of decorrelating detector was analyzed in [61] for a Gaussian channel and in [89] for a frequency nonselective Rayleigh fading channel.

Multistage detectors [62] [63] and decision-feedback detectors [10]-[12] are other examples of suboptimal detectors. In the former, the n^{th} stage uses the tentative decisions made at the $(n-1)^{th}$ stage to cancel MAI. In theory, the number of stages can be made as big as desired and hence improve the detector's performance, however, due to the delay and the complexity constraints, the number of stages is usually limited to very few. In the latter, the users' received power strengths are sorted first, information of the strong users are detected next, then in detecting the week users' information signal strong users' decisions are utilized allowing for interference cancellation to take place. The decision-feedback detector mentioned in the above references are mainly for Gaussian channels. Analysis for a fading channel can be found in [77]-[79], where it was concluded that in the time-varying fading channel, the use of these type of detectors depend on the the channel fading rapidity. In the case of slow fading, the channel can be estimated accurately [55], where on the other hand, for fast fading, channel estimation is difficult, and hence interference cancellation will be hard to carry out. Another combined decorrelator and canceler scheme is proposed in [57] for the synchronous channel in which two stages are used for interference cancellation. The first stage uses a decorrelator, and the second stage uses a canceler. The decorrelator output of the first stage provides a tentative decision for the second stage to form estimates of MAI for each user, and then subtracts them from the matched filter output directly and this is followed by the final decision. This detector is near-far resistant, and can gain performance improvement over the decorrelator when the interfering users' energy is relatively strong compared to that of the desired user. The asynchronous version of the above detector in the Gaussian channel was proposed in [58] in which the decorrelator in the first stage was realized in [82]. Specifically, each bit interval is subdivided into K (number of users)

blocks according to the users' relative delays. Each block is viewed as a synchronous channel, and after performing decorrelation on all blocks over one bit interval of a specific user, optimal weighs are derived to reconstruct the original signal carrying the information bit. The second stage still uses a canceler.

Successive interference cancellation ideas are implicit or explicit in a number of references. Assume user 1 is the weaker user in the two-user example given in section 1.2, and user 1's information needs to be detected. In order to cancel MAI we have to get the estimation of $\rho\sqrt{a_2}c_2b_2$. If ρ is known and $\sqrt{a_2}c_2$ can be estimated or tracked by using an adaptive algorithm, the rest is to get the decision user 2's bit decision $\hat{b}_2$. So the detection should always be made starting from the strongest user for two reasons: the stronger user experiences less MAI, correspondingly, the stronger user's decision is better and the stronger user contributes a bigger MAI to the weaker user. After detection of the stronger user's information, its MAI can be cancelled to the benefit of the weaker user's decision. A practical implementation of the successive interference cancellation for DS/CDMA systems was presented in [14].

Adaptive multiuser detectors have the feature of self-adapting to the unknown changing environment. A pretty comprehensive survey of adaptive multiuser detectors can be found in [69]. Algorithms are needed to implement the adaptive features of these detectors that more or less assume the availability of at least partial knowledge of the communications environment. For example, the detector for asynchronous system in [51] assumes the availability of the desired user's timing and the training sequence, and the detector for the synchronous system in [5] assumes the knowledge of all users' signature sequences, although without having to calculate their cross-correlation. A blind adaptive algorithm is presented in [21] in which an MMSE multiuser detector is implemented without training sequences. The only knowledge needed in [21] is the desired user's signature waveform and timing. In

[87] [86], although it is termed an adaptive multiuser detector, the adaptive feature actually lies only in that the channel is estimated adaptively using previous bit decisions (decision feedback) for performing coherent detection.

1.3.3 Limitations of the Present Multiuser Detectors

The optimal multiuser detector is prohibitively complex to be implemented for a practical system. Some of the aforementioned suboptimal detectors are not readily realizable in practical situations either. Interference cancellation employing interference users' decisions requires accurate estimates of interference users' instantaneous power (interference users' power adjusted by fading channel) in order to reconstruct interference, and is very vulnerable to estimation error, although they may work very well in a Gaussian channel because of its time-invariant nature. Decorrelating detectors seem to exhibit greater robustness when compared to these multiuser detectors in time-varying fading channels [77]-[79] The performance of interference cancellation type of detectors combining a decorrelator as the first stage, and the decision feedback, or adaptive algorithm implemented in the second stage degrades as both the desired user and interference users' channel estimation quality degrade. Tracking error makes such detectors not near-far resistant. A comprehensive study of robustness of different suboptimal multiuser detectors is presented in [80]. It was concluded that the performance of successive interference cancellation (SIC) and parallel interference cancellation (PIC) schemes degrades as the number of users increases, while the performance of multistage and decision feedback detectors are very sensitive to the channel mismatch. The decorrelator is robust to channel mismatch and has lower complexity than these detectors, however in the asynchronous channel the decorrelator realization is not simple. The infinite horizon decorrelator in the frequency nonselective asynchronous channel results in a linear noncausal K-input K-output filter [48], while in the frequency selective channel it

results in a KL input KL output linear time-invariant filter [83], where K is the total number of users and L is the number of resolvable paths. This filter is by no means easy to implement, and as one or more users add to or drop out of the system, the filter coefficients have to be changed correspondingly. Moreover, L, the number of resolvable paths is also a random variable as the vehicle moves within a mobile environment. The full length decorrelator causes excessive processing delay, and the sliding windows decorrelator in [76] introduces edge effects. The window length is another design parameter which shows the tradeoff between the detector complexity and performance.

Although the decorrelator is robust to the channel mismatch, un-avoidable in the time-varying channel, the delay estimation error significantly affects the decorrelator performance [60]. Therefore, accurate delay estimators are needed for implementing the decorrelator. If delay information can be obtained accurately, practical implementation of a decorrelator in both frequency nonselective and selective asynchronous channels is an important research direction.

1.4 Communication in Time-Varying Fading Channel

Any effective radio network design requires an accurate characterization of the channel. Channel characteristics are, however, different from one environment to another, rendering a universally applicable channel characterization impossible. We will focus our discussion on the statistically known, but dynamically changing channels, and we will assume Rayleigh time-varying, frequency selective and nonselective fading channels of the wide-sense stationary uncorrelated scattering (WSSUS) type.

1.4.1 Fading and Multipath Channels

Extensive studies on radio channel modeling can be found in [59] [17]. The channel's time-varying nature comes from the the fact that the physical position of the communications link is changing most of the time. Fading rapidity can be measured by channel Doppler frequency f_d which can be determined from the vehicle's moving speed and moving direction relative to the communication link. The channel coherence time can be calculated approximately as $(\Delta t)_c \approx 1/f_d$ [55]. This absolute fading rate measure is not very useful regarding data detection because the actual data rate in digital communication is not involved. The meaningful measure of fading rate is the relative value of the symbol period T to $(\Delta t)_c$, or equivalently the normalized channel Doppler bandwidth f_dT. Given this quantity and the WSS assumption, the channel correlation property in time can be described by the spaced-time correlation function $\Phi(\Delta t) = E\{c^*(t)c(t+\Delta t)\}$. Different models for this correlation function are adopted in literature. Jakes' model (land mobile) [24] is given by $\Phi(\Delta t) = J_0(2\pi f_d Deltat)$, where $J_0(\cdot)$ is the zero-th order Bessel function of the first kind, and the first order autoregressive (AR) model (first order Butterworth) is given by $\Phi(\Delta t) = exp(-2\pi f_d \Delta t)$. Jakes' model seems to provide the best fit to most of the practical channels, although the first order AR model is used widely in the literature possibly because the channel governed by this model is computationally the easiest to generate and can be estimated by using a Kalman filter. Others include Gaussian, second order AR, rectangular and second order Butterworth, etc.

The channel frequency selective nature comes from the fact that the channel coherence bandwidth $(\Delta f)_c$ is not infinite, hence different frequency components of a signal whose bandwidth exceeds $(\Delta f)_c$ fade differently. Channel coherence bandwidth is related to the multipath delay spread T_m as [55] $(\Delta f)_c \approx 1/T_m$. For a fixed communication link, T_m is determined solely by the physical arrangement

of objects such as buildings, vehicles, etc. With respect to the receiver, whether the channel exhibits multipath or not depends on the relative value of the information signal bandwidth W and the channel coherence bandwidth $(\Delta f)_c$. Because the achievable multipath profile resolution at the receiver is $1/W$, the number of resolvable fading paths is $L = WT_m + 1$. So even in the same physical channel, a larger bandwidth of the transmitted signal results in more resolvable multipaths. When the vehicle is moving, it experiences the time-varying delay spread of channel, so the resolvable paths also change with respect to time.

1.4.2 Detection in Fading Channels

In this dissertation, we will limit our discussion to PSK signals only. It is well known that either coherent or differentially coherent (DPSK) detection can be applied to the PSK signals. The detection method should be used according to the specific application and the channel environment. For slow fading, the channel can be estimated more accurately [55], so that coherent detection can be employed in such a channel because of its higher power efficiency compared with differentially coherent detection. On the other hand, if the channel exhibits rapid phase fluctuation making the channel estimation difficult, DPSK can be resorted to because of its robustness and simplicity. In DPSK, the phase of the received signal in the previous symbol interval is used as the reference phase for the current symbol detection thus providing channel estimation free detection. The validity of this method is based on the assumption that the channel induced phase does not change appreciably over the two consecutive symbol intervals. The performance of DPSK over an additive white Gaussian channel and frequency nonselective slow Rayleigh fading channel [6] is well known [55]. However, channel fading statistics have to be taken into consideration when the fading bandwidth is nonzero and the complex fading channel process

[6]Channel is assumed constant for at least two consecutive symbol intervals.

changes as a function of time [7]. The bit error rate analysis of M-ary differential phase shift keying (MDPSK) in such a channel was given in [31] and the error floor expression was derived. Although this irreducible error can not be lowered by increasing the transmitted power, it can be lowered or even eliminated by proper receiver design. In [20] and [9], multiple-symbol differential detection of differentially encoded PSK is analyzed; the scheme uses maximum likelihood sequence detection of N symbols to gain performance over the conventional two symbol differential detection. When $N \longrightarrow \infty$, the performance of the multiple-symbol differential detector in a Gaussian channel approaches that of coherent detection with differential encoding [9]. In a correlated Rayleigh fading channel, it was shown that the error floor can be lowered or even eliminated by proper choice of N [20]. An optimal algorithm for implementing multiple-symbol differential detection was given in [27].

Despite so many advantages of DPSK in a fading channel, there are still strong reasons to perform coherent detection. First, if a good carrier recovery can be achieved, coherent detection is more power efficient. Second, in order to eliminate error floor in DPSK, a system design requires additional complexity. Third, when a pilot tone or a pilot symbol can be inserted easily in a system, these techniques can be used to perform channel estimation and hence obtain coherent detection. For example in [8] [50], pilot tone, and in [4] [1] pilot symbol assisted carrier recovery were used to mitigate the effects of fading. The common idea of the pilot symbol aided carrier recovery is to insert a known symbol in every group of transmitted symbols, and utilize the known inserted symbols for fading process estimation. A comprehensive study of performance versus various parameters such as interpolator

[7]For convenience of analysis and mathematical tractability, the usual way is to assume that the channel fading process fluctuates from one symbol interval to another, but still can be approximately treated as constant over one symbol interval when obtaining the discrete-time channel model. For special purposes, if we have multiple samples per symbol, the discrete-time channel model allows the channel to change from one sample interval to another according to the channel second order statistics, but remains constant during one sample interval.

size, pilot symbol space etc., can be found in [4]. In [23], a combined pilot symbol and decision feedback channel estimation method is studied, where a symbol-aided tracker which makes use of only the known inserted symbols as the initial estimator, and then symbol decisions in between the known symbols to further improve the detector performance. A reference-symbol aided channel estimation for coherent detection in a CDMA reverse link was analyzed in [40]. When such information is not available, decision feedback MMSE type of carrier recovery can be designed in fading channels. These methods and analysis were carried out extensively in [16] [29] [30] [32]-[35] [64]. Coherent detection of PSK signals by using decision-directed fading channel estimates also exhibits error floor in time-varying channel. Phase reversal phenomena can happen in coherent detection with the decision-directed channel estimation structure. One remedy to this is the use of differential encoding as demonstrated in [79]. Performance of coherent detection with differential encoding is worse [8] than that of pure coherent detection, but the detector is robust.

The effective detection method for multipath channels are RAKE or RAKE based receivers in which resolvable multipath components are utilized in an optimal way for an improved performance receiver design. But problems such as error floor due to ISI caused by delay spread, fading variations and interference caused by non-zero path cross-correlation still need to be solved. A detailed study of the effects of time delay spread on digital radio communications performance is given in [6]. Extensive simulation results indicate that when delay spread is not severe, the major cause of error floor is not the timing error caused by delay spread, but the fading.

The idea of fractional sampling was used in fading channels for improved performance receiver design. In [74] [75], the so called "*multisampling Viterbi receiver (MSVR)*" was proposed based on more than one sample per symbol for a frequency nonselective fast Rayleigh fading channel. In [74], rectangular system

[8]The value will be different depending on the channel; in the random error frequency nonselective Rayleigh fading channel, the difference is approximately $3dB$.

impulse response of duration equal to signaling interval was assumed. Further analysis of this method using bandlimited pulses was carried out in [75]. Another multiple sample per symbol differential detection method of PSK in frequency nonselective Rayleigh fading channels is given in [7], in which K samples [9] were obtained in each symbol interval followed by a maximum likelihood detection applied on the $2K$ samples snapshot over two consecutive symbol intervals. Channel second order statistics are initially assumed known, and then it was shown that the actual channel statistics can be estimated by an adaptive algorithm. For the Jakes' channel model used in [7], the error floor was not observed in the SNR region of interest, and the detector performance was almost invariant to the fading rate. The fractionally-sampled detector employing DPSK in time-varying dispersive (frequency selective) fading channels was presented in [49], and significant performance improvement over symbol-spaced receiver was observed. Promising performance of multi-sampling techniques was observed in all these situations.

1.5 Problem Definition

1.5.1 Motivation

In [66], it was claimed that multiuser detection techniques were not suitable to cellular CDMA system for reasons such as that the intercell interference is uncancelable, that the capacity is limited by the number of code dimensions, that adaptive algorithms can not adapt to changing of channel, etc. As mentioned in Section 1.3, multiuser detection needs at least partial information of the desired and interfering users' signals (e.g., signature waveforms of all or a subset of users, timing). In a cellular system, the same cell interference is usually treated as cancelable while other cell interference is not [66] [13]. Given the other cell to the same cell interference

[9] $K (K \geq 2)$ is a design parameter.

ratio $f = 0.6$, the maximum achievable performance improvement (genie-aided interference cancellation) factor in such a system is 4.3 dB [70]. However, objectives of multiuser detection are not only in the potential system capacity improvement, but also in the relaxation of the power control requirement which will be shown in Section 2.4 to be very difficult in mobile radio channels. Although the present CDMA system interference level is very sensitive to a large variance of the received signal to interference plus background noise density ratio due to imperfect power control, CDMA techniques do give us more potential and flexibility for an increased capacity and improved performance system design. Multiuser detection is an approach which could push a CDMA system to its full potential based on the conviction that present multiuser detectors can be improved or modified, and their complexity can be lowered to yield significant improvement in overall system performance.

In a time-varying fading channel, a major problem for coherent or differentially coherent detection of the phase shift keying signal is the error floor which can not be lowered by increasing the transmitted power. This will be a big challenge for receiver design for data communication. For voice communication, the probability of error of 10^{-3} will maintain a reasonably good voice quality, however in data communication, the required probability of error usually needs to be as low as 10^{-6}. This requirement will be hard to maintain for the conventional differentially coherent or coherent detection of a PSK signal in a fast fading channel even in a single user environment. With the multiple access interference being another big detrimental factor to the receiver performance, this situation will be even worse. In a multipath CDMA time-varying fading channel, error floor of conventional RAKE type of receivers is caused by many factors: multiple access interference, path cross-correlation interference, the imperfection of channel estimates because of the channel's time-varying nature associated with Doppler spread and the intersymbol interference, etc. When there is an error floor, we can not lower the error rate by decreasing the total number of

active users in a multiple access system, hence a more efficient receiver design for such a system is called for.

1.5.2 Objectives

We consider multiuser detection problems in an asynchronous CDMA time-varying frequency nonselective or selective fading channels with the emphasis on high quality data or voice communication that requires very low error probability. The receiver performance is required to exhibit a greatly reduced error floor even when the desired user's signal is exposed to a strong interference in a time-varying fading channel. The proposed detectors will be of decorrelating type that exploit the implicit time diversity in the time-varying fading and multipath channels for improved detector performance. Low complexity and real time processing aspects of the decorrelator design are also major objectives of the dissertation. Specifically we consider

- problems of the present CDMA systems in time-varying fading channels: analysis will be made to demonstrate the potential benefit of multiuser detection for a CDMA system in which power control makes the present CDMA system successful to some extent, but it also limits the inherent advantages of DSSS-CDMA over other multiple access techniques like TDMA in mobile channels.

- design a computationally efficient decorrelator in asynchronous CDMA frequency nonselective time-varying fading channels employing both DPSK and BPSK modulation. We intend to design a decorrelator which not only cancels MAI at a low computational complexity, but also lowers the error floor. For BPSK, a novel channel estimator is proposed to lower the error floor caused by imperfect channel estimates. Our channel estimation method will be universally applicable for any given channel spaced-time correlation function, unlike the Kalman filter estimator which can be implemented as an optimal

decision-feedback channel estimator for Markovian type of channel models only.

- propose a fractionally-spaced bit-by-bit multipath decorrelator with low complexity in frequency selective fading channels. In addition, we want to lower the error floor of the conventional receivers in a multiple access time-varying multipath environment.

1.6 Dissertation Outline

In this dissertation, we will consider time-varying spread spectrum asynchronous CDMA frequency nonselective and frequency selective Rayleigh fading channels. Both BPSK and DPSK will be used and channel second order statistics (spaced-time correlation function) will be assumed known. For coherent detection no additional means such as pilot symbol or pilot tone will be assumed available to assist the channel estimation, so decision-feedback type of channel estimators will be used.

Chapter 2 proposes a method of analyzing the effect of imperfect power control on the IS-95 reverse link multiple access interference. To maintain a certain communications quality, the mobiles' required transmitted power is obtained through solving a set of linear equations. The received signal to interference plus noise density ratio (SINR) is assumed to be a random variable with lognormal distribution after power control. The total interference above the noise level is calculated for different values of the standard deviation of the received SINR due to an imperfect power control.

In Chapter 3, a lower complexity fractionally-spaced bit-by-bit decorrelator structure is proposed for frequency nonselective and frequency selective Rayleigh fading CDMA asynchronous channels. Statistical description of the time-varying fading channels and the preliminary knowledge for both types of channels with the associated received baseband equivalent signals in these channels are also discussed in this chapter.

Chapter 4 describes a differentially coherent decorrelating detector for a K-user reverse link CDMA environment that exhibits time-varying Rayleigh fading. The mobile channel is modeled as providing only a single fading path for each user and with no additional means to achieve diversity. The detector's design is based on using fractionally sampled matched filter outputs over each bit interval of the desired user, thus enabling the realization of a bit-by-bit decorrelator that requires smaller size matrices only. Oversampling is also utilized in forming the maximum likelihood decision rule, which results in an effective increase of the correlation in the fading process and hence a diminished error floor. Analytical evaluation and simulation of the error probability of the detector will be given. Comparison is made between performance of the this detector and that of the conventional DPSK detector (one sample per bit) operating in a single user environment.

In Chapter 5 a coherent multiuser detector for an asynchronous CDMA frequency nonselective time-varying Rayleigh fading channel is proposed. A fractionally sampled decorrelator is exploited to achieve the effective diversity implicit in the time-varying fading channel. A decision feedback MAP channel estimation method is proposed for this detector structure. In contrast to the Kalman filter which can be implemented as the optimal MMSE channel estimator for Markovian type of channels only, this estimator is optimal and universally applicable for any channel model with known first and second order statistics. Coherent detection with differential encoding is proposed in order to prevent the "run away" phenomenon of the channel estimator which operates in a decision feedback mode. This detector provides a simple multiuser detector with an improved performance.

Chapter 6 deals with a time-varying frequency selective fading channel, in which performance can be improved through both time and frequency domain processing. The wideband nature of each user's information signal relative to the

channel coherence bandwidth results in L ($L > 1$) resolvable paths at the receiver, and this can be viewed as another method for obtaining frequency diversity of order L [55], although this diversity is exploited in time domain by the use of RAKE or RAKE-type of receivers in a way similar to time diversity. The effective time diversity which can be achieved by obtaining multiple samples per bit is another approach for an improved performance receiver design in the time-varying fading channel. A novel structure of fractionally-sampled bit-by-bit multipath asynchronous decorrelator with the ML detection of differentially encoded data is proposed. This structure provides full utilization of both frequency and time domain diversity for an improved performance and a robust multiuser receiver design because no channel estimation is needed.

Following the bit-by-bit multipath decorrelator structure of Chapter 3, a coherent detection is analyzed in Chapter 7. The MAP channel estimator is used to obtain the channel estimates and performance comparison is made between the performance of the proposed detector in a multiuser environment and that of ideal RAKE (that assumes zero path cross-correlation and no ISI) in a single user environment. Effects of number of samples per bit and fading rapidity on performance of the proposed detector are also addressed.

In Chapter 8, a summary of the dissertation is drawn and future research based on the accomplishments of this dissertation is proposed.

CHAPTER 2

IMPACT OF IMPERFECT POWER CONTROL ON IS-95 MULTIPLE ACCESS INTERFERENCE

2.1 Introduction

The Erlang capacity analysis of the IS-95 CDMA system was given in [73], with analytical expressions for Erlang capacity as a function of the blocking probability and standard deviation of the received bit energy to interference density ratio caused by imperfect power control derived. By assuming a frequency reuse factor equal to 7 in a 3-slot TDMA system, it was claimed that the Erlang capacity of the present IS-95 CDMA system was about sevenfold that of the 3-slot TDMA system [73]. In the CDMA cellular system interference analysis [71], it was assumed that all cells are equally loaded, with the same number of users per cell uniformly distributed within each sector. The Erlang capacity under non-uniform distribution with light loading of cells surrounding the desired one was presented in [38].

In [73], the Erlang capacity of a CDMA system is derived by setting the interference-to-noise ratio I/N_0 at the base station to 10 dB, because beyond this value, interference increases nonlinearly for one additional user. In theory, there is no hard interference level limit on the CDMA system; one more user can join the system at the expense of all of them transmitting a higher power, provided that a particular communication quality can be maintained.

While the evaluation of the system capacity is essential for assessing the theoretical loading limit of the system, the actual system design requires the calculation of other system parameters as well. In a sectored cellular CDMA system, transmitted power of other mobiles both inside and outside of the desired sector act as an interference source. One very important practical parameter is the mobiles' transmitted power for a given loading of the system. For some predetermined

service quality level, loading and the coverage area, a proper system design requires transmitted power to be as low as possible.

For a fair loading capability comparison between CDMA and TDMA, one additional constraint, the mobiles' transmitted power requirement, should be taken into consideration. This is because in TDMA and FDMA systems the number of radio channels is determined by the total bandwidth available, and this number can be directly and uniquely converted into Erlangs for a certain blocking probability. The CDMA system is different, the capacity is soft, and we can always trade an increase in the mobiles' transmitted power for a higher loading while maintaining communication quality. But from the practical consideration, handsets have maximum available transmitted power, and also operating at high interference level makes the system unstable.

Imperfect power control affects IS-95 CDMA system Erlang capacity and the system interference level. A closed-loop power control bit is sent every 1.25 ms to inform the mobile station (MS) to either increase or decrease its power by one dB. This power control method is effective in mitigating slow channel gain variations caused by shadowing effects, but may not be effective for the short term channel gain variations caused by fast fading.

A model for computing transmitted power of mobiles in a sectored CDMA system reverse link under imperfect power control and shadowing is proposed. Users are assumed to be randomly distributed over the service area which consists of N_{sec} sectors according to the uniform distribution. The received signal to interference plus noise density ratio is assumed to be a random variable with lognormal distribution after power control. A set of linear equations is then formed for each realization of the distribution of the mobiles over the service area. By solving these equations, the transmitted power of the mobiles is obtained, making it possible to completely measure the reverse link performance. All important parameters measuring CDMA

system reverse link performance such as interference margin for a given loading, other sectors to the same sector interference ratio, and the system Erlang capacity can be obtained readily. This method can be applied to the practical CDMA system reverse link performance analysis directly.

Upon establishing the mobiles' transmitted power model, we will simulate impact of imperfect power control on the reverse link interference. Relative interference above the white Gaussian noise level is calculated for different path loss exponent and lognormal shadowing standard deviation with respect to different standard deviation of imperfect power control. Then, an actual fading channel is generated, and we will show that in a fast fading channel the IS-95 CDMA close-loop power control method is not effective. This observation motivated our research efforts in seeking near-far resistant detectors for CDMA systems that provide a robust system for mobile communication with an improved performance.

2.2 Definition of System Parameters and Propagation Model

The service area defined as one cell in the center and two tiers of out-cells is shown in Fig. 2.1. Each cell consists of three sectors.

The following is a partial list of the notations:

W = System bandwidth

R = Bit rate

N_0 = Thermal noise power spectral density

I_0 = Total interference plus thermal noise power spectral density

α = Voice activity factor

μ = Path loss exponent

E_b = Received energy per bit

σ_s = Lognormal shadowing standard deviation

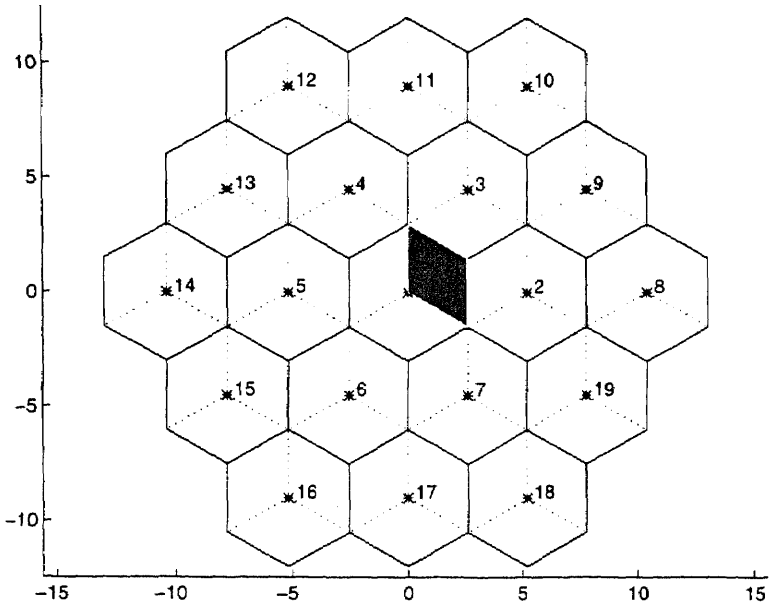

Figure 2.1 The service area considered

σ_p = Received E_b/I_0 standard deviation due to imperfect power control

N_{sec} = Total number of sectors in the service area

N_{tot} = Total number of users in the service area

N_k = Total number of users hosted by the k^{th} sector

$a_{i,kl}$ = Propagation attenuation from l^{th} user of k^{th} sector to i^{th} base

$\xi_{i,kl}$ = Gaussian random variable, where $10^{\xi_{i,kl}/10}$ represents the lognormal shadowing random variable for l^{th} user in k^{th} sector to i^{th} base

$r_{i,kl}$ = Distance of l^{th} user of k^{th} sector to i^{th} base

$G_{i,kl}$ = Relative antenna gain from l^{th} user of k^{th} sector to i^{th} base

x_{kl} = Transmitted power of l^{th} user in k^{th} sector

The mobile transmitted power propagation losses in decibels with the antenna gain included are

$$10\log(a_{i,kl}) = A_0 - 10\mu\log(r_{i,kl}) + \xi_{i,kl} + G_{i,kl}, \tag{2.1}$$

where A_0 is the propagation loss defined at one mile. Notice here when $r_{i,kl} \longrightarrow 0$, the above equation is not defined. From practical consideration, when $r_{i,kl}$ is smaller than a threshold, we can substitute this threshold into the above equation. A lognormal shadowing random variable for all mobiles to all sectors can be generated the same way as presented in [72]. Each of them consists of two parts, the first part is common for each mobile to all sectors, but independent from mobile to mobile. The second part is independent not only from mobile to mobile, but also independent from each mobile to different cells [1].

Using equation (2.1), the hosting sector of each mobile can be determined by calculating the minimum attenuation from the mobile to all sectors. We also assume that no mobile is communicating with more than one sector at a time.

2.3 Mobile Transmitted Power Calculation

Because of imperfect power control the received signal to interference plus noise density ratio d_{kl} of the l^{th} user hosted by the k^{th} sector is assumed to be a lognormal random variable [73] with

$$d_{kl} = \left(\frac{E_b}{I_0}\right)_{kl} = 10^{\zeta_{kl}/10}, \tag{2.2}$$

where ζ_{kl} is a Gaussian random variable with $E\{\zeta_{kl}\} = (E_b/I_0)_{required}$, and the standard deviation σ_p.

Each mobile's transmitted power has to satisfy the following equation

$$\begin{aligned} \left(\frac{E_b}{I_0}\right)_{kl} &= \frac{x_{kl}a_{k,kl}/R}{N_0 + \alpha(I_{kl}/W)} = \frac{g x_{kl} a_{k,kl}}{N_0 W + \alpha I_{kl}} \\ &= d_{kl} \end{aligned} \tag{2.3}$$

$$k = 1, 2, \ldots N_{sec}, \quad l = \text{all mobiles hosted by sector } k,$$

[1] Each cell has three sectors, and this part is assumed to be the same for a mobile to all three sectors in the same cell.

where $g = W/R$ is the processing gain, and I_{kl}, the interference for the l^{th} mobile in the k^{th} sector, is given by

$$I_{kl} = \sum_{\substack{j \\ j \neq l}} x_{kj} a_{k,kj} + \sum_{i \neq k} \sum_{j} x_{ij} a_{k,ij} \tag{2.4}$$

Let

$$\boldsymbol{X}_k = [x_{k1}, x_{k2}, \ldots, x_{kN_k}]^T$$

be the transmitted power of all mobiles in the k^{th} sector,

$$\boldsymbol{D}_k = [d_{k1}, d_{k2}, \ldots, d_{kN_k}]^T$$

the received E_b/I_0 of all mobiles in the k^{th} sector,

$$\boldsymbol{A}_{ik} = -\begin{bmatrix} a_{i,k1} & a_{i,k2} & \cdots & a_{i,kN_k} \\ a_{i,k1} & a_{i,k2} & & a_{i,kN_k} \\ \vdots & & & \\ a_{i,k1} & a_{i,k2} & & a_{i,kN_k} \end{bmatrix}, \text{ for } i \neq k \text{ and}$$

$$\boldsymbol{A}_{kk} = -\begin{bmatrix} -g a_{k,k1}/(\alpha d_{k1}) & a_{k,k2} & \cdots & a_{k,kN_k} \\ a_{k,k1} & -g a_{k,k2}/(\alpha d_{k2}) & & a_{k,kN_k} \\ \vdots & & & \\ a_{k,k1} & a_{k,k2} & & -g a_{k,kN_k}/(\alpha d_{kN_k}) \end{bmatrix}$$

$i, k = 1, 2, \ldots, N_{sec}$.

Equation (2.3) can now be arranged in the matrix form as

$$\begin{aligned} \boldsymbol{AX} &= \begin{bmatrix} \boldsymbol{A}_{11} & \boldsymbol{A}_{12} & \cdots & \boldsymbol{A}_{1N_{sec}} \\ \boldsymbol{A}_{21} & \boldsymbol{A}_{22} & & \boldsymbol{A}_{2N_{sec}} \\ \vdots & & & \\ \boldsymbol{A}_{N_{sec}1} & \boldsymbol{A}_{N_{sec}2} & & \boldsymbol{A}_{N_{sec}N_{sec}} \end{bmatrix} \begin{bmatrix} \boldsymbol{X}_1 \\ \boldsymbol{X}_2 \\ \vdots \\ \boldsymbol{X}_{N_{sec}} \end{bmatrix} \\ &= (N_0 W/\alpha)\mathcal{I}, \end{aligned} \tag{2.5}$$

where $\mathcal{I}$ is a $N_{tot} \times 1$ vector with all elements equal to one. Hence the transmitted power of all mobiles in the service area can be computed as

$$\boldsymbol{X} = (N_0 W/\alpha)\boldsymbol{A}^{-1}\mathcal{I}. \tag{2.6}$$

In order to get the transmitted power of all mobiles in the service area, we need to invert a matrix with the size $N_{tot} \times N_{tot}$. As a special case when perfect power control

is assumed, the dimension of the matrix $\boldsymbol{A}$ in equation (2.5) decreases to $N_{sec} \times N_{sec}$, because the following governing equations hold

$$x_{k1}a_{k,k1} = x_{k2}a_{k,k2} = \ldots = x_{kN_k}a_{k,kN_k} = Y_k, \qquad k = 1, 2, \ldots N_{sec},$$

or equivalently

$$\begin{bmatrix} x_{k1} \\ x_{k2} \\ \vdots \\ x_{kN_k} \end{bmatrix} = \begin{bmatrix} a_{k,k1}^{-1} \\ a_{k,k2}^{-1} \\ \vdots \\ a_{k,kN_k}^{-1} \end{bmatrix} Y_k, \qquad k = 1, 2, \ldots N_{sec}. \tag{2.7}$$

By using the above relation, equation (2.5) can be reformulated as

$$\begin{bmatrix} S_{11} & S_{12} & \ldots & S_{1N_{sec}} \\ S_{21} & S_{22} & & S_{2N_{sec}} \\ \vdots & & & \\ S_{Ns1} & S_{Ns2} & \ldots & S_{N_{sec}N_{sec}} \end{bmatrix} \begin{bmatrix} Y_1 \\ Y_2 \\ \vdots \\ Y_{N_{sec}} \end{bmatrix} = (N_0 W/\alpha)\mathcal{I}, \tag{2.8}$$

where

$$\begin{aligned} S_{mk} &= -\sum_{l=1}^{N_k} \frac{a_{m,kl}}{a_{k,kl}}, \; k \neq m \\ S_{kk} &= g/(\alpha d) - (N_k - 1), \qquad \text{where } d \text{ is the required } E_b/I_0. \end{aligned}$$

2.4 Numerical Examples and Discussions

The following parameters will be used for all numerical examples: the average number of users per sector is 10, $\left(\frac{E_b}{I_0}\right) = 5$ or 7 dB, the cell radius is taken to be 3 miles, $W = 1.2288$ MHz, $R = 9.6$ kbps, and $\alpha = 0.4$. Two tiers of cells outside the target cell are considered. A 90° antenna with the maximum gain of 14.5 dB is applied.

Fig. 2.2 shows the average other sectors to the same sector interference ratio versus σ_s, with $\sigma_p = 0$ (perfect power control). Fig. 2.3 shows the average interference margin versus σ_s for different σ_p. In Fig. 2.4 the average other-sectors to the same-sector interference ratio versus path loss exponents with $\sigma_p = 0$ is shown. Fig. 2.5 shows the interference margin versus path loss exponents for different values of σ_p.

From Fig. 2.3 and Fig. 2.5, it is clear that imperfect power control will affect the system interference level appreciably as the power control mechanism deteriorates. Relatively tight power control is needed in order for the IS-95 CDMA system to operate effectively.

Considering a mobile moving at 100 km/h, and transmitting at the rate of 9600 bps with carrier frequency $f_c = 835\ MHz$, the maximum Doppler frequency is calculated as: $f_d = \frac{vf_c}{c} = 87\ Hz$. A power control bit is sent every 1.25×10^{-3} second in the IS-95 CDMA system. If Jakes' model is used for the channel spaced-time correlation function, the channel gain is plotted in Fig. 2.6 for an interval of 20 power control bits. Obviously, the IS-95 CDMA power control method can not compensate for the short term channel variations in the above example. In mobile cellular communications, mobiles may move in the range of 20 to 70 miles per hour resulting in a possible relatively fast fading channel, making IS-95 CDMA power control ineffective for the short-term fading. For such a fast fading, however, coding with finite depth interleaving becomes more effective. Power control can be effective to compensate for shadowing effects or slow fading (low mobility), wherein coding is not so effective because of its finite depth interleaving in a slowly changing channel. The combined effect of power control and coding will probably result in a different required E_b/I_0 in order to maintain a certain communications quality for the whole practical mobility range. It should be noted that in our interference analysis, we did not take these facts into consideration, i.e, we assumed that the required E_b/I_0 to maintain a certain communications quality is the same regardless of the fading rapidity.

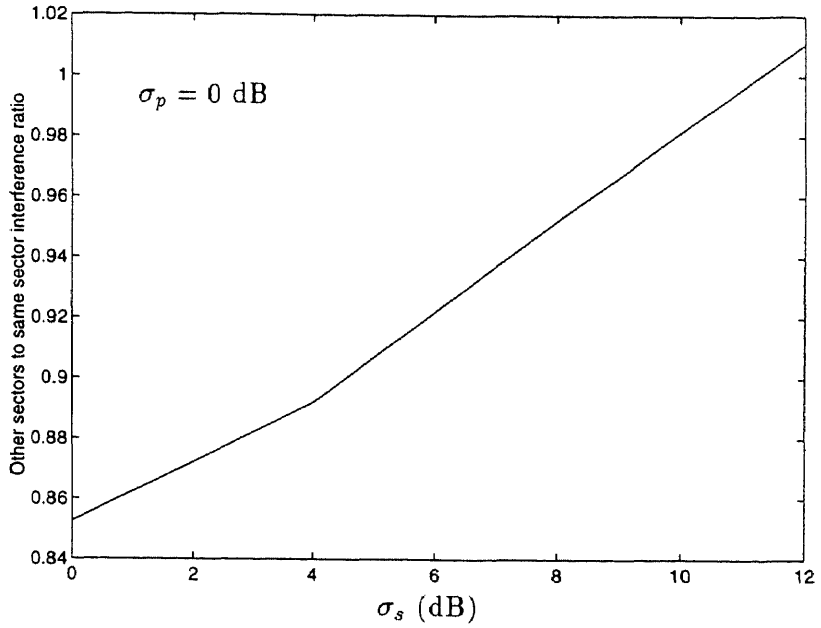

Figure 2.2 Other-sectors to the same-sector interference ratio vs. $\sigma_s(\mu = 4)$

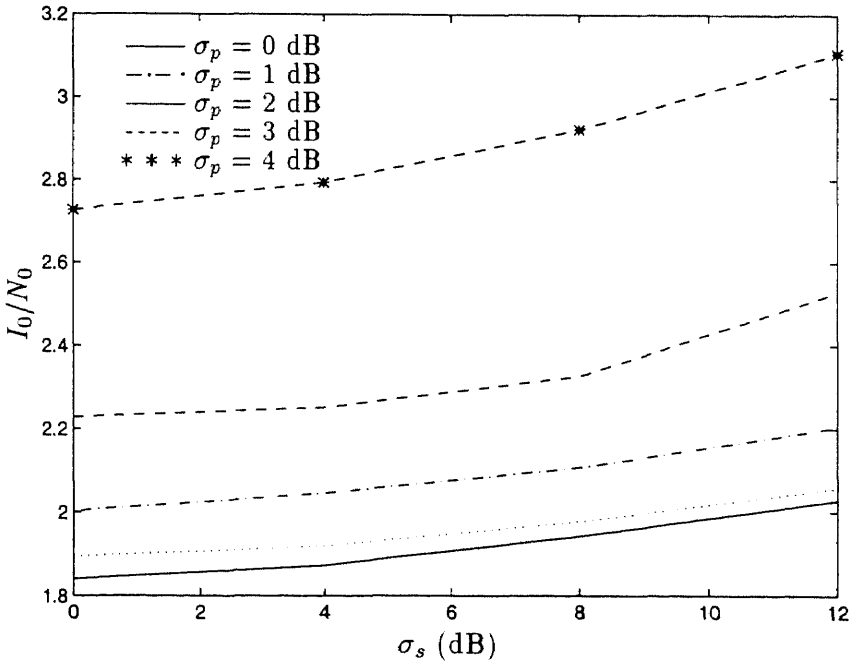

Figure 2.3 Interference plus noise to noise density ratio vs. $\sigma_s(\mu = 4)$

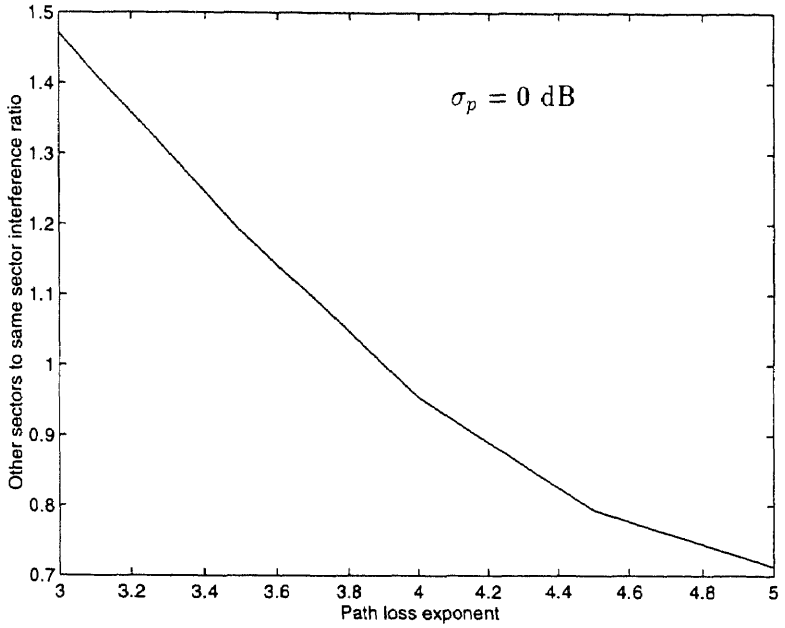

Figure 2.4 Other-sectors to the same sector interference ratio vs. $\mu(\sigma_s = 8dB)$

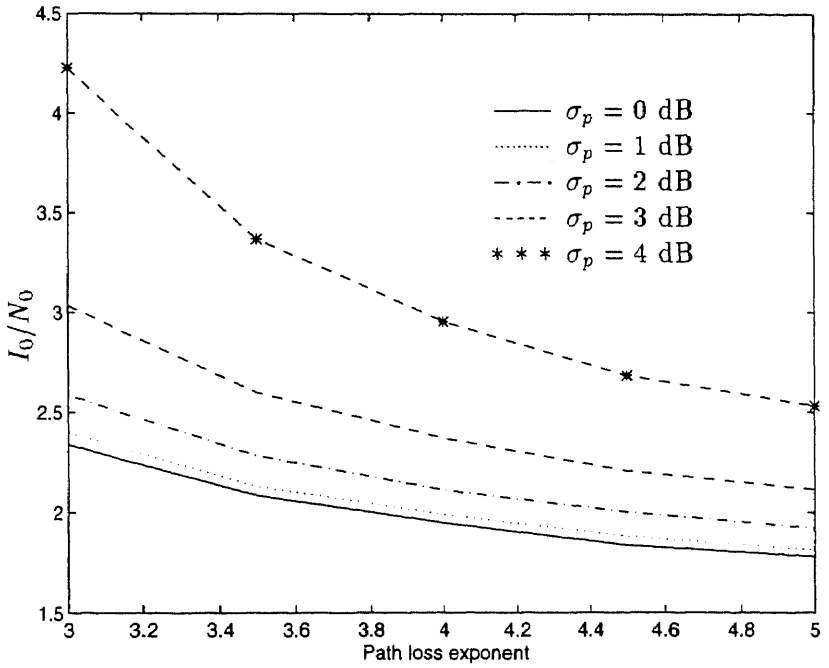

Figure 2.5 Interference plus noise to noise density ratio vs. $\mu(\sigma_s = 8dB)$

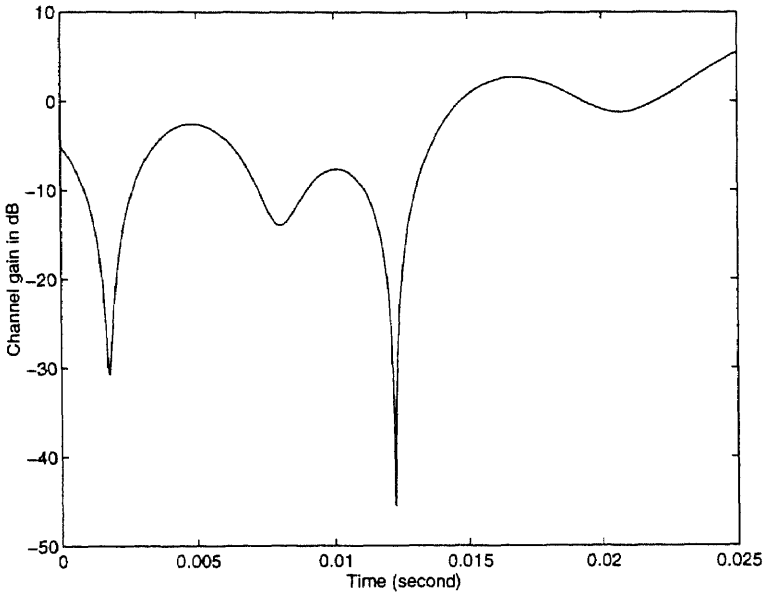

Figure 2.6 Rayleigh fading channel gain variation during an interval of 20 power control bits

CHAPTER 3

FRACTIONALLY-SPACED DECORRELATOR FOR TIME-VARYING FADING CHANNELS

3.1 Introduction

As was mentioned in Chapter 1, in a time-varying [1] fading environment a decorrelator appears to be more robust than multistage multiuser detectors wherein interference has to be estimated first and then subtracted from the composite signal of the desired user when performing the desired user's information detection. Previous work on the decorrelating type of multiuser detectors for fading channels was mainly focussed on an infinite horizon decorrelator (e.g., [91] [88]). In addition to the excessive processing delay, variations in the number of users and in their relative delays will result in a corresponding change of the correlation matrix [26], thus requiring an intensive computation. Sliding window approximation to the infinite horizon decorrelator is one way to obtain a finite memory-length decorrelator, however, it causes other problems such as an edge effect. This edge effect can be resolved by the isolation bit insertion method proposed in [81] at the expense of losing bandwidth efficiency and additionally it requires some form of synchronism between users [26]. The choice of the window size is another issue which reflects the tradeoff between the detector complexity and the bandwidth efficiency.

We will develop the realization of a low complexity bit-by-bit decorrelator in an asynchronous multiuser scenario in which each user's transmission propagates through a single time-varying fading path. Then, we will extend this bit-by-bit decorrelator structure for an asynchronous CDMA frequency selective channel wherein each resolvable path is subject to time-varying fading with a known spaced-time

[1] Often an unquantifiable term "slow fading" is used in referring to the channels whose gains remain constant, and therefore perfectly estimable, over the entire transmission horizon. The terms "fast" or "rapid" fading are, then, used to characterize channels that do not conform to the above assumption. It seems that time-invariant and time-varying channels are more appropriate respective descriptions, e.g., [65], wherein the fading rapidity of the latter type can be quantified by an appropriate parameter.

correlation function that directly relates the fading rapidity to the channel Doppler shift. To overcome the limitations of the infinite horizon or the windowed decorrelator, the first step in our approach will be to utilize fractionally sampled matched filter outputs in realizing a lower complexity bit-by-bit decorrelator, which was originally described in [68] and is based on the realization presented in [82] for an AWGN channel.

The goal of this chapter is to present a lower complexity decorrelator structure for the asynchronous CDMA channel. The chapter is organized as follows. In Section 3.2, we provide some basic description of the time-varying frequency nonselective and frequency selective fading channels. The statistical description of the time-varying characteristic of the channels and the received baseband equivalent signals in these channels are also given in this Section. Section 3.3 presents the fractionally-spaced bit-by-bit decorrelator for the frequency nonselective channel with the correlation matrix singularity problem addressed in Section 3.3.1. Section 3.4 describes the fractionally-spaced bit-by-bit decorrelator for the frequency selective channel Concluding remarks on the proposed fractionally-spaced decorrelator are given in Section 3.5.

3.2 Preliminaries

Consider K users transmitting asynchronously in a CDMA mobile environment. The unit energy signature waveform $s_k(t), k = 1, \ldots, K$ of duration T, and the chip period T_c is assigned to each user. Information bit [2] $b_k(i) \in \{-1, 1\}$ for the i^{th} bit interval of user k also has duration T. In a frequency nonselective environment, the channel for each user is modeled as an independent, narrowband Rayleigh fading channel having multipath spread much shorter than T, resulting in negligible inter-symbol interference at the receiver. The channel gain for user k then represents

[2] Differentially encoded for DPSK

multiplicative distortion modeled as a normalized, independent, zero-mean complex-valued wide-sense stationary Gaussian process $c_k(t)$ [55]. The received baseband equivalent complex signal $r(t)$ can therefore be expressed as

$$r(t) = \sum_i \sum_{k=1}^{K} b_k(i)\sqrt{a_k}c_k(t)s_k(t - iT - \tau_k) + n_w(t), \tag{3.1}$$

where a_k and τ_k are the received energy per bit and relative delay for user k, respectively, and $n_w(t)$ is a zero-mean, complex white Gaussian noise with the one-sided power spectral density N_0.

In a frequency selective channel, we consider the wide-sense-stationary uncorrelated scattering (WSSUS) Rayleigh fading. Assuming each user's signal is bandlimited to $W = 1/T_c$, the channel with L resolvable paths can be modeled as a tapped delay line with the tap spacing T_c [55], i.e., the channel impulse response for each user is

$$c_k(\tau, t) = \sum_{l=0}^{L-1} c_{kl}(t)\delta(\tau - lT_c),$$

where $c_{kl}(t)$, $k = 1, \ldots, K$, $l = 1, \ldots, L$ are mutually independent zero-mean, complex Gaussian random processes. The number of resolvable paths L at the receiver for each user is $L = WT_m + 1$ [55], where T_m is the channel multipath spread. We assume that the channel is time-varying with a known spaced-time correlation function.

Using this tapped delay line channel model, if the transmitted signal is $s_k(t)$, the received noiseless signal is

$$h_k(t) = \sum_{l=0}^{L-1} c_{kl}(t)s_k(t - lT_c).$$

For the multiuser communications in this scenario, the received baseband equivalent complex signal $r(t)$ is expressed as

$$r(t) = \sum_i \sum_{k=1}^{K} \sqrt{a_k}b_k(i) \sum_{l=0}^{L-1} c_{kl}(t)s_k(t - iT - \tau_k - lT_c) + n_w(t). \tag{3.2}$$

The time-varying statistics of the fading channel are described by the spaced-time correlation function $\Phi(\Delta t)$ defined as

$$\Phi_{kl}(\Delta t) = E\{c_{kl}(t)c_{kl}^{*}(t+\Delta t)\}, \quad k=1,\ldots,K, \text{ and } l=1,\ldots,L, \tag{3.3}$$

where $E\{\cdot\}$ denotes statistical expectation, * denotes conjugate, and $\Phi_{kl}(0)=1$ due to the normalization.

One of the often used models in the literature (e.g., [32], [2]), for describing time variations of a channel is a simple, first-order Markov process, which results in the exponential correlation function

$$\Phi_{kl}(\Delta t) = e^{-2\pi f_d T|\Delta t/T|} = \varrho^{|\Delta t/T|}, \tag{3.4}$$

where the correlation parameter $\varrho = \Phi(T)/\Phi(0)$ determines the fluctuation rate of the fading channel, and f_d represents the maximum Doppler shift.

Another model due to Jakes [24], also referred to as the land-mobile channel model, yields the following correlation function:

$$\Phi_{kl}(\Delta t) = J_0(2\pi f_d \Delta t), \tag{3.5}$$

where $J_0(\cdot)$ is a Bessel function of the first kind.

In (3.4) and (3.5) for a frequency nonselective channel, $L=1$. For numerical examples in this dissertation, the time-varying fading channel will be generated by employing both models.

3.3 Fractionally-Spaced Decorrelator for Frequency Nonselective Fading Channels

Fractionally sampled matched filter outputs, with relative spacing of the sampling instants coinciding with the users' relative delays, will be used for the realization of the decorrelator. Without loss of generality, we assume that $0=\tau_1<\tau_2<\ldots<$

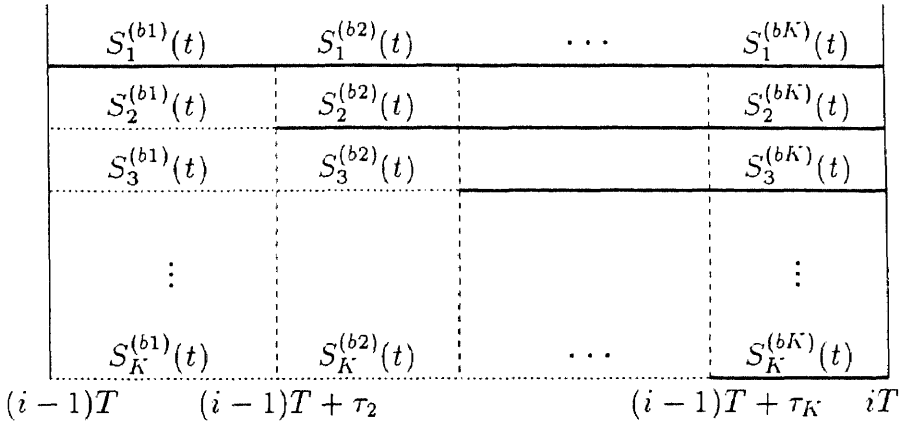

Figure 3.1 Partition of the i^{th} bit interval of user 1 into blocks

$\tau_K < \tau_{K+1} = T$, and we focus on bit i of user 1 that we, as shown in Fig. 3.1, position in the interval $[(i-1)T, iT]$. (To simplify notations, the time index will be omitted whenever possible).

We can view each block of time $[\tau_j, \tau_{j+1}]$ $j = 1, \ldots, K$ as a $K-$user synchronous channel with unit-energy waveforms $\overline{s}_k^{(bj)}(t) = s_k^{(bj)}(t)/\sqrt{\epsilon^{(bj)}}$ $k, j = 1, \ldots, K$, where

$$s_k^{(bj)}(t) = \begin{cases} s_k(t + \beta_{kj}T - \tau_k) & \tau_j < t < \tau_{j+1} \\ 0 & \text{otherwise} \end{cases}$$

$$\beta_{kj} = \begin{cases} 1 & j < k \\ 0 & \text{otherwise,} \end{cases}$$

and

$$\epsilon^{(bj)} = \int_{\tau_j}^{\tau_{j+1}} s_k^2(t + \beta_{kj}T - \tau_k)dt = \int_0^T \left[s_k^{(bj)}(t)\right]^2 dt, \quad k = 1, \ldots, K.$$

In all notations the superscript $^{(bj)}$ denotes block j.

By introducing matrix $\boldsymbol{P}^{(bj)}$, whose $(m,l)^{th}$ element, $p_{ml}^{(bj)}$, is defined as

$$p_{ml}^{(bj)} = \frac{1}{\epsilon^{(bj)}} \int_0^T s_m^{(bj)}(t) s_l^{(bj)}(t)dt \qquad m, l \in (1, \ldots, K),$$

the fractionally sampled matched filter output for the j^{th} block in the i^{th} bit interval is [3]

$$\boldsymbol{x}^{(bj)} = \sqrt{\epsilon^{(bj)}}\boldsymbol{P}^{(bj)}\boldsymbol{A}\boldsymbol{C}^{(bj)}\boldsymbol{b}^{(bj)} + \boldsymbol{n}^{(bj)}, \quad j = 1, \ldots, K, \tag{3.6}$$

where

$$\begin{aligned} \boldsymbol{x}^{(bj)} &= [x_1^{(bj)}, x_2^{(bj)}, \ldots, x_K^{(bj)}]^T \\ \boldsymbol{b}^{(bj)} &= [b_1(i), \ldots, b_j(i), b_{j+1}(i-1), \ldots, b_K(i-1)]^T \\ \boldsymbol{A} &= \mathrm{diag}[\sqrt{a_1}, \ldots, \sqrt{a_K}]. \end{aligned}$$

The additive noise vector for each block, $\boldsymbol{n}^{(bj)} = [n_1^{(bj)}, \ldots, n_K^{(bj)}]^T$, has the covariance matrix $E\{\boldsymbol{n}^{(bj)}\boldsymbol{n}^{(bj)H}\} = N_0\boldsymbol{P}^{(bj)}$, where ^{H} denotes Hermitian transpose.

In the discrete-time channel formulation adopted here, the fading process is piecewise-constant in each block of time [4] $[\tau_j, \tau_{j+1}]$ so that $\boldsymbol{C}^{(bj)}$, the matrix of the channel fading coefficients in block j, is given as

$$\begin{aligned} \boldsymbol{C}^{(bj)} &= \mathrm{diag}[c_1^{(bj)}, \ldots, c_K^{(bj)}] \\ &= \mathrm{diag}[c_1(t)|_{t=(i-1)T+\tau_{j+1}}, \ldots, c_K|_{t=(i-1)T+\tau_{j+1}}]. \end{aligned} \tag{3.7}$$

After performing a decorrelating operation on K synchronous users in the j^{th} block, the resulting multiuser interference-free vector is

$$\boldsymbol{z}^{(bj)} = (\boldsymbol{P}^{(bj)})^{-1}\boldsymbol{x}^{(bj)} = \sqrt{\epsilon^{(bj)}}\boldsymbol{A}\boldsymbol{C}^{(bj)}\boldsymbol{b}^{(bj)} + \boldsymbol{\xi}^{(bj)} \quad j = 1, \ldots, K, \tag{3.8}$$

where

$$\boldsymbol{z}^{(bj)} = [z_1^{(bj)}, \ldots, z_K^{(bj)}]^T, \tag{3.9}$$

and

$$\begin{aligned} \boldsymbol{\xi}^{(bj)} &= [\xi_1^{(bj)}, \ldots, \xi_K^{(bj)}]^T \\ &= (\boldsymbol{P}^{(bj)})^{-1}\boldsymbol{n}^{(bj)}, \end{aligned} \tag{3.10}$$

[3] We assumed that the channel variations have no effect on the matched filtering operation.

[4] The details of this nonuniform piece-wise approximation of channel gains over the interval $[0, T]$ are given in Section 4.3.

represents the noise vector for all K users in the j^{th} block, and has the covariance matrix

$$E\{\boldsymbol{\xi}^{(bj)}\boldsymbol{\xi}^{(bj)H}\} = N_0(\boldsymbol{P}^{(bj)})^{-1}.$$

The decorrelating operation requires an inversion of $K \times K$ matrices and can commence as soon as the vector $\boldsymbol{x}^{(bj)}$ at the corresponding time instant becomes available.

3.3.1 Singularity Problem

Correlation matrix singularity may occur for any decorrelating type of multiuser detectors. For the realization of the above decorrelator in the asynchronous system, a portion of the signature waveforms for each user is taken to form the correlation matrix in each block. If two consecutive relative delays are closer to each other, the correlation matrix in such a block is more likely to be singular because of the linearly dependence of the spreading sequences over that block. When the user population in the system is not too high (e.g., 20 users for a processing gain of 128), one remedy to this problem is to discard those short blocks (out of total of K blocks) whose correlation matrices are singular. The remaining blocks carrying the same information will be sufficient for performing a proper detection because the users' energy contained in the discarded short blocks is small, resulting in a very small signal to noise ratio penalty.

As the number of active users in the system increases, relative delays become closer to each other, and hence more correlation matrices in all the K blocks over one bit interval are likely to become singular or ill-conditioned. In this case, the correlation matrix singularity problem can be avoided by reducing the number of samples per bit, resulting in an increased interval between any two consecutive sampling points and hence a less likely linear dependence among the portion of spreading sequences over each block. More importantly, the gain due to fractional sampling

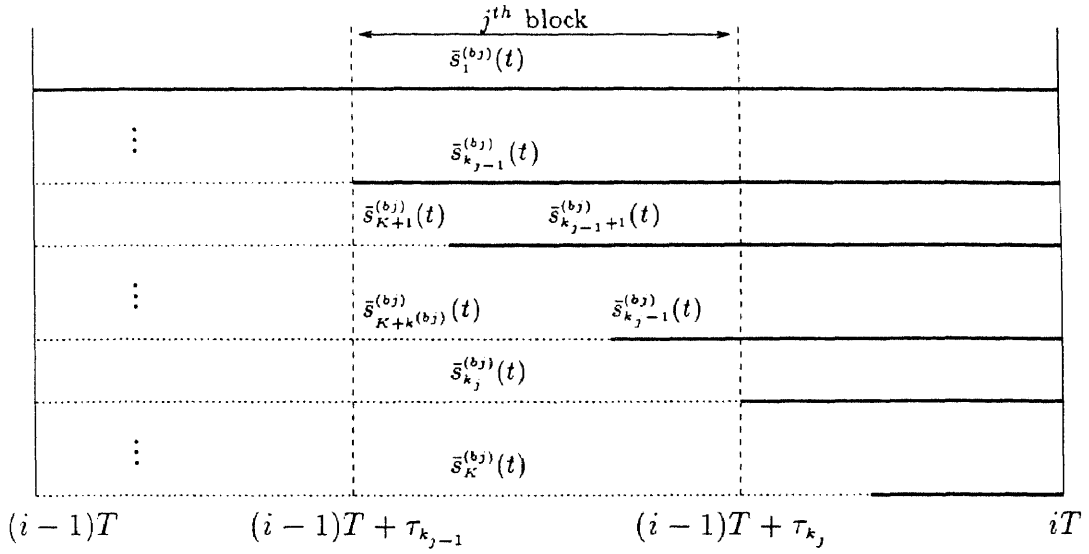

Figure 3.2 Partition of users over one bit interval of user 1 into J blocks

can be maintained almost completely if we take as few as two to three samples per bit. This will be demonstrated in later chapters by examples.

Fig. 3.2 shows the way of grouping the K users into J groups and obtaining J samples over the i^{th} bit interval of user 1. In order to obtain the J samples, we partition the i^{th} bit interval of user 1 into J blocks in which the initial time of the j^{th} block starts at the initial time of the $(k_{j-1})^{th}$ user and ends at the initial time of the $(k_j)^{th}$ user. Correspondingly, the j^{th} block spans the time interval $[(i-1)T + \tau_{k_{j-1}},\ (i-1)T + \tau_{k_j}]$, $j = 1, \ldots, J$ and we take samples at the end of each block that correspond to time instants $(i-1)T + \tau_{k_j}$, $j = 1, \ldots, J$ for the i^{th} bit interval of user 1.

Notice that in the above formulation, $k_0 = 0$, $\tau_{k_0} = 0$, $k_J = K + 1$ and $\tau_{k_J} = T$. By letting $k^{(bj)} = k_j - k_{j-1} + 1$ represent the total number of users whose initial time of the i^{th} bit interval falls in the j^{th} block, we can view the j^{th} block as an equivalent $N_j = K + k^{(bj)} - 1$ user synchronous system with the spreading sequences for each

of them defined as

$$s_n^{(bj)}(t) = \begin{cases} s_n(t+\beta_n^{(bj)}T-\tau_n) & n=1,\ \ldots,\ K \\ s_{n-K+k_{j-1}}(t+\beta_n^{(bj)}T-\tau_{n-K+k_{j-1}}) & n=K+1,\ \ldots,\ K+k^{(bj)} \\ 0 & \text{otherwise,} \end{cases}$$

for the interval of $\tau_{k_{j-1}} \leq t < \tau_{k_j}$. In the above equation $\beta_n^{(bj)}$, $j = 1,\ \ldots,\ J$, $n = 1,\ \ldots,\ K + k^{(bj)}$ are defined as

$$\beta_n^{(bj)} = \begin{cases} 0 & n \leq k_j - 1 \\ 1 & \text{otherwise.} \end{cases}$$

The normalized spreading sequences for each equivalent user over each block can be written as $\bar{s}_n^{(bj)}(t) = s_n^{(bj)}(t)/\epsilon_n^{(bj)}$ and the energy for each sequence, $\epsilon_n^{(bj)}$, is defined as

$$\epsilon_n^{(bj)} = \int_0^T \left[s_n^{(bj)}(t)\right]^2 dt,\ j = 1,\ \ldots\ J.$$

The correlation matrix for the j^{th} block $\boldsymbol{P}^{(bj)}$ has dimension $N_j \times N_j$. Its $(n_r, n_c)^{th}$ element, $p_{n_r,n_c}^{(bj)}$, can be calculated as

$$p_{n_r,n_c}^{(bj)} = \int_0^T \bar{s}_{n_r}^{(bj)}(t)\bar{s}_{n_c}^{(bj)}(t)dt,$$

where $n_r, n_c \in (1, \ldots, N_j)$. Having the correlation matrices for each block $\boldsymbol{P}^{(bj)}, j = 1, \ldots J$, all the rest of the derivation above applies except that here the matrix dimension becomes $N_j \times N_j$.

The complexity of this realization of the decorrelator is a little bit higher than that of the relative delay spaced decorrelator, but it provides us with more flexibility in terms of matrix invertibility, the number of samples per bit we want to take in order to achieve the effective diversity, etc.

Limited simulations are performed on the correlation matrix singularity problem of the proposed fractionally spaced decorrelator. The worst situation for the singularity problem, albeit unrealistic, is when unfiltered (rectangular) signature waveforms are assumed with relative delays chosen to be integer multiples

of a chip. In this case, if a block spans $\mathcal{K}$ chips, the rank of the cross-correlation matrix for this block is always less than or equal to $\mathcal{K}$ with a very high probability of equality. For a more practical situation, we assume that the relative delays are randomly distributed (according to the uniform distribution) over one bit interval and each chip is shaped into the main lobe of a raised cosine pulse with a roll-off factor of 1. Based on computer simulation under the above assumptions, the table below shows the percentage of occurance when the correlation matrices resulting from Gold sequences of length 31 are non-singular.

$K = 6$	$K = 8$	$K = 10$	$K = 12$
96.78%	90.53%	82.29%	75.4%

Given that there are K blocks over one bit interval, and each of them carries the same information bit, the proposed detection scheme can still work as long as we have at least one block with a non-singular correlation matrix. From the above simulation results, we can conclude that the probability that all K correlation matrices are singular simultaneously approaches zero for the user population up to $K = 12$ [5] because the singular matrices come from the short blocks in the total K un-equal length blocks, if we have a short block, there have to be other longer blocks to compensate for it.

When the number of samples are reduced to two for the above simulation conditions, it was never found through our limited simulation that we could not find the sampling points which result in non-singular matrices over each block.

3.4 Fractionally-Spaced Decorrelator for Frequency Selective Fading Channels

The fractionally-spaced decorrelator for the asynchronous multipath channel is implemented using a bit-by-bit approach. Without loss of generality, we assume that

[5] We should point out that for a practical system, $K = 12$ is not a small number for a processing gain of 31.

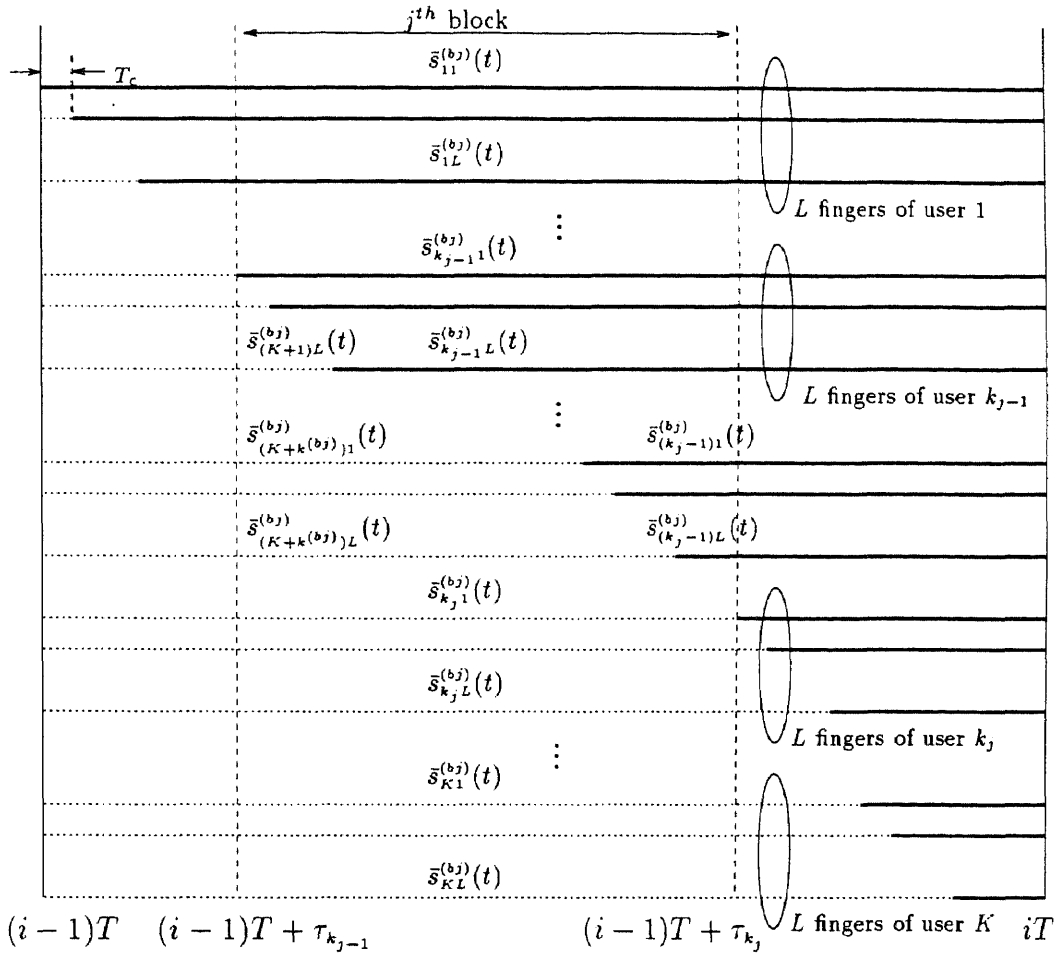

Figure 3.3 Partition of the i^{th} bit interval of user 1 into J blocks

$0 = \tau_1 < \tau_2 < \ldots < \tau_J < \tau_{K+1} = T$, and focus on the detection of the i^{th} bit of the desired user (assumed to be user 1) that we, as shown in Fig. 3.3, position in the time interval $[(i-1)T, iT]$ (To simplify notations, the time index will be omitted whenever possible).

We want to obtain J samples over the i^{th} bit interval for user 1. In order to achieve the fractional sampling and perform multiuser detection in a multiuser multipath environment, we partition the i^{th} bit interval of user 1 into J blocks as shown in Fig. 3.3 in which the initial time of the j^{th} block starts at the initial time of the $(k_{j-1})^{th}$ user and ends at the initial time of the $(k_j)^{th}$ user. Correspondingly,

the j^{th} block spans time interval $[(i-1)T+\tau_{k_{j-1}},\ (i-1)T+\tau_{k_j}]$, $j=1,\ \ldots,\ J$ and we take samples at the end of each block that corresponds to time instant $(i-1)T+\tau_{k_j}$, $j=1,\ \ldots,\ J$ for the i^{th} bit interval of user 1.

Notice that in the above formulation, $k_0=0$, $\tau_{k_0}=0$, $k_J=K+1$ and $\tau_{k_J}=T$. Let $k^{(bj)}=k_j-k_{j-1}+1$ represent total number of users whose initial time of the i^{th} bit interval falls in the j^{th} block, we can view the j^{th} block as an equivalent $N_j=(K+k^{(bj)})L-1$ user synchronous system with the spreading sequences for each defined as [6]

$$s_{nl}^{(bj)}(t)=$$
$$\begin{cases} s_n(t+\beta_n^{(bj)}T-\tau_n-(l-1)T_c) & n=1,\ \ldots,\ K \\ s_{n-K+k_{j-1}}(t+\beta_n^{(bj)}T-\tau_{n-K+k_{j-1}}-(l-1)T_c) & n=K+1,\ \ldots,\ K+k^{(bj)} \\ 0 & \text{otherwise} \end{cases}$$

for the period of $\tau_{k_{j-1}}\le t<\tau_{k_j}$ and $l=1,\ \ldots,\ L$. In the above equation $\beta_n^{(bj)}$, $j=1,\ \ldots,\ J$ and, $n=1,\ \ldots,\ K+k^{(bj)}$ are defined as

$$\beta_n^{(bj)} = \begin{cases} 0 & n\le k_j-1 \\ 1 & \text{otherwise.} \end{cases}$$

Also notice that in the definition of $s_{nl}^{(bj)}(t)$, $j=1,\ \ldots,\ J$, when $n=K+1$, l takes values from $(2,\ldots L)$ because for $n=K+1$, $l=1$, $s_{nl}^{(bj)}(t)=0$, thus giving a total $N_j=(K+k^{(bj)})L-1$ equivalent users for block j. The normalized spreading sequences for each equivalent user over each block can be written as $\bar{s}_{nl}^{(bj)}(t)=s_{nl}^{(bj)}(t)/\epsilon_{nl}^{(bj)}$ and the energy for each sequence $\epsilon_{nl}^{(bj)}$ is defined as

$$\epsilon_{nl}^{(bj)}=\int_0^T\left[s_{nl}^{(bj)}(t)\right]^2dt,\ j=1,\ \ldots\ J.$$

Again, in all notations the superscript $^{(bj)}$ denotes block j.

The channel fading process $c_{kl}(t)$ is assumed to be constant over one block interval but is allowed to change from one block to another according to its spaced-time correlation function. It will be assumed that the time variations of the channel

[6] Because $s_{nl}^{(bj)}(t)$,and $p_{mn}^{(bj)}$, $j=1,\ldots,J$ are bit index invariant, for simplicity $i=1$ will be chosen in their definitions below.

coefficient $c_{kl}(t)$ are such to render the piecewise constant over each block discrete time model approximation valid [7].

The correlation matrix $\boldsymbol{P}^{(bj)}$ has dimension $N_j \times N_j$, and its $(n_r, n_c)^{th}$ element, $p^{(bj)}_{n_r,n_c}$, can be calculated as

$$\begin{aligned} p^{(bj)}_{n_r,n_c} &= \int_0^T \bar{s}^{(bj)}_{n_1 l_1}(t)\bar{s}^{(bj)}_{n_2 l_2}(t)dt, \\ n_r &= (n_1 - 1)L + l_1, \\ n_c &= (n_2 - 1)L + l_2, \end{aligned}$$

where $n_1, n_2 \in (1, \ldots, N_j)$, $l_1, l_2 \in (1, \ldots, L)$ and $j = 1, \ldots, L$.

Having $\boldsymbol{P}^{(bj)}$ for each block, decorrelation can be performed on the equivalent N_j synchronous users for each block to get the MAI-, path cross-correlation interference- and ISI-free signals for all equivalent users, with the adjusted background noise due to the decorrelation. For user 1, L fingers in each block corresponding to the same information bit are available. Define the decorrelated output in each block for user 1 as

$$\begin{aligned} \boldsymbol{z}^{(b1)}(i) &= [z^{(b1)}_{11}(i), \ldots, z^{(b1)}_{1L}(i)]^T \\ &\vdots \\ \boldsymbol{z}^{(bJ)}(i) &= [z^{(bJ)}_{11}(i), \ldots, z^{(bJ)}_{1L}(i)]^T. \end{aligned}$$

The decorrelated signal for user 1 over the J blocks in the i^{th} bit interval can be written in vector form as

$$\boldsymbol{z}(i) = \begin{bmatrix} \boldsymbol{z}^{(b1)}(i) \\ \vdots \\ \boldsymbol{z}^{(bJ)}(i) \end{bmatrix} = b_1(i)\sqrt{a_1}\mathcal{E}\boldsymbol{C}(i) + \boldsymbol{\xi}(i), \tag{3.11}$$

where

$$\mathcal{E} = \text{diag}[\sqrt{\epsilon^{(b1)}_{11}}, \ldots, \sqrt{\epsilon^{(b1)}_{1L}}, \ldots, \sqrt{\epsilon^{(bJ)}_{11}}, \ldots, \sqrt{\epsilon^{(bJ)}_{1L}}]$$

[7] Compared with the symbol interval spaced discrete time realization of the time-varying channel this one is more accurate because a block interval is shorter than the bit interval.

$$= \text{diag}[\mathcal{E}^{(b1)}(i), \ \ldots, \ \mathcal{E}^{(bJ)}(i)], \tag{3.12}$$

$$\begin{aligned} \boldsymbol{C}(i) &= [c_{11}^{(b1)}(i), \ldots, c_{1L}^{(b1)}(i), \ \ldots, c_{11}^{(bJ)}(i), \ldots, c_{1L}^{(bJ)}(i)]^T \\ &= [\boldsymbol{C}^{(b1)}(i)^T, \ \ldots, \ \boldsymbol{C}^{(bJ)}(i)^T]^T, \end{aligned} \tag{3.13}$$

$$\begin{aligned} \boldsymbol{\xi}(i) &= [\xi_{11}^{(b1)}(i), \ldots, \xi_{1L}^{(b1)}(i), \ \ldots. \ \xi_{11}^{(bJ)}(i), \ldots, \xi_{1L}^{(bJ)}(i)]^T \\ &= [\boldsymbol{\xi}^{(b1)}(i)^T, \ \ldots, \ \boldsymbol{\xi}^{(bJ)}(i)^T]^T. \end{aligned} \tag{3.14}$$

In equation (3.13),

$$c_{1l}^{(bj)}(i) = c_{1l}(t)|_{t=(i-1)T+\tau_{k_j+1}}.$$

The statistics of the channel vector $\boldsymbol{C}(i)$ can be obtained from the spaced-time correlation of $c_{kl}(t)$. The covariance matrix of $\boldsymbol{C}(i)$ has a special form for our piecewise constant over each block, discrete time channel. It is convenient to define

$$\varrho_{jm} = \Phi_{1l}(|\tau_{k_j+1} - \tau_{k_m+1}|)/\Phi_{1l}(0),$$

then we can calculate

$$E[\boldsymbol{C}^{(bj)}(i)\boldsymbol{C}^{(bm)}(i)^H] = \varrho_{jm}\boldsymbol{I}_{L\times L}, \tag{3.15}$$

correspondingly, $\boldsymbol{R}_c$ can be obtained as

$$\begin{aligned} \boldsymbol{R}_c &= E\left[\boldsymbol{C}(i)\boldsymbol{C}(i)^H\right], \\ &= \begin{bmatrix} \boldsymbol{I}_{L\times L} & \varrho_{12}\boldsymbol{I}_{L\times L} & \cdots & \varrho_{1J}\boldsymbol{I}_{L\times L} \\ \varrho_{12}\boldsymbol{I}_{L\times L} & \boldsymbol{I}_{L\times L} & \cdots & \varrho_{2J}\boldsymbol{I}_{L\times L} \\ \vdots & & & \\ \varrho_{1J}\boldsymbol{I}_{L\times L} & \varrho_{2J}\boldsymbol{I}_{L\times L} & \cdots & \boldsymbol{I}_{L\times L} \end{bmatrix}. \end{aligned} \tag{3.16}$$

Partitioning $\left(\boldsymbol{P}^{(bj)}\right)^{-1}$, the inverse of the $N_j \times N_j$ cross-correlation matrix in each block, into four reduced size matrices as

$$\left(\boldsymbol{P}^{(bj)}\right)^{-1} = \begin{bmatrix} \left(\boldsymbol{P}_{i,11}^{(bj)}\right)_{L\times L} & \boldsymbol{P}_{i,12}^{(bj)} \\ \boldsymbol{P}_{i,21}^{(bj)} & \boldsymbol{P}_{i,22}^{(bj)} \end{bmatrix}, \tag{3.17}$$

the statistics of the noise vector $\boldsymbol{\xi}^{(bj)}(i)$ can be calculated as

$$E\left[\boldsymbol{\xi}^{(bj)}(i)\boldsymbol{\xi}^{(bj)}(i)^H\right] = N_0\boldsymbol{P}_{i,11}^{(bj)}, \tag{3.18}$$

where $\boldsymbol{\xi}^{(bj)}(i)$ and $\boldsymbol{\xi}^{(bm)}(i)$ are uncorrelated with each other for $j \neq m$. Correspondingly, the $JL \times JL$ covariance matrix of $\boldsymbol{\xi}(i)$ defined in (3.14) can be written as

$$\boldsymbol{R}_{\xi} = E\left[\boldsymbol{\xi}(i)\boldsymbol{\xi}(i)^{H}\right] = N_0 \text{ diag}\left[\boldsymbol{P}_{1,11}^{(b1)}, \ldots. \boldsymbol{P}_{1,11}^{(bJ)}\right]. \tag{3.19}$$

Observe that in this decorrelator structure and the desired user's signal formulation in (3.11), we discarded $l-1$ chips of energy for the l^{th} finger of user 1 in the first block over each bit interval. This discarded energy is minimal especially for small delay spread channels.

3.5 Conclusions

We proposed fractionally-spaced decorrelator for the time-varying frequency nonselective and frequency selective Rayleigh fading asynchronous CDMA channels. The proposed decorrelators are of lower complexity and have the processing latency of one bit interval; both features being achieved through fractional sampling. The matrix singularity problem is addressed and solutions to the problem are suggested. Such a realization of the decorrelator for the frequency nonselective Rayleigh fading channel in a K-user CDMA environment needs the inversion of $K \times K$ matrices only. The realization of the decorrelator for the frequency selective fading channel has the ability to eliminate MAI, ISI, and the non-zero path cross-correlation effect simultaneously. Additionally, as will be shown in the chapters hereafter, it provides the basis to achieve an effective diversity in the time-varying fading environment for a significant performance improvement.

CHAPTER 4

DIFFERENTIALLY COHERENT DETECTION FOR TIME-VARYING FREQUENCY NONSELECTIVE RAYLEIGH FADING CHANNELS

4.1 Introduction

A decorrelator used in conjunction with the differentially coherent phase shift keying (DPSK) modulation does not require channel estimates and seems to be an attractive choice for the multiuser time-varying fading environment. The effect of fading dynamics on such a receiver was given in [87]. It was shown that the error floor for a differentially coherent decorrelating detector is the same as in the case of a single-user channel. As fading rapidity increases, this error floor worsens. So the receiver in a mobile multiple access communications system suffers from both MAI and the effect of channel variation associated with the movement of the vehicle.

Following the mathematical formulation of the proposed fractionally-spaced decorrelator in Section 3.3, we will develop the differentially coherent multiuser detection scheme for the time-varying frequency nonselective Rayleigh fading CDMA channel. Multiple samples at the decorrelator output over each bit of the desired user are available, thus allowing for a maximum likelihood (ML) detection on the vector of multiple samples per bit over two consecutive bit intervals to be applied. As a result, we achieve a significant reduction in the error floor in comparison to the decorrelating detector used with conventional single sample per bit differentially coherent detection. In addition to the usual requirement for timing and signature sequences of the users, the proposed detector needs only the statistical description of the fading channel, and not the actual realizations of the fading process.

The chapter is organized as follows. The ML detection procedure, derivation of the decision variable and analytical error probability of the multiuser detector are presented in Section 4.2. Numerical examples and their interpretations are provided in Section 4.3.

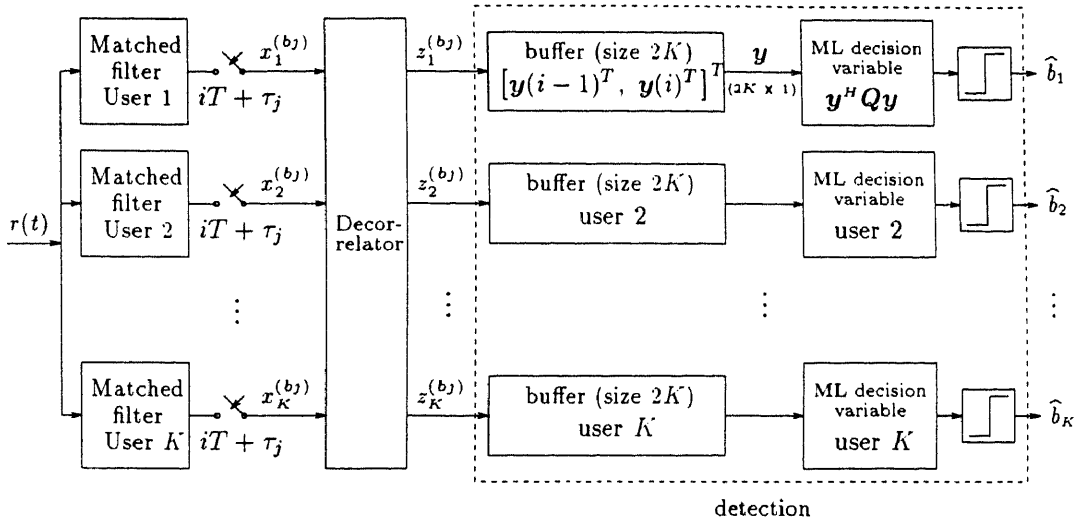

Figure 4.1 The fractionally-spaced DPSK multiuser detector

4.2 Detector Structure

The proposed multiuser detector has a bank of K matched filters as its front end, with each filter matched to the user's signature sequence $s_k(t)$. It will be assumed that the time variations of the channel coefficient $c_k(t)$ are such to render the piecewise constant discrete time model approximation valid. The detection structure is shown in Fig. 4.1. Its front end includes the decorrelator proposed in Section 3.3 and the detection procedure is described in the following subsection.

4.2.1 Detection Procedure

The $2K$-sample snapshot of decorrelated outputs in (3.8) over two adjacent symbol intervals $(i-1)$ and i, which will be used to detect the i^{th} information bit of the desired user[1], can be written in a $2K \times 1$ vector as

$$\begin{aligned} \boldsymbol{y} &= [z_1^{(b1)}(i-1),\ \ldots,\ z_1^{(bK)}(i-1), z_1^{(b1)}(i),\ \ldots,\ z_1^{(bK)}(i)]^T \\ &= [\boldsymbol{y}(i-1)^T,\ \boldsymbol{y}(i)^T]^T \\ &= \sqrt{a_1}\boldsymbol{B}_1\ \mathcal{E}_1\boldsymbol{C}_1 + \boldsymbol{\xi}_1, \end{aligned} \tag{4.1}$$

[1]The decorrelated outputs can be obtained for all K users, but performance analysis of user 1, without loss of generality, will only be considered.

where

$$\begin{aligned}
\boldsymbol{B}_1 &= \mathrm{diag}[\underbrace{b_1(i-1),\ldots,b_1(i-1)}_{K},\ \underbrace{b_1(i),\ldots,b_1(i)}_{K}] \\
&= \mathrm{diag}[\boldsymbol{B}_1(i-1),\ \boldsymbol{B}_1(i)], \\
\mathcal{E}_1 &= \mathrm{diag}[\sqrt{\epsilon^{(b1)}},\ldots,\sqrt{\epsilon^{(bK)}},\ \sqrt{\epsilon^{(b1)}},\ldots,\sqrt{\epsilon^{(bK)}}] \\
&= \mathrm{diag}[\mathcal{E}_1(i),\ \mathcal{E}_1(i)], \\
\boldsymbol{C}_1 &= [c_1^{(b1)}(i-1),\ldots,c_1^{(bK)}(i-1),\ c_1^{(b1)}(i),\ldots,c_1^{(bK)}(i)]^T \\
&= [\boldsymbol{C}_1(i-1)^T,\ \boldsymbol{C}_1(i)^T]^T, \\
\boldsymbol{\xi}_1 &= [\xi_1^{(b1)}(i-1),\ldots,\xi_1^{(bK)}(i-1),\ \xi_1^{(b1)}(i),\ldots,\xi_1^{(bK)}(i)]^T \\
&= [\boldsymbol{\xi}_1(i-1)^T,\ \boldsymbol{\xi}_1(i)^T]^T.
\end{aligned}$$

Once $\boldsymbol{y}$, the multiuser interference-free signal over a two-symbol period, is obtained, the detection approach of [7] can be applied. The $2K \times 2K$ covariance matrix of $\boldsymbol{y}$ is

$$\begin{aligned}
\boldsymbol{R}_y &= E\{\boldsymbol{y}\boldsymbol{y}^H\} \\
&= E\{a_1\boldsymbol{B}_1\mathcal{E}_1\boldsymbol{C}_1\boldsymbol{C}_1^H\mathcal{E}_1^H\boldsymbol{B}_1^H\} + E\{\boldsymbol{\xi}_1\boldsymbol{\xi}_1^H\} \\
&= a_1\boldsymbol{B}_1\mathcal{E}_1\boldsymbol{R}_{c_1}\mathcal{E}_1^H\boldsymbol{B}_1^H + \boldsymbol{R}_{\xi_1}, \qquad (4.2)
\end{aligned}$$

where

$$\boldsymbol{R}_{c_1} = E\{C_1C_1^H\}$$

is the covariance matrix of the fading process at the decorrelator output, and

$$\boldsymbol{R}_{\xi_1} = E\{\boldsymbol{\xi}_1\boldsymbol{\xi}_1^H\} = N_0\boldsymbol{F}_1$$

is the additive noise covariance matrix at the decorrelator output. In the above equation,

$$\begin{aligned}
\boldsymbol{F}_1 &= \mathrm{diag}[F_1^{(b1)},\ \ldots,\ F_1^{(bK)},\ F_1^{(b1)},\ \ldots,\ F_1^{(bK)}] \\
&= \mathrm{diag}[\boldsymbol{F}_1(i)^T,\ \boldsymbol{F}_1(i)^T] \qquad (4.3)
\end{aligned}$$

accounts for the noise enhancement in $2K$ blocks over symbols $(i-1)$ and i due to decorrelation, and $F_1^{(bj)} = (\boldsymbol{P}^{(bj)})^{-1}_{1,1}$ $j = 1, \ldots, K$ is the $(1,1)^{st}$ element of the matrix $(\boldsymbol{P}^{(bj)})^{-1}$.

Because we assumed that the fading process is wide-sense stationary and normalized, $\boldsymbol{R}_{c_1}$ is Hermitian and positive semi-definite with diagonal elements equal to one.

The decorrelator output vector $\boldsymbol{z}_1$ being the sum of two independent complex Gaussian random vectors (due to the Rayleigh type of fading), has a $2K$-variate complex Gaussian distribution [3], [7]

$$p(\boldsymbol{y}) = \frac{1}{\pi^{2K}|\boldsymbol{R}_y|} e^{-\boldsymbol{y}^H \boldsymbol{R}_y^{-1} \boldsymbol{y}}, \tag{4.4}$$

where $|\boldsymbol{R}_y|$ is the determinant of $\boldsymbol{R}_y$.

Let hypothesis "H_1" correspond to transmitting the information bit 1, i.e., pairs of differentially encoded symbols $(-1, -1)$ or $(1, 1)$ over two consecutive symbol intervals, and let hypothesis "H_0" correspond to transmitting the information bit -1. The likelihood ratio can be written as

$$\Lambda(\boldsymbol{y}) = \frac{p(\boldsymbol{y}|H_1)}{p(\boldsymbol{y}|H_0)} = \frac{\frac{1}{\pi^{2K}|\boldsymbol{R}_{y(1)}|} e^{-\boldsymbol{y}^H \boldsymbol{R}_{y(1)}^{-1} \boldsymbol{y}}}{\frac{1}{\pi^{2K}|\boldsymbol{R}_{y(-1)}|} e^{-\boldsymbol{y}^H \boldsymbol{R}_{y(-1)}^{-1} \boldsymbol{y}}}, \tag{4.5}$$

where $\boldsymbol{R}_{y(1)}$ and $\boldsymbol{R}_{y(-1)}$ are the covariance matrices of $\boldsymbol{y}$ corresponding to transmitted information bits 1 and -1, respectively. These covariance matrices can be written as

$$\boldsymbol{R}_{y(1)} = \mathcal{E}_1 \boldsymbol{R}_{c_1} \mathcal{E}_1^H + \boldsymbol{R}_{\xi_1} = \boldsymbol{R} \tag{4.6}$$

$$\boldsymbol{R}_{y(-1)} = (\mathcal{E}_1 \boldsymbol{R}_{c_1} \mathcal{E}_1^H + \boldsymbol{R}_{\xi_1}) \bigotimes \begin{bmatrix} \mathbf{1} & -\mathbf{1} \\ -\mathbf{1} & \mathbf{1} \end{bmatrix}. \tag{4.7}$$

In equation (4.7), $\mathbf{1}$ is a $K \times K$ square matrix with all elements equal to 1, and $\bigotimes$ stands for the Hadamard product, giving element by element multiplication. The maximum *a posteriori* (MAP) decision rule can be formulated as

$$\Lambda(\boldsymbol{y}) \underset{H_0}{\overset{H_1}{\gtrless}} \frac{\Pr(H_0)}{\Pr(H_1)}. \tag{4.8}$$

Assuming equally likely information bits, the determinant of $\boldsymbol{R}_y$ doesn't depend on the sign of the transmitted bit. By taking the logarithm of both sides of (4.8), the decision statistics for the i^{th} information bit can be expressed as

$$\lambda_i = \boldsymbol{y}^H(\boldsymbol{R}_{y(-1)}^{-1} - \boldsymbol{R}_{y(1)}^{-1})\boldsymbol{y} = \boldsymbol{y}^H\boldsymbol{Q}\boldsymbol{y}. \tag{4.9}$$

The decision rule is thus

$$\lambda_i \begin{cases} > 0 & \text{decide "1"} \\ < 0 & \text{decide "}-1\text{"}. \end{cases}$$

4.2.2 Error Performance Analysis

A transformation, as done in [56] and [7], can be performed on the quadratic form of the decision variable in (4.9). The details of the derivation are shown in the Appendix A, where the decision variable in (A.1) is reduced to a diagonal Hermitian form with independent variates. Specifically, there exists a linear transformation $\boldsymbol{w} = \boldsymbol{T}\boldsymbol{S}$, such that

$$\lambda_i = d_1(i)\boldsymbol{w}^H\boldsymbol{\Gamma}\boldsymbol{w}, \tag{4.10}$$

where $d_1(i)$ is the i^{th} information bit of user 1 before differential encoding, i.e., $d_1(i) = b_1(i)b_1(i-1)$, and $\boldsymbol{w} = [w_1 \ \ldots \ w_{2K}]^T$ is a complex Gaussian random vector with unit variance and independent elements, i.e., $E\{\boldsymbol{w}\boldsymbol{w}^H\} = \boldsymbol{I}$, with $\boldsymbol{I}$ being the unit matrix, and

$$\boldsymbol{\Gamma} = \text{diag}[\gamma_1, \ \ldots, \ \gamma_{2K}],$$

where γ_u, $k = 1, \ \ldots, \ 2K$ are the eigenvalues of the $2K \times 2K$ matrix $\boldsymbol{R}\boldsymbol{Q}$. Without loss of generality, we assume $d_1(i) = 1$ when performing error performance analysis of the detector. The characteristic function of the quadratic form in (4.10) for this case is

$$\psi_\lambda(j\omega) = \frac{1}{\det(\boldsymbol{I} - j\omega\boldsymbol{\Gamma})} = \prod_{u=1}^{2K} \frac{1}{1 - j\omega\gamma_u} = \sum_{u=1}^{2K} \frac{\beta_u}{1 - j\omega\gamma_u}, \tag{4.11}$$

where β_u are the coefficients of the partial fraction expansion of $\psi_\lambda(j\omega)$, i.e.,

$$\beta_u = \prod_{\substack{v=1 \\ v \neq u}}^{2K} \frac{\gamma_u}{\gamma_u - \gamma_v}.$$

In the case of distinct nonzero eigenvalues (which occurs in situations of practical interest), the probability of error of this quadratic form is given by [3] [92]

$$P_e = P\{\lambda_i < 0\} = \sum_{\gamma_u < 0} \beta_u = \sum_{\gamma_u < 0} \prod_{\substack{v=1 \\ v \neq u}}^{2K} \frac{\gamma_u}{\gamma_u - \gamma_v}. \tag{4.12}$$

4.3 Numerical Examples and Discussion

As mentioned in Section 3.3, the piece-wise constant representation of the fading process in each block of time exhibits nonuniformity along the time axis. For convenience, in our numerical examples the blocks of time were chosen as integer multiples of the chip period T_c.

In all our simulations, the channel fading process is generated in a discrete-time form according to the specific spaced-time correlation function. It is well known that the first-order Markov type of fading process can be generated in a recursive way as

$$c_k((n+1)T_c) = \varrho' c_k(nT_c) + \chi(nT_c),$$

where the correlation parameter ϱ' in the above recursion was modified as $\varrho' = \varrho^{\frac{T_c}{T}}$, and $\chi(nT_c)$ is a zero-mean complex Gaussian random variable with the variance $1 - \varrho'^2$. The elements of the vector of channel coefficients C_1 in (4.1) are the values at the time instants corresponding to the users' relative delays.

The channel fading process whose spaced-time correlation is modeled by Jakes' model in (3.5) is generated the same way as described in [24]. The fading process is

$$c(t) = \frac{C_0}{\sqrt{2S_0 + 1}} \left[X_c(t) + jX_s(t)\right],$$

where

$$X_c(t) = 2\sum_{n=1}^{S_0} \left[cos(\phi_n)cos(\omega_n t)\right] + \sqrt{2}cos(\phi_N)cos(\omega_m t),$$

$$X_s(t) = 2\sum_{n=1}^{S_0}[sin(\phi_n)cos(\omega_n t)] + \sqrt{2}sin(\phi_N)cos(\omega_m t).$$

In the above equations, S_0 is the total number of sinusoids [2], and

$$\omega_m = 2\pi f_d,$$
$$\omega_n = \omega_m cos(2\pi n/S).$$

The relationship between S and S_0 is $S = 2(2S_0 + 1)$, and we use $S_0 = 16$ sinusoids for our simulation. Other values of parameters we used are $\phi_S = 0$, $\phi_n = \pi n/(S_0 + 1)$ and $C_0 = 1$ to satisfy the normalized channel fading process assumption. The corresponding statistics of $X_c(t)$, $X_s(t)$ and $c(t)$ are

$$E\{X_c^2(t)\} = S_0,$$
$$E\{X_s^2(t)\} = S_0 + 1,$$
$$E\{|c(t)|^2\} = C_0 = 1.$$

The elements of the vector of channel coefficients $\boldsymbol{C}_1$ in (4.1) for Jakes' model are the values at the time instants corresponding to the users' relative delays.

A three-user scenario with signature waveforms chosen from Gold sequences of length 31 assigned to each of them was considered. In the examples presented the relative delays were set at $\tau_1 = 0$, $\tau_2 = \frac{3}{31}T$, and $\tau_3 = \frac{15}{31}T$, resulting in the following value of the corresponding noise enhancement matrix in (4.3): $\boldsymbol{F}_1 = \text{diag}[1.5\ 1.0345\ 1.1852\ 1.5\ 1.0345\ 1.1852]$. With the previous assumption of $E\{|c_k|^2\} = 1$, the signal to noise ratio for user 1 was defined as $SNR_1 = a_1/N_0$.

The error performance of the proposed detector is compared to that of the conventional DPSK receiver in a single-user environment that utilizes one sample per symbol. Fig. 4.2 provides the performance comparison for the channel modeled by the first-order Markov process. The fading rates $f_dT = 0.04$ and $f_dT = 0.08$

[2] Jakes suggests that $S_0 = 8$ sinusoids will give a pretty good approximation.

in (3.4) were chosen, and for both fading rates the proposed detector demonstrates clear superiority by significantly lowering the error floor. In Fig. 4.3 the Jakes model with $f_dT = 0.08$ and $f_dT = 0.16$ in (3.5) was employed for the same SNR range used with the previous model, but the error floor did not appear. In both fading channel models the theoretical curves were, as much as it was feasible, confirmed by simulation.

To assess the reasons for the performance improvement of the proposed detector, (4.10) is rewritten as

$$\lambda_i = d_1(i) \sum_{u=1}^{2K} \gamma_u |w_u|^2 = d_1(i) \sum_{u=1}^{2K} \gamma_u \alpha_u. \tag{4.13}$$

Because $\boldsymbol{w}$ is a complex Gaussian random vector with independent elements w_k, α_k, $k = 1, \ldots, 2K$, are i.i.d. random variables with a chi-square distribution. The form of equation (4.12) bears similarity to the analysis of a single user diversity reception in nonselective Rayleigh fading (Ch. 11 in [56]). In the proposed scheme the decision process involves $2K$ random variables, each corresponding to the same information bit, albeit with a lowered SNR in each block. For a fading process with $\varrho < 1$ (i.e., one that is not completely correlated), the receiver's structure may be considered as one that explores a form of time diversity. One can also invoke the explanation for the performance improvement given in [7] wherein the receiver, by applying the maximum likelihood principle on the fractionally sampled data, effectively increases the correlation in the fading process, resulting in the lowered error floor.

With the proposed detector, fractionally sampled matched filter outputs of the received multiuser signal are utilized for a dual benefit. Besides providing the basis for ML detection to lower the error floor, fractional sampling also provides the means for realizing a lower complexity bit-by-bit decorrelator, which requires inversion of $K \times K$ matrices only. The number of samples per symbol is implied by the number

of users for our analysis performed before, however, it could be a design parameter in principle as was discussed in Section 3.3.

It was observed that the variation of the distribution of the users' relative delays does not appear to affect the performance when the Jakes model is used, while much greater sensitivity resulted with the first-order Markov model.

In the example in Fig. 4.3 the proposed detector did not exhibit the error floor within the specified range of SNR values. [3] In order to provide an intuitive and yet quantitative explanation of the displayed behavior, we analyze the nonzero eigenvalues of matrix $\boldsymbol{RQ}$, which depend, among other parameters, on the fading rate. It can be observed from (4.13) that if information bit +1 is transmitted, a decision error is made if the sum of the negative eigenvalues exceeds the sum of the positive ones. For the fading rates of interest, numerical examples suggest that there is a dominant positive eigenvalue for both fading models, and a dominant negative (in absolute value) eigenvalue for the first-order Markov model. Plots of the ratio of the absolute values of the largest positive and negative eigenvalues vs. the SNR are shown in Figs. 4.4 and 4.6 for the same fading rates used in our numerical examples. The SNR value at which the eigenvalue ratio flattens out can serve as a rough estimate of the SNR at which the probability of error curve does the same, i.e., where the error floor is exhibited. Figs. 4.5 and 4.7 show the corresponding analytical error performance curves for both models, over a wide range of SNR values. The respective error floors for both fading rates appear at approximately 30 dB and 35 dB for the first order Markov model and at approximately 110 dB and 140 dB for Jakes' model, as suggested by Figs. 4.4 and 4.6.

[3] A higher value of f_dT, which would certainly cause the error floor to appear at more "reasonable" SNR values, would preclude obtaining matched filter outputs in the form given in (3.6).

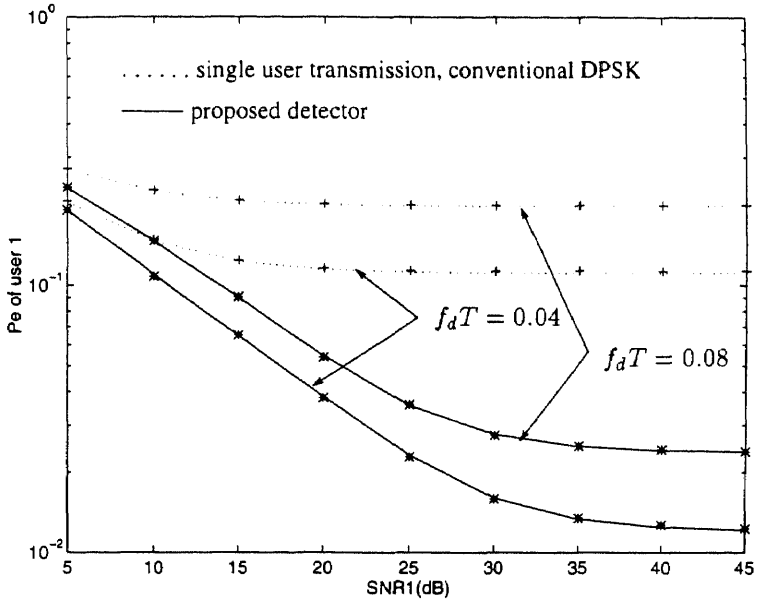

Figure 4.2 Analytical and simulated ($* * *$) error performance with first-order Markov model

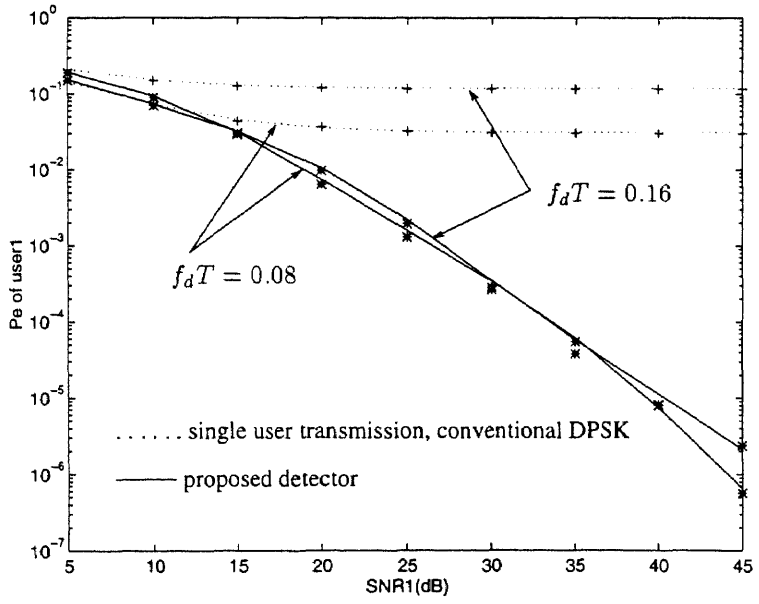

Figure 4.3 Analytical and simulated ($* * *$) error performance with Jakes model

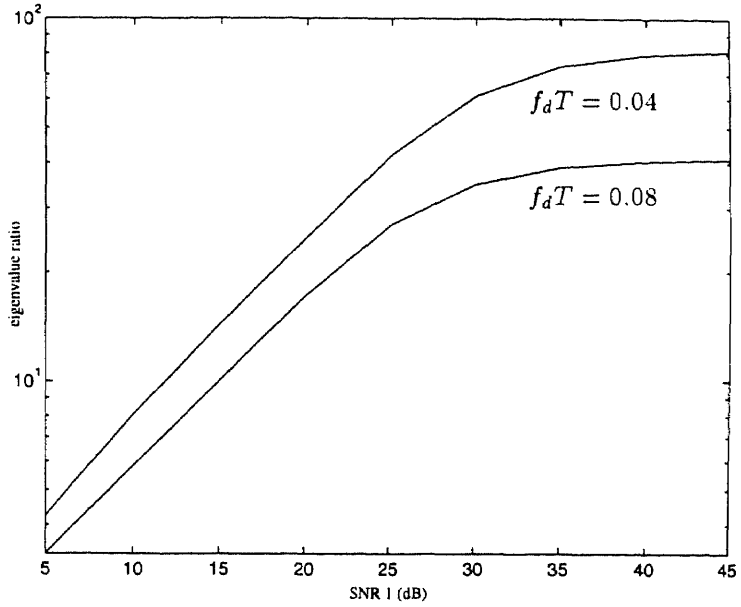

Figure 4.4 Eigenvalue ratio with first-order Markov model

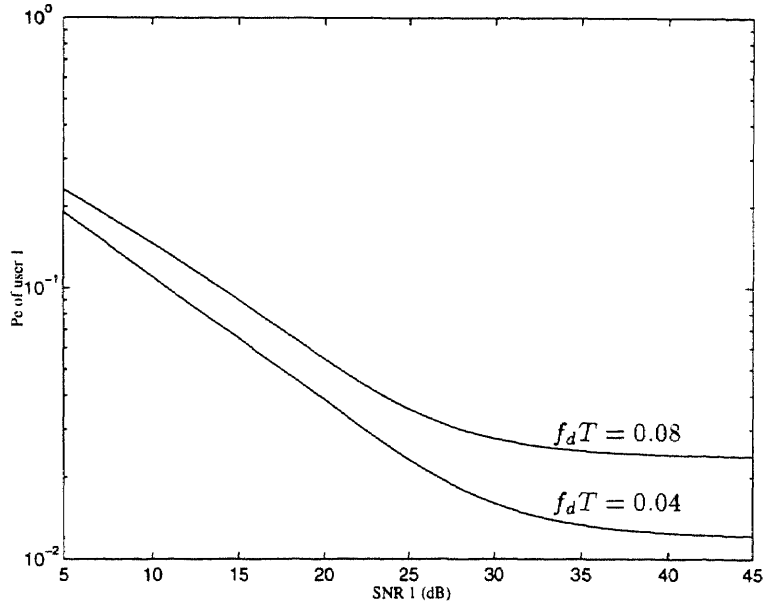

Figure 4.5 Analytical error performance with first-order Markov model over wide range of SNR values

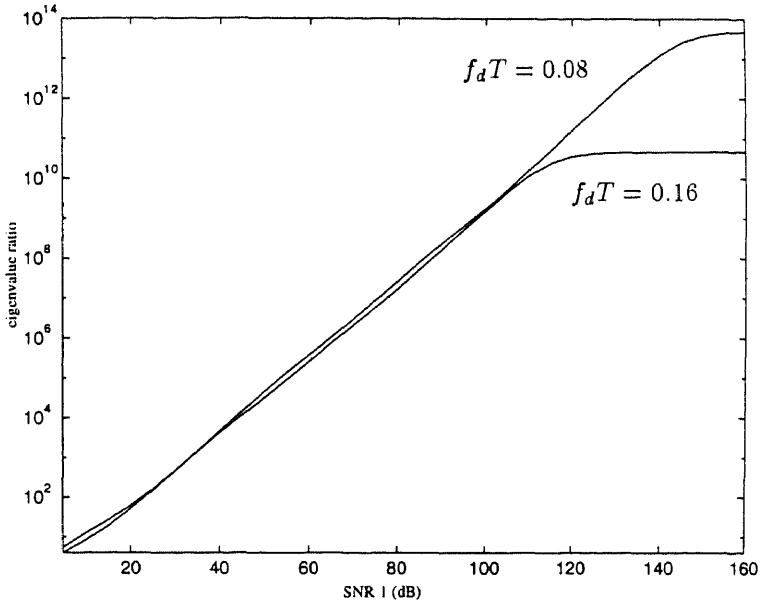

Figure 4.6 Eigenvalue ratio with Jakes model

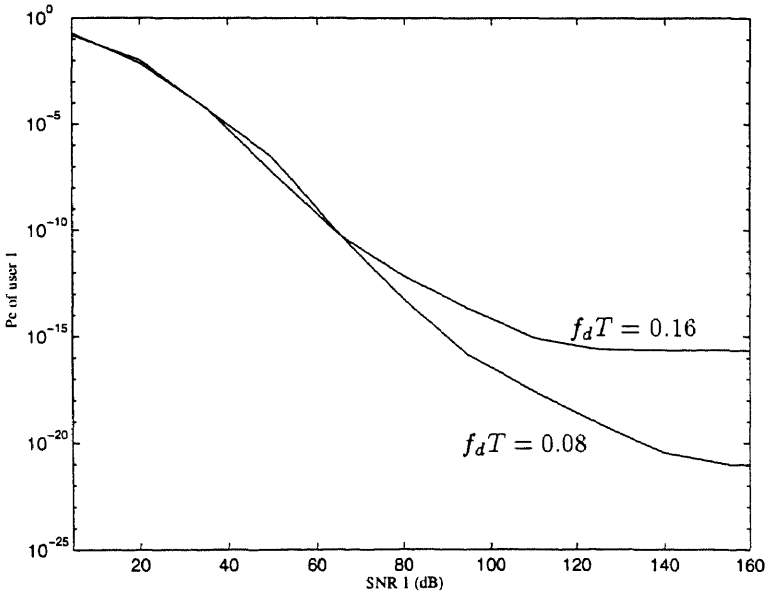

Figure 4.7 Analytical error performance with Jakes model over wide range of SNR values

CHAPTER 5

COHERENT DETECTION FOR TIME-VARYING FREQUENCY NONSELECTIVE RAYLEIGH FADING CHANNELS

5.1 Introduction

It is well known that DPSK is not as power efficient as BPSK, but it provides a simple and robust detector because no carrier recovery is necessary. Error floor is a shortcoming of DPSK for the conventional differential detection, but from the analysis and the examples given in Chapter 4, we demonstrated that a carefully designed DPSK receiver can have significantly lowered error floor even when the channel exhibits fairly fast fading. It is our belief that if a good carrier recovery algorithm is available, a fractionally spaced coherent multiuser detection will give a better performance than the fractionally spaced differentially coherent multiuser detection proposed in the Chapter 4.

In this chapter, we propose and analyze a coherent multiuser detector for an asynchronous CDMA single-path time-varying Rayleigh fading channel. The fractionally spaced decorrelator is realized the same way as presented in Section 3.3. Effective diversity implicit in a time-varying fading channel is achieved by applying a maximum ratio combining (MRC) rule on the decorrelated signal vector of the desired user. A decision feedback MAP channel estimation method is proposed for this detector structure for coherent detection. In contrast to the Kalman filter which can be implemented as the optimal decision feedback MMSE channel estimator for fading processes of the Markovian type only, this MAP channel estimator is universally applicable for Rayleigh fading channels with an arbitrary spaced-time correlation function model.

This chapter is organized as follows. By employing the decorrelator structure described in Section 3.3, the coherent detection procedure with perfect channel estimates and its error performance analysis are presented in Section 5.2. In Section

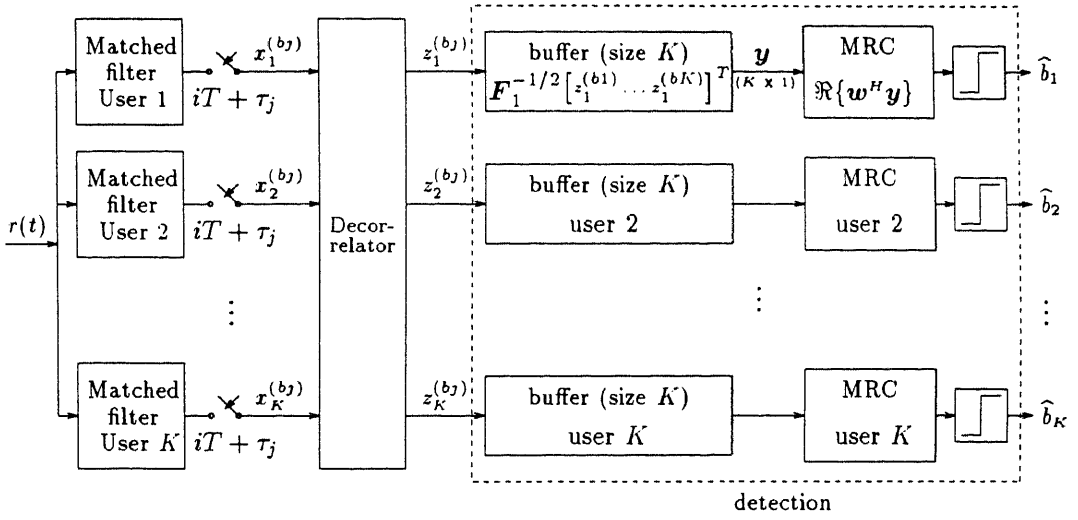

Figure 5.1 The coherent multiuser detector with perfect channel estimates

5.3.1, we derive a single-stage and a two-stage decision feedback MAP channel estimator. Then in Section 5.4, coherent detection with the adaptive channel estimates is given, and analytical error performance for this detector structure with adaptive channel estimates is also given. In Section 5.5, numerical examples are presented for coherent detection with both perfect channel estimates and adaptive channel estimates. In order to compare the performance of the differentially coherent detector proposed in the previous chapter and the coherent detector with differential encoding utilizing adaptive channel estimates, numerical results for both schemes are presented in this Section.

5.2 Coherent Detection with Perfect Channel Estimates

The received baseband equivalent signal $r(t)$ for the K-user asynchronous CDMA Rayleigh fading channel is the same as in (3.1). The whole detection procedure of the coherent detector with perfect channel estimates is shown in 5.1, and its mathematical formulation is given as following.

Following the bit-by-bit fractionally sampled decorrelator structure proposed in Section 3.3 and the decorrelated output in each block in (3.8), the K-sample snapshot of decorrelated outputs for the desired user over the i^{th} bit interval can then be written in vector form as

$$\boldsymbol{z}_1 = [z_1^{(b1)}(i),\ \ldots,\ z_1^{(bK)}(i)]^T = \sqrt{a_1}\mathcal{E}_1\boldsymbol{C}_1 b_1 + \boldsymbol{\xi}_1, \tag{5.1}$$

where

$$\begin{aligned}
\mathcal{E}_1 &= [\sqrt{\epsilon^{(b1)}}, \ldots, \sqrt{\epsilon^{(bK)}}]^T \\
\boldsymbol{C}_1 &= [c_1^{(b1)}(i), \ldots, c_1^{(bK)}(i)]^T \\
\boldsymbol{\xi}_1 &= [\xi_1^{(b1)}(i), \ldots, \xi_1^{(bK)}(i)]^T.
\end{aligned}$$

The covariance matrix of $\boldsymbol{\xi}_1$ is

$$\boldsymbol{R}_{\xi_1} = E\{\boldsymbol{\xi}_1\boldsymbol{\xi}_1^H\} = N_0\boldsymbol{F}_1, \tag{5.2}$$

where matrix $\boldsymbol{F}_1$ accounts for noise enhancement in each block over one bit interval of user 1, and can be obtained as

$$\begin{aligned}
\boldsymbol{F}_1 &= \mathrm{diag}[F_1^{(b1)},\ \ldots,\ F_1^{(bK)}] \\
&= \mathrm{diag}[(\boldsymbol{P}^{(b1)})_{(1,1)}^{-1},\ \ldots,\ (\boldsymbol{P}^{(bK)})_{(1.1)}^{-1}],
\end{aligned} \tag{5.3}$$

in which $(\boldsymbol{P}^{(bj)})_{(1,1)}^{-1}$, $j = 1, \ldots, K$ stands for the $(1,1)^{st}$ element of $(\boldsymbol{P}^{(bj)})^{-1}$, the inverse code correlation matrix for the j^{th} block derived in Section 3.3. Each element of $\boldsymbol{F}_1$ is always finite and greater than 1 if $\boldsymbol{P}^{(bj)}$, $j = 1,\ \ldots,\ K$ are not singular, so $\boldsymbol{F}_1^{-1/2}$ can be used to normalize the noise vector $\boldsymbol{\xi}_1$. Define

$$\begin{aligned}
\boldsymbol{y} &= \boldsymbol{F}_1^{-1/2}\boldsymbol{z}_1 \\
&= \sqrt{a_1}\boldsymbol{F}_1^{-1/2}\mathcal{E}_1\boldsymbol{C}_1 b_1 + \boldsymbol{F}_1^{-1/2}\boldsymbol{\xi}_1 \\
&= \sqrt{a_1}\boldsymbol{w} b_1 + \boldsymbol{\zeta},
\end{aligned} \tag{5.4}$$

where $\boldsymbol{w} = \boldsymbol{F}_1^{-1/2}\mathcal{E}_1\boldsymbol{C}_1$ stands for the equivalent channel vector which is obtained from the actual channel vector $\boldsymbol{C}_1$, adjusted by energy in each block and noise enhancement due to decorrelation over one bit interval. It is easy to show that

$$E\{\zeta\zeta^H\} = N_0\boldsymbol{I}, \tag{5.5}$$

where $\boldsymbol{I}$ is the $K \times K$ identity matrix, indicating that the noise components in (5.4) are mutually independent. Assuming the availability of the channel vector $\boldsymbol{w}$ (or $\boldsymbol{C}_1$), the detection can be done by using the maximum ratio combining (MRC) on the elements of $\boldsymbol{y}$ [56] [54]. The decision variable can thus be written as

$$\lambda_i = \Re\{\boldsymbol{w}^H\boldsymbol{y}\}. \tag{5.6}$$

Error performance analysis for this detector is similar to that of the quadratic receivers [3]. Introducing a $2K \times 1$ vector

$$\boldsymbol{v} = \begin{bmatrix} \boldsymbol{w} \\ \boldsymbol{y} \end{bmatrix},$$

the decision variable in (5.6) can be reformulated as

$$\begin{aligned} \lambda_i &= \begin{bmatrix} \boldsymbol{w} \\ \boldsymbol{y} \end{bmatrix}^H \begin{bmatrix} \mathbf{o} & 0.5\boldsymbol{I} \\ 0.5\boldsymbol{I} & \mathbf{o} \end{bmatrix} \begin{bmatrix} \boldsymbol{w} \\ \boldsymbol{y} \end{bmatrix} \\ &= \boldsymbol{v}^H\boldsymbol{Q}\boldsymbol{v}, \end{aligned} \tag{5.7}$$

where $\mathbf{o}$ is a $K \times K$ matrix with all elements equal to zero. The $2K \times 2K$ covariance matrix of $\boldsymbol{v}$ can be obtained as

$$\begin{aligned} \boldsymbol{V} &= E\{\boldsymbol{v}\boldsymbol{v}^H\} \\ &= E\left\{\begin{bmatrix} \boldsymbol{w} \\ \boldsymbol{y} \end{bmatrix}[\boldsymbol{w}^H\boldsymbol{y}^H]\right\} \\ &= E\begin{Bmatrix} \boldsymbol{w}\boldsymbol{w}^H & \boldsymbol{w}\boldsymbol{y}^H \\ \boldsymbol{y}\boldsymbol{w}^H & \boldsymbol{y}\boldsymbol{y}^H \end{Bmatrix}, \end{aligned} \tag{5.8}$$

and the $2K \times 2K$ matrix $\boldsymbol{V}\boldsymbol{Q}$ can be calculated as

$$\begin{aligned} \boldsymbol{V}\boldsymbol{Q} &= 0.5E\begin{Bmatrix} \boldsymbol{w}\boldsymbol{y}^H & \boldsymbol{w}\boldsymbol{w}^H \\ \boldsymbol{y}\boldsymbol{y}^H & \boldsymbol{y}\boldsymbol{w}^H \end{Bmatrix} \\ &= 0.5\begin{bmatrix} \sqrt{a_1}\boldsymbol{R}_w & \boldsymbol{R}_w \\ a_1\boldsymbol{R}_w + N_0\boldsymbol{I} & \sqrt{a_1}\boldsymbol{R}_w \end{bmatrix}. \end{aligned}$$

In the above equation $\boldsymbol{R}_w$ can be obtained from the channel covariance matrix $\boldsymbol{R}_{c_1}$, the energy in each block $\mathcal{E}_1$, and the noise enhancement matrix $\boldsymbol{F}_1$, as

$$\boldsymbol{R}_w = \boldsymbol{F}_1^{-1/2} \mathcal{E}_1 \boldsymbol{R}_{c_1} \mathcal{E}_1 \boldsymbol{F}_1^{-1/2}.$$

The probability of error of the quadratic decision variable in (5.7) is the one given in [3]

$$P_e = P\{\lambda_i < 0\} = \sum_{\gamma_l < 0} \prod_{\substack{m=1 \\ m \neq l}}^{2K} \frac{\gamma_l}{\gamma_l - \gamma_m}, \tag{5.9}$$

in which $\gamma_1, \ldots, \gamma_{2K}$ are the eigenvalues of the matrix $\boldsymbol{VQ}$.

The error performance in (5.9) is the ultimate performance lower bound of this fractionally spaced coherent multiuser detector assuming the availability of the channel vector $\boldsymbol{w}(i)$. In practice, however, $\boldsymbol{w}(i)$ has to be estimated before detection of $b_1(i)$. We therefore propose a coherent detector and analyze its performance assuming that we have no other methods, like pilot tone or pilot symbol, to assist in channel estimation, so we have to use decision feedback to provide channel estimates.

5.3 DF MAP Estimator for Statistically Known Channels

In this section we derive a fractionally sampled decision feedback MAP channel estimator in a single user transmission scenario. This estimator, however, can be applied to our coherent multiuser detector directly because the decorrelator outputs for the desired user is the same as a single user transmission except for the enhanced noise due to decorrelation. A single-stage DF MAP channel estimator is proposed first, then a two-stage channel estimator is derived for better channel estimation, although we will use the single-stage channel estimates for coherent detection.

5.3.1 Single-Stage Estimator

The received baseband equivalent complex signal $r(t)$ in a single path Rayleigh fading channel is expressed as

$$r(t) = \sum_i \sqrt{a} b(i) s(t - iT) c(t) + \xi(t), \tag{5.10}$$

where a, $b(i) \in \{-1, 1\}$, $s(t)$, and $\xi(t)$ denote bit energy, the information bit, a waveform of duration T with energy normalized to unity, and an additive, zero-mean, complex white Gaussian noise with the one-sided power spectral density N_0, respectively. The fading channel process $c(t)$ is modeled as a normalized, zero-mean complex-valued wide-sense stationary Gaussian process with a known spaced-time correlation function. We obtain K samples at the matched filter output at time instants $(i-1)T + \tau_1, \ldots, (i-1)T + \tau_K$ over the i^{th} bit interval [1]. A K-sample snapshot of the received signal over the i^{th} bit interval can be written in a vector form as

$$\begin{aligned} \boldsymbol{y}(i) &= [r^{(1)}(i), \ldots, r^{(K)}(i)]^T \\ &= \sqrt{a}\mathcal{E}\boldsymbol{C}(i)b(i) + \boldsymbol{\xi}(i), \end{aligned} \tag{5.11}$$

where

$$\begin{aligned} \mathcal{E} &= \mathrm{diag}[\sqrt{\epsilon^{(1)}}, \ldots, \sqrt{\epsilon^{(k)}}] \\ \boldsymbol{C}(i) &= [c^{(1)}(i), \ldots, c^{(K)}(i)]^T \\ &= [c(t)|_{t=(i-1)T+\tau_1}, \ldots, c(t)|_{t=(i-1)T+\tau_K}]^T \\ \boldsymbol{\xi}(i) &= [\xi^{(1)}(i), \ldots, \xi^{(K)}(i)]^T \end{aligned}$$

[1] The time instants are not necessarily to be uniformly distributed over the i^{th} bit interval, but it is required that $0 = \tau_0 < \tau_1 < \ldots < \tau_K = T$. Also notice the difference of the definition of τ_j here and that in the multiuser asynchronous communication scenario which for the latter represents the relative delays of each user with $\tau_1 = 0$ assumed.

represent signal energy matrix, channel vector and noise vector for each sample, respectively. In (5.11) we adopted a discrete-time fading channel formulation, specifically, the channel is assumed to be constant during one sample interval, but allowed to change from one sample to another.

The actual realization of this oversampling scheme can be achieved by an integrate-and-dump operation. Mathematically, it can be realized the same way as described in Section 3.3 for the fractionally-spaced decorrelator output by defining

$$\begin{aligned} s^{(j)}(t) &= \begin{cases} s(t) & \tau_{j-1} < t < \tau_j \\ 0 & \text{otherwise} \end{cases}, \\ \epsilon^{(j)} &= \int_{\tau_{j-1}}^{\tau_j} s^2(t)dt = \int_0^T \left[s^{(j)}(t)\right]^2 dt, \\ \overline{s}^{(j)}(t) &= s^{(j)}(t)/\sqrt{\epsilon^{(j)}}. \end{aligned}$$

Let $\boldsymbol{w}(i) = \mathcal{E}\boldsymbol{C}(i)$, which represents the equivalent channel vector obtained from the actual channel vector $\boldsymbol{C}(i)$, and adjusted by energy contained in each sample. Then (5.11) can be re-written as

$$\boldsymbol{y}(i) = \sqrt{a}\boldsymbol{w}(i)b(i) + \boldsymbol{\xi}(i). \tag{5.12}$$

The covariance matrix of $\boldsymbol{\xi}(i)$ is

$$\boldsymbol{R}_\xi = E\{\boldsymbol{\xi}(i)\boldsymbol{\xi}(i)^H\} = N_0\boldsymbol{I}, \tag{5.13}$$

where $\boldsymbol{I}$ is a $K \times K$ identity matrix. Define the $MK \times 1$ vector

$$\mathcal{Y}_{i-1} = [\tilde{\boldsymbol{y}}(i-M)^T\ \tilde{\boldsymbol{y}}(i-M+1)^T\ \ldots\ \tilde{\boldsymbol{y}}(i-1)^T]^T, \tag{5.14}$$

where $\tilde{\boldsymbol{y}}(i-m) = \boldsymbol{y}(i-m)\hat{b}(i-m)$, $m = 1, \ldots, M$, and $\hat{b}(i-m)$ is the decision on the information bit $b(i-m)$. $\mathcal{Y}_{i-1}$ stands for the received signal vector over $(i-M)^{th}$ to $(i-1)^{th}$ bit intervals with the information bit removed [2]. Also, define

[2] Because the information bit removal is achieved by using the corresponding bit decision, if a decision error happens, the removed information bit is not correct. However, for a reliable communication, the bit error rate is usually very small, making the decision error effect very small.

the $(M+1)K \times 1$ vector

$$\mathcal{Y} = [\mathcal{Y}_{i-1}^T,\ \boldsymbol{w}(i)^T]^T, \tag{5.15}$$

whose covariance matrix can be written as

$$\boldsymbol{R}_{\mathcal{Y}} = E\{\mathcal{Y}\mathcal{Y}^H\} = \begin{bmatrix} \boldsymbol{R}_{y11} & \boldsymbol{R}_{y12} \\ \boldsymbol{R}_{y21} & \boldsymbol{R}_{y22} \end{bmatrix}, \tag{5.16}$$

where

$$\boldsymbol{R}_{y11} = E\{\mathcal{Y}_{i-1}\ \mathcal{Y}_{i-1}^H\}, \qquad (MK \times MK) \tag{5.17}$$

$$\boldsymbol{R}_{y12} = E\{\mathcal{Y}_{i-1}\ \boldsymbol{w}(i)^H\}, \qquad (MK \times K) \tag{5.18}$$

$$\boldsymbol{R}_{y21} = E\{\boldsymbol{w}(i)\ \mathcal{Y}_{i-1}^H\}, \qquad (K \times MK) \tag{5.19}$$

$$\boldsymbol{R}_{y22} = E\{\boldsymbol{w}(i)\ \boldsymbol{w}(i)^H\}. \qquad (K \times K) \tag{5.20}$$

The covariance matrices (5.17) - (5.19) depend not only on the channel spaced-time correlation function, but also on the previous bit decisions. An error on the previous bit decisions could happen with a certain probability and hence these matrices need to be calculated by combining both the channel statistics and probability of error. From the practical point of view, for a reliable communication the decision error is usually small enough, so these matrices can be calculated by using channel correlation information only, that is, previous bit decisions can be assumed as being correct for computing $\boldsymbol{R}_{y11}$, $\boldsymbol{R}_{y12}$ and $\boldsymbol{R}_{y21}$, although the matrices depend on $\mathcal{Y}_{i-1}$ which is data decision dependent. Given this approximation, the matrices are assumed decision independent and can be calculated *a priori*.

The MAP channel estimates of $\boldsymbol{w}(i)$ can be obtained by maximizing $p\{\boldsymbol{w}(i)|\mathcal{Y}_{i-1}\}$, i.e.

$$\max_{\boldsymbol{w}(i)}\ p\{\boldsymbol{w}(i)|\mathcal{Y}_{i-1}\}. \tag{5.21}$$

The whole procedure is illustrated in Fig. 5.2.

In (5.15), since both $\mathcal{Y}_{i-1}$ and $\boldsymbol{w}(i)$ are complex Gaussian random vectors, so is $\mathcal{Y}$. The conditional probability density function in equation (5.21) can be written

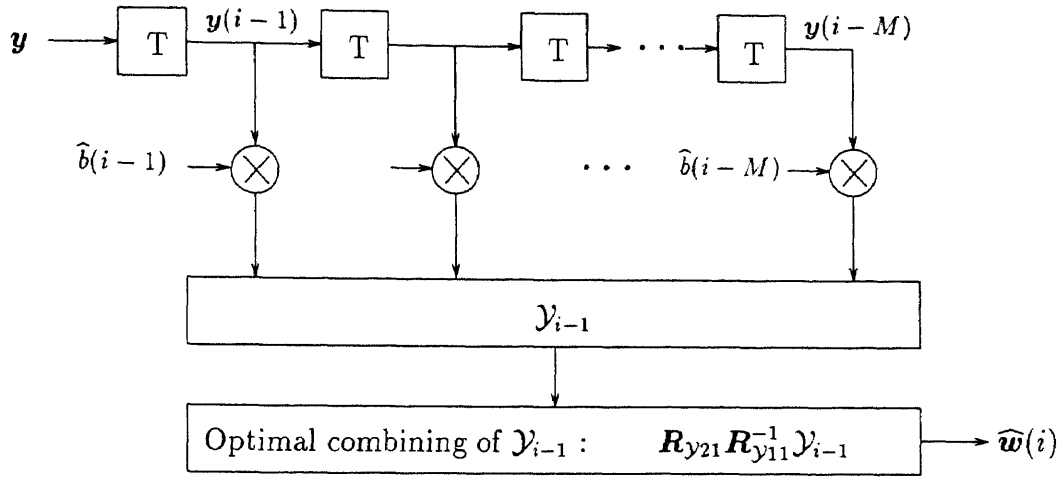

Figure 5.2 The single-stage DF MAP channel estimator

as

$$\begin{aligned} p\{\boldsymbol{w}(i)|\mathcal{Y}_{i-1}\} &= \frac{p\{\mathcal{Y}_{i-1}, \boldsymbol{w}(i)\}}{p\{\mathcal{Y}_{i-1}\}} \\ &= \frac{\frac{1}{\pi^{(M+1)K}|\boldsymbol{R}_y|}e^{-\mathcal{Y}^H\boldsymbol{R}_y^{-1}\mathcal{Y}}}{\frac{1}{\pi^{MK}|\boldsymbol{R}_{y11}|}e^{-\mathcal{Y}_{i-1}^H\boldsymbol{R}_{y11}^{-1}\mathcal{Y}_{i-1}}}. \end{aligned} \tag{5.22}$$

By using the partitioned matrix inversion from [36], $\boldsymbol{R}_y^{-1}$ can be expressed as

$$\boldsymbol{R}_y^{-1} = \begin{bmatrix} \boldsymbol{R}_{y11} & \boldsymbol{R}_{y12} \\ \boldsymbol{R}_{y21} & \boldsymbol{R}_{y22} \end{bmatrix}^{-1} = \begin{bmatrix} \boldsymbol{R}_{yi11} & \boldsymbol{R}_{yi12} \\ \boldsymbol{R}_{yi21} & \boldsymbol{R}_{yi22} \end{bmatrix}, \tag{5.23}$$

where

$$\boldsymbol{R}_{yi11} = (\boldsymbol{R}_{y11} - \boldsymbol{R}_{y12}\boldsymbol{R}_{y22}^{-1}\boldsymbol{R}_{y21})^{-1}, \tag{5.24}$$

$$\boldsymbol{R}_{yi22} = (\boldsymbol{R}_{y22} - \boldsymbol{R}_{y21}\boldsymbol{R}_{y11}^{-1}\boldsymbol{R}_{y12})^{-1}, \tag{5.25}$$

$$\boldsymbol{R}_{yi12} = -\boldsymbol{R}_{yi11}\boldsymbol{R}_{y12}\boldsymbol{R}_{y22}^{-1}, \tag{5.26}$$

$$\boldsymbol{R}_{yi21} = -\boldsymbol{R}_{yi22}\boldsymbol{R}_{y21}\boldsymbol{R}_{y11}^{-1}. \tag{5.27}$$

Maximizing the conditional probability density function in (5.22) is equivalent to minimizing the following quadratic function

$$l = \mathcal{Y}^H\boldsymbol{R}_y^{-1}\mathcal{Y} - \mathcal{Y}_{i-1}^H\boldsymbol{R}_{y11}^{-1}\mathcal{Y}_{i-1}. \tag{5.28}$$

The derivative of l with respect to $\boldsymbol{w}(i)$ gives

$$\begin{aligned}\widehat{\boldsymbol{w}}(i) &= -\boldsymbol{R}_{y_{i22}}^{-1}\boldsymbol{R}_{y_{i21}}\mathcal{Y}_{i-1} \\ &= \boldsymbol{R}_{y21}\boldsymbol{R}_{y11}^{-1}\mathcal{Y}_{i-1}, \end{aligned} \tag{5.29}$$

where, as mentioned before, $\widehat{\boldsymbol{w}}(i)$ denotes the estimate of $\boldsymbol{w}(i)$. This single-stage channel estimate depends on $\mathcal{Y}_{i-1}$ which is decision dependent, so any erroneous previous bit decisions will affect the incoming channel vector estimation and hence the incoming bit decision. This is of course a common characteristic of a decision feedback channel estimator of any type, including the Kalman filter implementation as a decision feedback MMSE channel estimator for the Markovian type of channels. Therefore, the proposed DF MAP channel estimator also suffers from the same problem.

In order to observe the properties of this channel estimator, we calculate the following statistics

$$E\{\widehat{\boldsymbol{w}}(i)\widehat{\boldsymbol{w}}(i)^H\} = \boldsymbol{R}_{y21}\boldsymbol{R}_{y11}^{-1}\boldsymbol{R}_{y12}, \tag{5.30}$$

$$E\{\widehat{\boldsymbol{w}}(i)\boldsymbol{w}(i)^H\} = \boldsymbol{R}_{y21}\boldsymbol{R}_{y11}^{-1}\boldsymbol{R}_{y12}, \tag{5.31}$$

$$E\{\boldsymbol{w}(i)\widehat{\boldsymbol{w}}(i)^H\} = \boldsymbol{R}_{y21}\boldsymbol{R}_{y11}^{-1}\boldsymbol{R}_{y12}. \tag{5.32}$$

Observe that $E\{\widehat{\boldsymbol{w}}(i)\widehat{\boldsymbol{w}}(i)^H\} = E\{\widehat{\boldsymbol{w}}(i)\boldsymbol{w}(i)^H\} = E\{\boldsymbol{w}(i)\widehat{\boldsymbol{w}}(i)^H\}$ which is interesting because except for the matrix form here, it resembles the orthogonality properties of the conventional MMSE channel estimator [18]. Let us refer to the equations (5.30)-(5.32) as the *generalized orthogonality* properties of the single-stage DF MAP channel estimator.

5.3.2 Two-Stage Estimator

The decision feedback channel estimator derived in Section 5.3.1 does not make full utilization of the available information in performing estimation of the equivalent channel vector $\boldsymbol{w}(i)$ since only the received signals and the bit decisions during the

previous bit intervals are used. Upon receiving $\boldsymbol{y}(i)$, more accurate channel estimates can be obtained if $\boldsymbol{y}(i)$ is used properly. Define

$$\tilde{\boldsymbol{y}}(i) = \boldsymbol{y}(i)\tilde{b}(i), \tag{5.33}$$

where $\tilde{b}(i)$ is the tentative bit decision on $b(i)$, and can usually be obtained by using the first stage channel estimates. Correspondingly, we want to maximize $p\{\boldsymbol{w}(i)|\mathcal{Y}_{i-1},\ \tilde{\boldsymbol{y}}(i)\}$ with respect to $\boldsymbol{w}(i)$, i.e.

$$\max_{\boldsymbol{w}(i)} p\{\boldsymbol{w}(i)|\mathcal{Y}_{i-1},\ \tilde{\boldsymbol{y}}(i)\}. \tag{5.34}$$

The conditional probability density function in (5.34), as shown in Appendix B, can be written as

$$p\{\boldsymbol{w}(i)|\mathcal{Y}_{i-1},\ \tilde{\boldsymbol{y}}(i)\} = \frac{p\{\mathcal{Y}_{i-1},\ \boldsymbol{w}(i)\}p\{\tilde{\boldsymbol{y}}(i),\ \boldsymbol{w}(i)\}}{p\{\mathcal{Y}_{i-1},\ \tilde{\boldsymbol{y}}(i)\}p\{\boldsymbol{w}(i)\}}, \tag{5.35}$$

The schematics of this two-stage channel estimator is shown in Fig. 5.3.

Let

$$\mathcal{Z} = [\tilde{\boldsymbol{y}}(i)^T,\ \boldsymbol{w}(i)^T]^T, \tag{5.36}$$

with its covariance matrix expressed as

$$\boldsymbol{R}_{\mathcal{Z}} = E\{\mathcal{Z}\mathcal{Z}^H\} = \begin{bmatrix} \boldsymbol{R}_{\mathcal{Z}11} & \boldsymbol{R}_{\mathcal{Z}12} \\ \boldsymbol{R}_{\mathcal{Z}21} & \boldsymbol{R}_{\mathcal{Z}22} \end{bmatrix}, \tag{5.37}$$

where

$$\boldsymbol{R}_{\mathcal{Z}11} = E\{\tilde{\boldsymbol{y}}(i)\ \tilde{\boldsymbol{y}}(i)^H\}, \tag{5.38}$$

$$\boldsymbol{R}_{\mathcal{Z}12} = E\{\tilde{\boldsymbol{y}}(i)\ \boldsymbol{w}(i)^H\}, \tag{5.39}$$

$$\boldsymbol{R}_{\mathcal{Z}21} = E\{\boldsymbol{w}(i)\ \tilde{\boldsymbol{y}}(i)^H\}, \tag{5.40}$$

$$\boldsymbol{R}_{\mathcal{Z}22} = E\{\boldsymbol{w}(i)\ \boldsymbol{w}(i)^H\}. \tag{5.41}$$

Similar to the definitions of $\boldsymbol{R}_{y11}$, $\boldsymbol{R}_{y12}$ and $\boldsymbol{R}_{y21}$ in the previous section, $\boldsymbol{R}_{\mathcal{Z}12}$ and $\boldsymbol{R}_{\mathcal{Z}21}$ in (5.39) and (5.40) are tentative decision $\tilde{b}(i)$ dependent, but these matrices

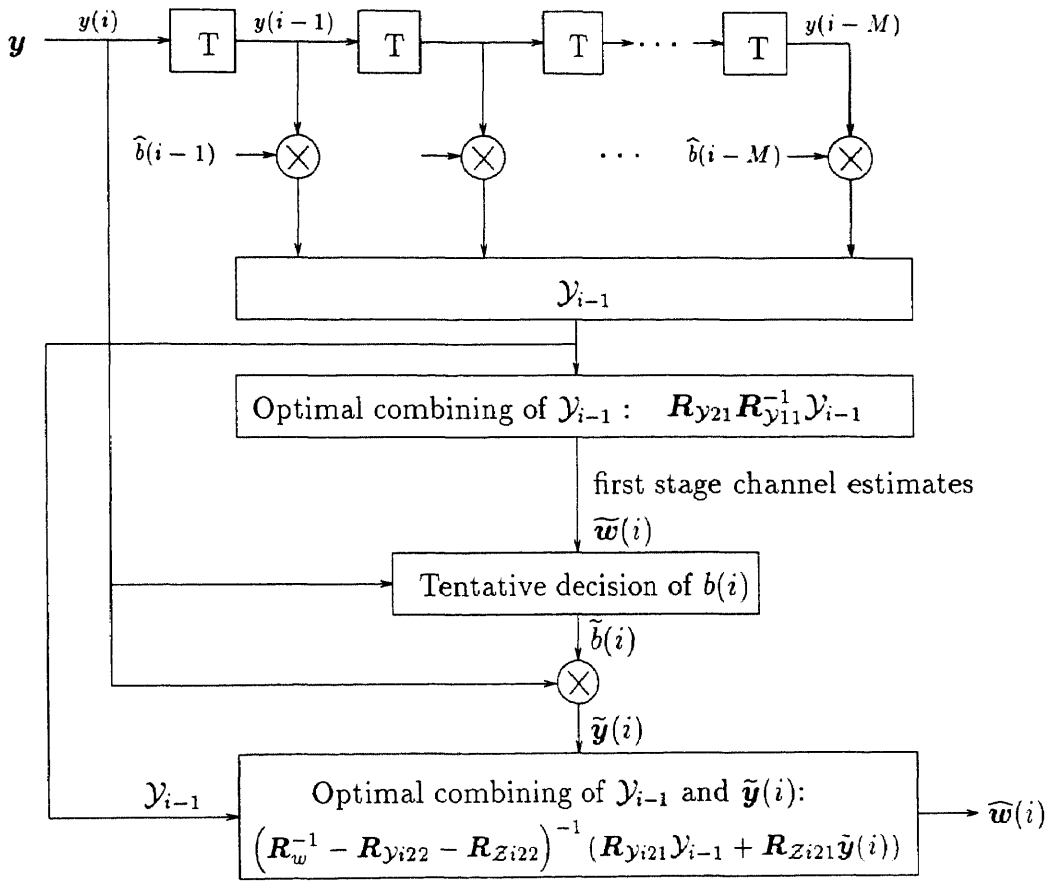

Figure 5.3 The two-stage DF MAP channel estimator

can be approximated by using the channel statistics only. This is justified as follows: let $\tilde{P}_e$ be the probability of error for the tentative decision, i.e., $\tilde{P}_e = P_r\{\tilde{b}(i) \neq b(i)\}$, so we have [3]

$$\begin{aligned} \boldsymbol{R}_{Z12} &= \sqrt{a}E\{\tilde{b}(i)b(i)\}E\{\boldsymbol{w}(i)\boldsymbol{w}(i)^H\} \\ &= (1-2\tilde{P}_e)\sqrt{a}\boldsymbol{R}_w. \end{aligned}$$

If $\tilde{P}_e$ is small enough so that $(1-2\tilde{P}_e) \longrightarrow 1$ (which is true for a reliable communication), $\boldsymbol{R}_{Z12}$ and $\boldsymbol{R}_{Z21}$ can be approximated by using the statistics of the channel only.

Notice that $\boldsymbol{R}_{Z22}$ in (5.41) and $\boldsymbol{R}_{y22}$ in (5.20) are the same; they are equal to the covariance matrix of the equivalent channel vector $\boldsymbol{w}(i)$ over one bit interval, i.e.

$$\boldsymbol{R}_{y22} = \boldsymbol{R}_{Z22} = \boldsymbol{R}_w = E\{\boldsymbol{w}(i)\boldsymbol{w}(i)^H\}.$$

Using the partitioned matrix inversion lemma, $\boldsymbol{R}_Z^{-1}$ can be obtained as

$$\boldsymbol{R}_Z^{-1} = \begin{bmatrix} \boldsymbol{R}_{Z11} & \boldsymbol{R}_{Z12} \\ \boldsymbol{R}_{Z21} & \boldsymbol{R}_{Z22} \end{bmatrix}^{-1} = \begin{bmatrix} \boldsymbol{R}_{Zi11} & \boldsymbol{R}_{Zi12} \\ \boldsymbol{R}_{Zi21} & \boldsymbol{R}_{Zi22} \end{bmatrix}, \tag{5.42}$$

where

$$\boldsymbol{R}_{Zi11} = (\boldsymbol{R}_{Z11} - \boldsymbol{R}_{Z12}\boldsymbol{R}_{Z22}^{-1}\boldsymbol{R}_{Z21})^{-1}, \tag{5.43}$$

$$\boldsymbol{R}_{Zi22} = (\boldsymbol{R}_{Z22} - \boldsymbol{R}_{Z21}\boldsymbol{R}_{Z11}^{-1}\boldsymbol{R}_{Z12})^{-1}, \tag{5.44}$$

$$\boldsymbol{R}_{Zi12} = -\boldsymbol{R}_{Zi11}\boldsymbol{R}_{Z12}\boldsymbol{R}_{Z22}^{-1}, \tag{5.45}$$

$$\boldsymbol{R}_{Zi21} = -\boldsymbol{R}_{Zi22}\boldsymbol{R}_{Z21}\boldsymbol{R}_{Z11}^{-1}. \tag{5.46}$$

As shown in Appendix C, some mathematical operations on equation (5.35) results in the following two-stage channel estimates

$$\widehat{\boldsymbol{w}}(i) = \left(\boldsymbol{R}_w^{-1} - \boldsymbol{R}_{yi22} - \boldsymbol{R}_{Zi22}\right)^{-1}\left(\boldsymbol{R}_{yi21}\boldsymbol{\mathcal{Y}}_{i-1} + \boldsymbol{R}_{Zi21}\check{\boldsymbol{y}}(i)\right). \tag{5.47}$$

[3] Although $\tilde{P}_e$ depends on $\tilde{\boldsymbol{w}}(i)$, the estimates of $\boldsymbol{w}(i)$, $\tilde{P}_e$ is independent of $\boldsymbol{w}(i)$ itself.

Comparing equation (5.29), the single-stage channel estimates and equation (5.47), the two-stage channel estimates, we find that the two-stage estimator uses more information, like $\tilde{\boldsymbol{y}}(i)$, and tries to combine both $\mathcal{Y}_{i-1}$ and $\tilde{\boldsymbol{y}}(i)$ in an optimal way to yield the channel estimates, while the single-stage estimator combines $\mathcal{Y}_{i-1}$ only. From the data detection point of view, using the two-stage channel estimates in (5.47) and using the single-stage channel estimates in (5.29) result in the same probability of error. This is because whenever the first stage makes a decision error, it results in a bad estimate of $\tilde{\boldsymbol{y}}(i)$ defined in (5.33), and correspondingly, the second stage will make an error. However, the second stage does give a more accurate average channel estimation, especially when signal to noise ratio is high. For the special case when $(a/N_0) \longrightarrow \infty$, the two stage channel estimator gives perfect estimates of $\boldsymbol{w}(i)$, but the first stage estimator usually does not give perfect estimates as long as the channel Doppler shift is not zero. So the two-stage estimator has an advantage when used in a time-varying fading channel for other purposes such as interference cancellation which needs estimation of the interference signal, etc. For simplicity, we will use the single-stage channel estimates for coherent detection throughout this dissertation.

The nice feature of this channel estimator is that it can be applied to a Rayleigh fading channel with any known spaced-time correlation function, unlike the Kalman filter which can be applied to the Markovian type of model only.

5.3.3 Comparison of the Single-Stage and Two-stage Estimator

We are interested in the performance comparison between the proposed channel estimators and other existing estimators. A Kalman filter can be implemented as the optimum decision feedback estimator only for the Markovian type of channels. For fading channels modeled by other models such as Jakes' model, A Kalman filter usually can not be implemented and we do not have a specific method for these type of channels, although in [80] the Jakes' model is approximated by using the

second order Markov model, and the resulting fading process is estimated by using the Kalman filter. So we will focus on the first-order Markov model with a Kalman filter as the optimal estimator and single sample per bit, which is a special case for the proposed estimator if $K = 1$ is set in equation (5.11). We will analyze the expected normalized estimation error variance when the signal to noise ratio is infinite and address the error floor for each case. The matched filter output of the received baseband equivalent signal in (5.10) in the i^{th} bit interval can be written as $r(i) = \sqrt{a}c(i)b(i) + \xi(i)$. When the channel estimation error is taken into account, the probability of error for this case is [87]

$$P_{BPSK} = \frac{1}{2}\left(1 - \sqrt{\frac{(a/N_0)(1-\Gamma)}{1+(a/N_0)}}\right),$$

where $\Gamma = E\{|c(i) - \hat{c}(i)|^2\}/E\{|c(i)|^2\}$ is the normalized estimation error variance. For Kalman filter estimation, the estimation error variance Γ (by assuming correct previous decisions) can be obtained by solving the Riccati equation [18] resulting in (also see [30] eq. 10)

$$E\Gamma^2 + (N_0 - a)(1-\varrho^2)\Gamma - N_0(1-\varrho^2) = 0,$$

where $\varrho = \Phi(T)/\Phi(0)$ was defined in Section 3.2 and solution to this equation is

$$\Gamma = \frac{(a-N_0)(1-\varrho^2) + \sqrt{(1-\varrho^2)(4aN_0 + (a-N_0)^2(1-\varrho^2))}}{2a}.$$

In the limiting case when the signal to noise ratio is infinity, we have the normalized estimation error variance as

$$\lim_{a/N_0 \to \infty} \Gamma = 1 - \varrho^2,$$

The error floor can then be obtained as

$$P_{BPSK,\infty} = (1-\varrho)/2.$$

For the proposed single-stage DF MAP channel estimator, if the buffer size $M = 1$ is used, the channel vector $\boldsymbol{w}(i)$ becomes a scalar and the channel state equation

can be written as $w(i) = \varrho w(i-1) + n(i-1)$, where $n(i-1)$ is a complex Gaussian random variable with the variance $1-\varrho^2$ and independent of $w(i-1)$. The channel estimates in (5.29) can be shown to be

$$\widehat{w}(i) = \frac{\sqrt{a}\varrho}{a+N_0}\left[\sqrt{a}w(i-1) + \xi(i-1)\right].$$

When $(a/N_0) \longrightarrow \infty$, we get $\widehat{w}(i) = \varrho w(i-1)$. The normalized channel estimation error variance for our estimator in this limiting case is $\Gamma = E\{|\widehat{w}(i) - w(i)|^2\}/E\{|w(i)|^2\} = 1-\varrho^2$, which is exactly the same as with the Kalman filter, and correspondingly, gives the same error floor. For a small signal to noise ratio, this single-stage estimator performs a little bit worse than the Kalman filter estimator. When we increase the buffer size ($M > 1$), the error floor is the same as for $M = 1$, but it improves the performance for the low signal to noise ratio.

The two-stage channel estimator for $M = 1$ gives the channel estimates as

$$\widehat{w}(i) = \left(\frac{a+N_0}{a+N_0-a\varrho^2} - \frac{a}{N_0}\right)^{-1}\left(-\frac{\sqrt{a}\varrho}{a+N_0-a\varrho^2}r(i-1)\widehat{b}(i-1) - \frac{\sqrt{a}}{N_0}\widetilde{r}(i)\right).$$

When $(a/N_0) \longrightarrow \infty$, we get the channel estimate as $\widehat{w}(i) = \widetilde{r}(i)/\sqrt{a} = w(i)b(i)\widetilde{b}(i)$, which gives perfect channel estimates if the tentative decision $\widetilde{b}(i)$ is correct. For other signal to noise ratio values, the channel estimate is an optimal combining of both $r(i-1)$ with information data removed and $\widetilde{r}(i)$.

5.4 Coherent Detection with Adaptive Channel Estimates

The decision feedback MAP channel estimator can be applied directly to the fractionally spaced decorrelator output to estimate the equivalent channel vector $\boldsymbol{w}$ of the desired user defined in (5.4). The whole detection procedure is similar to 5.1 except here a channel estimation block is added as shown in 5.4.

For the single-stage channel estimator, the estimate of $\widehat{\boldsymbol{w}}$ of $\boldsymbol{w}$ is

$$\widehat{\boldsymbol{w}} = \boldsymbol{R}_{y21}\boldsymbol{R}_{y11}^{-1}\mathcal{Y}_{i-1}. \tag{5.48}$$

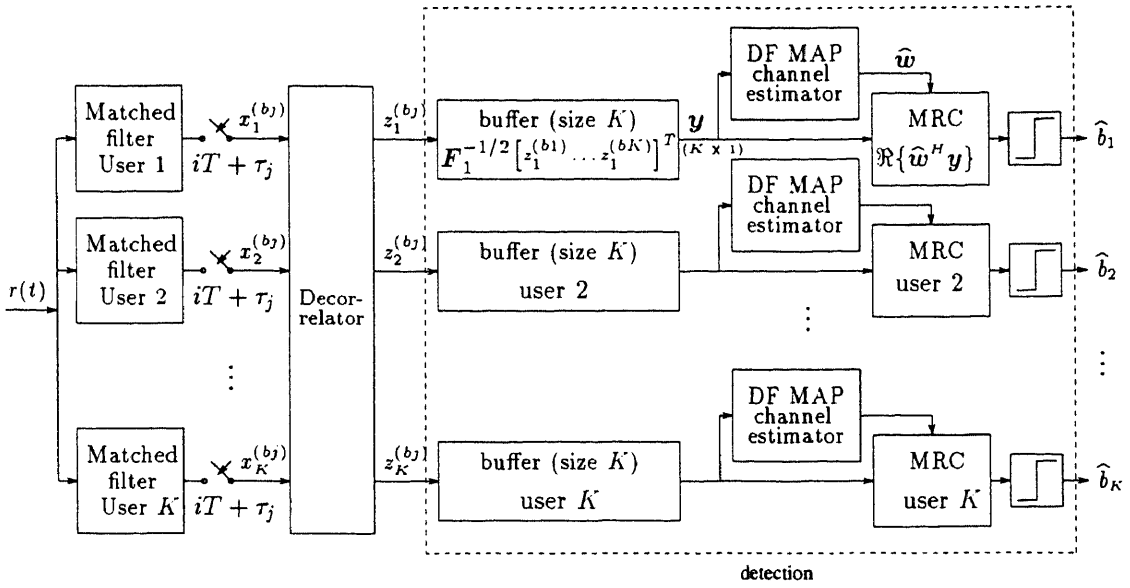

Figure 5.4 The coherent multiuser detector with the DF MAP channel estimates

Given this estimate, the decision variable for the i^{th} bit of the desired user can be written as

$$\lambda_i = \Re\{\widehat{\boldsymbol{w}}^H \boldsymbol{y}\}. \tag{5.49}$$

The adaptive feature of this coherent detection lies in the fact that for detecting the incoming bit, the previous received signal and bit decisions within a window of M bits are used to form the incoming channel estimate vector according to the MAP rule, that will adapt to the changing channel for detecting a new bit from the incoming received signal.

Without loss of generality, we will assume that the transmitted bit is 1 when deriving the error probability of the detector whose decision variable is given in (5.49). The analysis is similar to that for the error performance of quadratic receivers [3] [92] [56].

Introducing a $2K \times 1$ vector

$$\boldsymbol{v} = \begin{bmatrix} \widehat{\boldsymbol{w}} \\ \boldsymbol{y} \end{bmatrix},$$

the decision variable in (5.49) can be written as

$$\begin{aligned}\lambda_i &= \begin{bmatrix} \widehat{\boldsymbol{w}} \\ \boldsymbol{y} \end{bmatrix}^H \begin{bmatrix} \mathbf{o} & 0.5\boldsymbol{I} \\ 0.5\boldsymbol{I} & \mathbf{o} \end{bmatrix} \begin{bmatrix} \widehat{\boldsymbol{w}} \\ \boldsymbol{y} \end{bmatrix} \\ &= \boldsymbol{v}^H \boldsymbol{Q} \boldsymbol{v}, \end{aligned} \tag{5.50}$$

where $\mathbf{o}$ is a $K \times K$ matrix with all elements equal to zero. The covariance matrix of $\boldsymbol{V}$ is

$$\boldsymbol{V} = E\{\boldsymbol{v}\boldsymbol{v}^H\} = E\left\{ \begin{bmatrix} \widehat{\boldsymbol{w}} \\ \boldsymbol{y} \end{bmatrix} [\widehat{\boldsymbol{w}}^H \boldsymbol{y}^H] \right\}.$$

From the results and definitions in Section 5.3.1, and $\boldsymbol{y}$ in (5.4), we have the following expressions

$$\begin{aligned} E\{\widehat{\boldsymbol{w}}\widehat{\boldsymbol{w}}^H\} &= \boldsymbol{R}_{y21}\boldsymbol{R}_{y11}^{-1}\boldsymbol{R}_{y12} \\ E\{\boldsymbol{y}\boldsymbol{y}^H\} &= a_1\boldsymbol{R}_{y22} + N_0\boldsymbol{I} \\ E\{\widehat{\boldsymbol{w}}\boldsymbol{y}^H\} &= \sqrt{a_1}\boldsymbol{R}_{y21}\boldsymbol{R}_{y11}^{-1}\boldsymbol{R}_{y12} \\ E\{\boldsymbol{y}\widehat{\boldsymbol{w}}^H\} &= \sqrt{a_1}\boldsymbol{R}_{y21}\boldsymbol{R}_{y11}^{-1}\boldsymbol{R}_{y12}. \end{aligned}$$

Therefore, the matrix $\boldsymbol{V}$ defined above can be expressed as

$$\boldsymbol{V} = E\left\{ \begin{matrix} \widehat{\boldsymbol{w}}\widehat{\boldsymbol{w}}^H & \widehat{\boldsymbol{w}}\boldsymbol{y}^H \\ \boldsymbol{y}\widehat{\boldsymbol{w}}^H & \boldsymbol{y}\boldsymbol{y}^H \end{matrix} \right\} = \begin{bmatrix} \boldsymbol{R}_{y21}\boldsymbol{R}_{y11}^{-1}\boldsymbol{R}_{y12} & \sqrt{a_1}\boldsymbol{R}_{y21}\boldsymbol{R}_{y11}^{-1}\boldsymbol{R}_{y12} \\ \sqrt{a_1}\boldsymbol{R}_{y21}\boldsymbol{R}_{y11}^{-1}\boldsymbol{R}_{y12} & a_1\boldsymbol{R}_{y22} + N_0\boldsymbol{I} \end{bmatrix},$$

and

$$\boldsymbol{V}\boldsymbol{Q} = 0.5 \begin{bmatrix} \sqrt{a_1}\boldsymbol{R}_{y21}\boldsymbol{R}_{y11}^{-1}\boldsymbol{R}_{y12} & \boldsymbol{R}_{y21}\boldsymbol{R}_{y11}^{-1}\boldsymbol{R}_{y12} \\ a_1\boldsymbol{R}_{y22} + N_0\boldsymbol{I} & \sqrt{a_1}\boldsymbol{R}_{y21}\boldsymbol{R}_{y11}^{-1}\boldsymbol{R}_{y12} \end{bmatrix}.$$

In the above equations, $\boldsymbol{R}_{y11}$,$\boldsymbol{R}_{y12}$,$\boldsymbol{R}_{y21}$ and $\boldsymbol{R}_{y22}$ are defined in equations (5.15) through (5.18) respectively. In the case of distinct eigenvalues, the probability of error of the quadratic decision variable is the one given in [3]

$$P_e = P\{\lambda_i < 0\} = \sum_{\gamma_l < 0} \prod_{\substack{m=1 \\ m \neq l}}^{2K} \frac{\gamma_l}{\gamma_l - \gamma_m}, \tag{5.51}$$

in which $\gamma_1, \ldots, \gamma_{2K}$ are the eigenvalues of the matrix $\boldsymbol{V}\boldsymbol{Q}$.

5.5 Numerical Examples and Discussion

A three-user scenario with signature waveforms chosen from Gold sequences of length 31 assigned to each user was considered. In the examples presented the relative delays were set at $\tau_1 = 0$, $\tau_2 = \frac{10}{31}T$, and $\tau_3 = \frac{22}{31}T$.

Discrete-time complex channel gain is generated the same way as described in Section 4.3. The error performance of the proposed detector is compared to that of the conventional single-user coherent PSK receiver in a single-user environment that utilizes *one sample per symbol.* Performance of the multiuser detector for perfect channel estimates, and estimates obtained by using the decision feedback MAP channel estimation algorithm derived in Section 5.3.1 are evaluated.

Fig. 5.5 provides the performance comparison for the perfectly estimated channel modeled by the first-order Markov process with the spaced-time correlation function given in equation (3.4). The fading rates $f_dT = 0.04$ and $f_dT = 0.08$ were chosen, and for both fading rates the error probability of the proposed detector is below that of the conventional single-user PSK receiver. In Fig. 5.6 the Jakes model with the correlation function given in equation (3.5) and $f_dT = 0.08$ and $f_dT = 0.16$ was employed, and with perfect channel estimates similar performance improvement is observed. As expected, in both models the error performance, under the assumption of perfect channel estimates, improves with the increased fading rate. The performance improvement of the proposed detector is due to the utilization of a form of the time diversity through multiple samples within the same information bit interval. By analyzing the eigenvalues of $\boldsymbol{R}_w = E\{\boldsymbol{w}\boldsymbol{w}^H\}$, we found that when fading becomes extremely slow, all but one eigenvalue become zero, so the proposed detector performance is the same as that of the conventional single user detector with the SNR that includes the effect of the noise enhancement induced by decorrelation.

Higher fading rates, however, make accurate estimation of the fading coefficients more difficult. In Fig. 5.7 and Fig. 5.8, performance lower bound of this

coherent multiuser detector with the proposed DF MAP channel estimates are given for Jakes' model by assuming the previous decisions are correct when performing channel estimation. Both theoretical error probability calculation according to equation (5.51) and Monte Carlo simulation of the multiuser detector performance are given.

Because of the nature of decision feedback type of the channel estimation algorithm, "phase reversal" phenomenon [77] could occur. In order to prevent this, differential encoding is proposed for this detector structure, and simulated performance is shown in Fig. 5.9 and Fig. 5.10 for different fading rates. Comparison is made between this multiuser detector in a three users scenario and that of the conventional differentially coherent detection (symbol spaced) in a single-user scenario whose error probability is given by

$$P_{e,DPSK} = \frac{1}{2}\left[1 - \frac{\varrho a_1/N_0}{1 + a_1/N_0}\right]. \tag{5.52}$$

Error floor is not observed for the proposed detector while the single user conventional differential detector performance saturated at the SNR values around 15 dB for $f_dT = 0.04$ and around 20 dB for $f_dT = 0.08$. The performance improvement of the proposed detector is essentially due to the fractional sampling which provides us a means to exploit a form of the time diversity implicit in the time-varying fading channel. We also found that the performance of the detector with differential encoding is very close to the performance lower bound which assume correct previous decisions in the DF MAP channel estimation. In a frequency nonselective Rayleigh fading channel, from the simple theoretical analysis under the assumption of perfect channel estimates that does not consider the fading dynamics, and fully interleaved channel which results in randomized errors, coherent detection with differential encoding is approximately 3 dB worse than that without differential encoding [55]. However, in a time-varying Rayleigh fading channel, errors usually happen in bursts and hence a good performance with differential encoding is expected. This

structure provides a robust detector design because the channel estimator is invariant to the channel correlation function model and "run away" is prevented by employing differential encoding with very little performance degradation.

In Chapter 4, we proposed a fractionally sampled differentially coherent detector in a time-varying frequency nonselective asynchronous CDMA channel. In this chapter we proposed a coherent multiuser detection with the DF MAP channel estimates in the same environment. For both detectors, we demonstrated their performance gain in a multiuser environment over the conventional differentially coherent and coherent detection for a single user transmission scenario. Next we provide a performance comparison between the error performance of the detector in Chapter 4 and the coherent detector proposed in this chapter under the same environment. Figs. 5.11 and 5.12 show the probability of error for both detectors under Jakes' model for $f_dT = 0.04$ and $f_dT = 0.08$, respectively. Other parameters used are: $M = 4$ and relative delays as above. From these figures, it can be concluded that the performance of the coherent detection with the DF MAP channel estimation combined with differential encoding is uniformly better than that of the differentially coherent detection, but the coherent detector, although robust because of the differential encoding, is more complex than the differentially coherent detector for which no channel estimation is needed.

Under the assumption of rectangular pulses of a spreading code, the performance difference of the proposed DPSK detector and the coherent detector differential encoding is not very large, so the choice of a detector should depend on a specific communication scenario. Unless we have particular reasons to estimate the channel, the limited numerical examples presented here under the assumption of no pulse shaping favors the DPSK detector, despite its slightly inferior performance,.

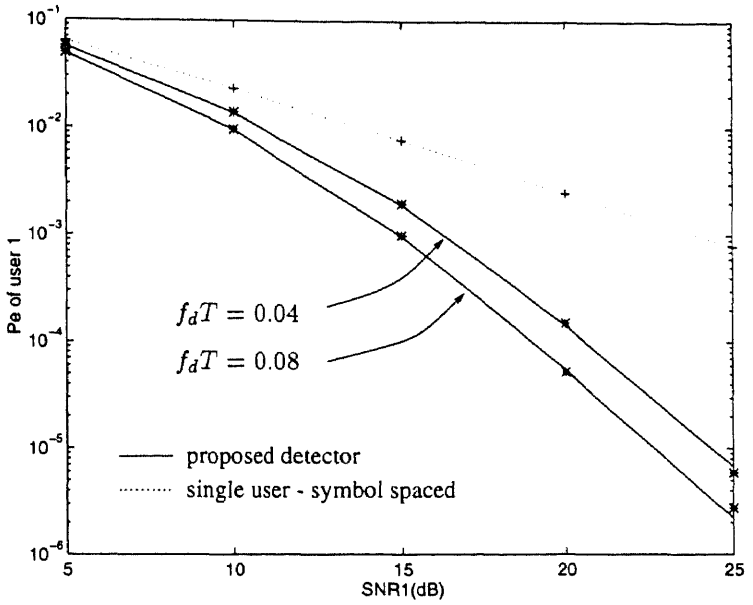

Figure 5.5 Analytical and simulated ($* * *$) error performance with first-order Markov model and perfect channel estimates

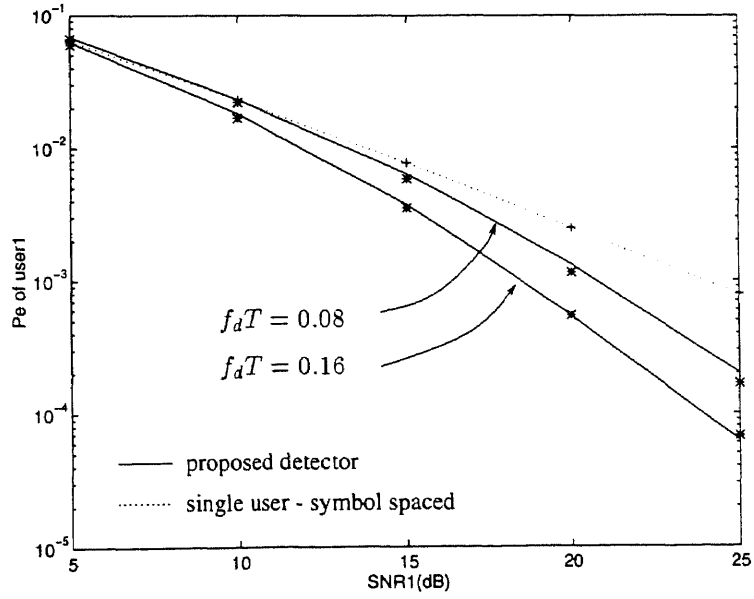

Figure 5.6 Analytical and simulated ($* * *$) error performance with Jakes model and perfect channel estimates

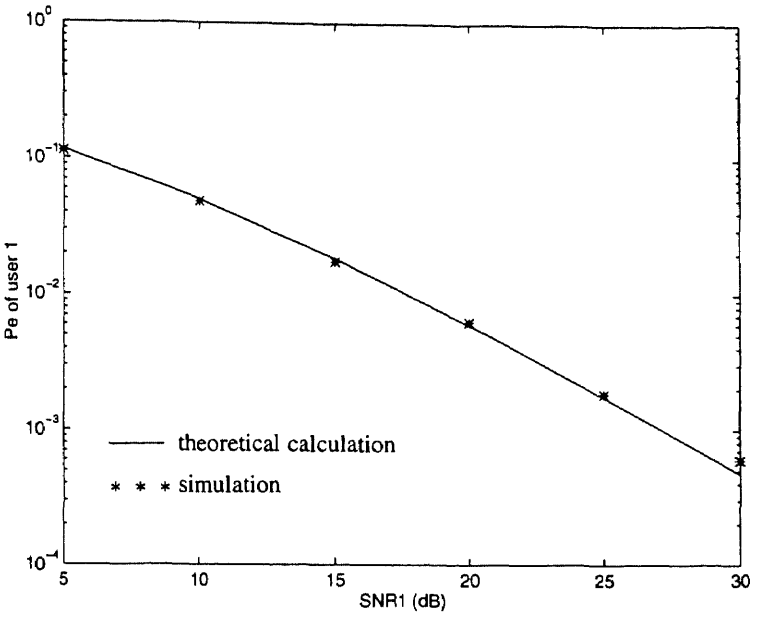

Figure 5.7 Analytical and simulated error lower bound of the detector with DF MAP channel estimates, $f_dT = 0.04$

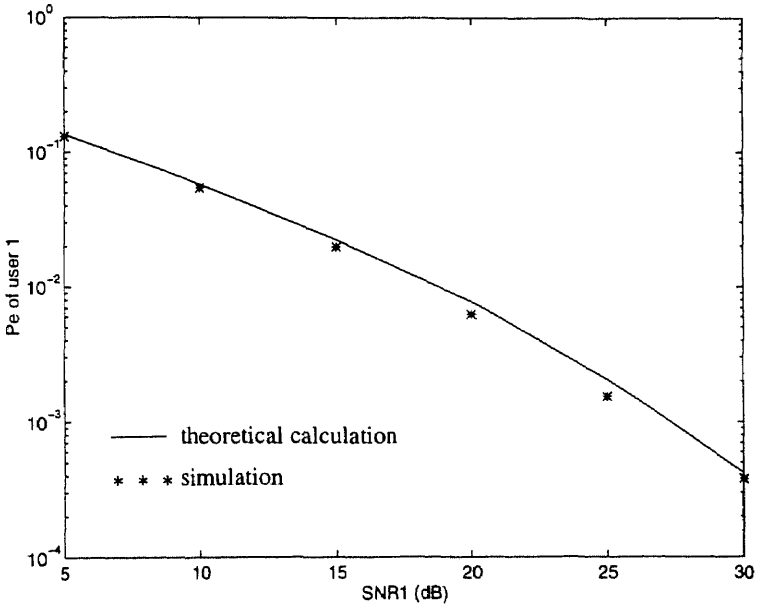

Figure 5.8 Analytical and simulated error lower bound of the detector with DF MAP channel estimates, $f_dT = 0.08$

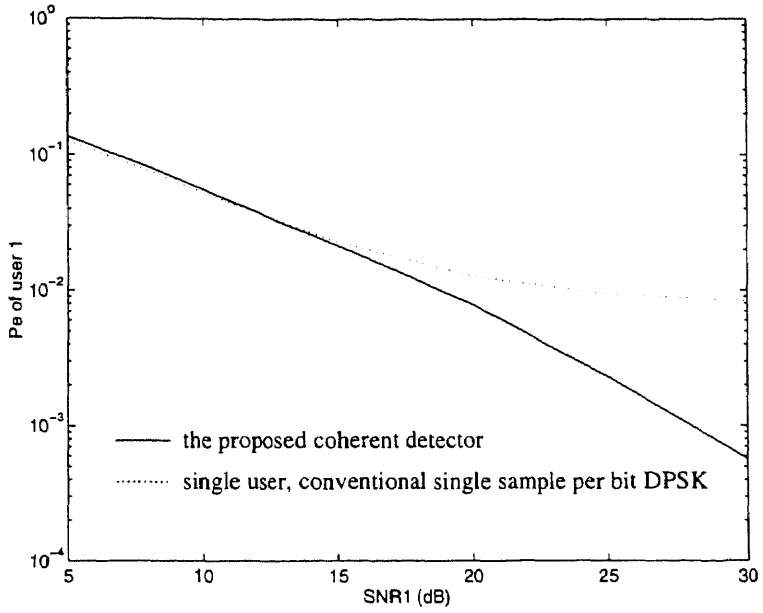

Figure 5.9 Simulated error performance with differential encoding, $f_dT = 0.04$

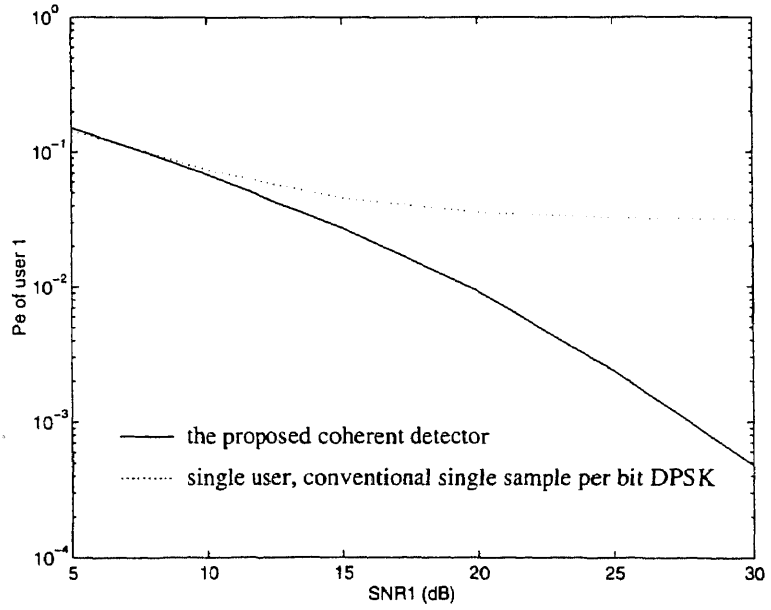

Figure 5.10 Simulated error performance with differential encoding, $f_dT = 0.08$

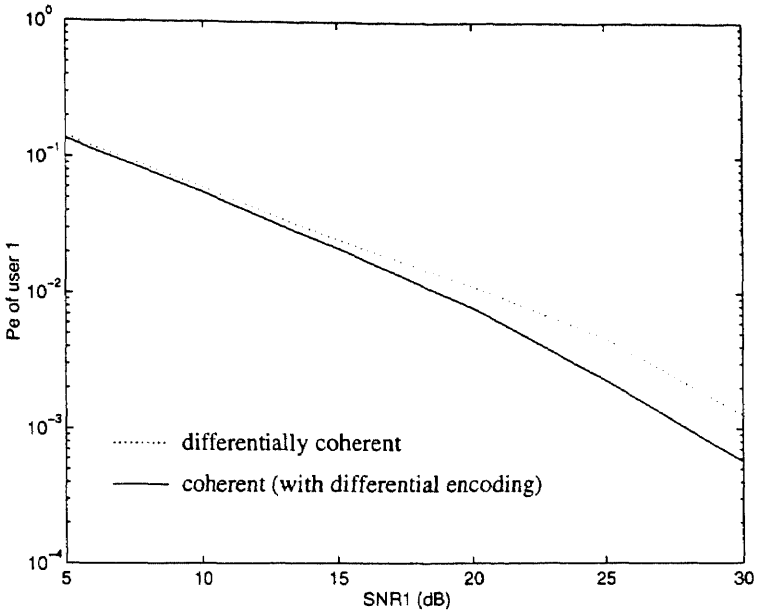

Figure 5.11 Performance comparison for differentially coherent detection and coherent detection, $f_dT = 0.04$

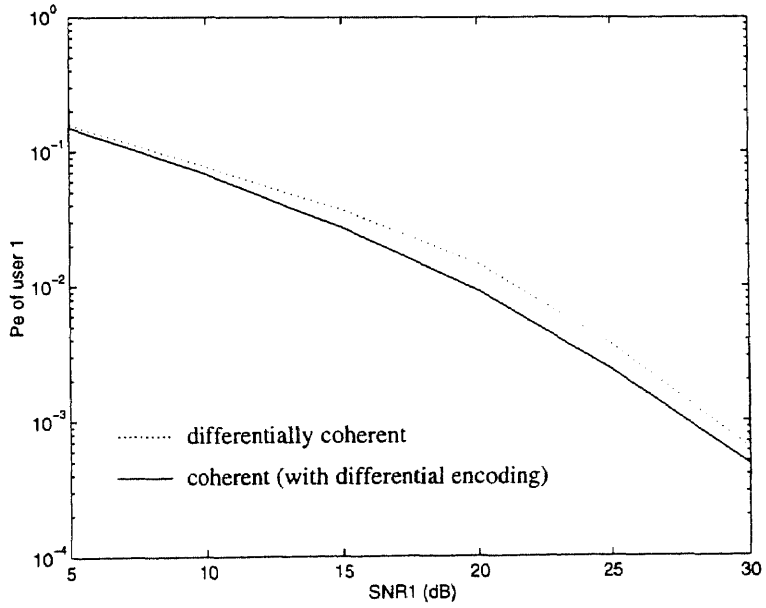

Figure 5.12 Performance comparison for differentially coherent detection and coherent detection, $f_dT = 0.08$

CHAPTER 6

DIFFERENTIALLY COHERENT DETECTION FOR TIME-VARYING FREQUENCY SELECTIVE RAYLEIGH FADING CHANNELS

6.1 Introduction

In Chapter 4, we proposed a low complexity fractionally-spaced decorrelator followed by a ML detection on the desired user's signal over two consecutive bit intervals in a frequency nonselective time-varying Rayleigh fading channel. We demonstrated that this DPSK detector can significantly reduce the error floor associated with the conventional DPSK detector in a time-varying fading channel in which channel Doppler shift can not be neglected. In Chapter 5, coherent detection in such a time-varying frequency nonselective environment is performed on the desired user's decorrelated output signal vector over one bit interval using maximum ratio combining of all K elements. A novel decision feedback maximum *a posteriori* channel estimator is proposed for this coherent detector which employs differential encoding. In both the differentially coherent and coherent detector, time variation is utilized through fractional sampling over one bit interval to improve the respective detectors' performance. Time-varying nature of the channel is quantitatively described by the channel's spaced-time correlation function such that the fading channel is not assumed to be slow (no changes for at least a few bits) or fully interleaved (channel realization is independent from one bit to another) like most of the research work in the literature does. In all our Monte Carlo simulations, complex channel gains are generated by using practical fading model, like Jakes model.

In a multipath time-varying fading channel, the wideband nature of each user's information signal relative to the channel coherence bandwidth results in L resolvable multipath paths at the receiver. This can be viewed as another method for obtaining frequency diversity of order L [55], although this diversity is exploited

in the time domain by RAKE or RAKE-type of receivers in a way similar to time-diversity. Another dimension that we can exploit for an improved performance receiver design in the time-varying fading channel is the effective time-diversity which can be achieved by obtaining multiple samples per bit.

In this chapter and hereafter, we will focus on a time-varying multipath fading channel with L resolvable paths. We will explore novel structures of low complexity multiuser detectors capable of mitigating the effects of MAI, path cross-correlation and ISI in a multiuser multipath fading channel and exploiting both the time-varying and frequency selective nature of a channel for maximum performance improvement.

Following the fractionally-spaced multipath decorrelator in Section 3.4, a maximum likelihood (ML) detection approach is applied for differentially encoded bit streams. In addition to the usual requirement for the availability of timing and signature sequences of the users, the proposed detector needs only the statistical description of a fading channel.

The chapter is organized as follows. The ML detection procedure and derivation of the decision variable for differentially encoded data stream and the error probability analysis are presented in Section 6.2. Numerical examples and discussion are provided in Section 6.3.

6.2 Detector Structure

The differentially coherent multiuser detector in a frequency selective fading channel will employ a decorrelator in the front-end followed by a maximum likelihood detection on the decorrelator output. Following the mathematical formulation of fractionally-spaced multipath decorrelator in Section 3.4, we will derive the ML detector structure and present its theoretical performance analysis in this section.

6.2.1 Detection Procedure

After decorrelating over two consecutive bit intervals spanning the time interval $[(i-2)T, iT]$ which corresponds to the $(i-1)^{th}$ and i^{th} bit interval of user 1, signals for user 1 can be written in vector form by combining the vector in equation (3.11) over the same bit intervals as a $2JL \times 1$ vector

$$\begin{aligned} \boldsymbol{y} &= [\boldsymbol{z}(i-1)^T,\ \boldsymbol{z}(i)^T]^T \\ &= \sqrt{a_1}\boldsymbol{B}_1\mathcal{E}_1\boldsymbol{C}_1 + \boldsymbol{\xi}_1, \end{aligned} \tag{6.1}$$

where

$$\begin{aligned} \boldsymbol{B}_1 &= \text{diag}[\underbrace{b_1(i-1), \ldots, b_1(i-1)}_{JL},\ \underbrace{b_1(i), \ldots, b_1(i)}_{JL}] \\ &= \text{diag}[\boldsymbol{B}_1(i-1),\ \boldsymbol{B}_1(i)], \\ \mathcal{E}_1 &= \text{diag}[\mathcal{E},\ \mathcal{E}], \\ \boldsymbol{C}_1 &= [\boldsymbol{C}(i-1)^T,\ \boldsymbol{C}(i)^T]^T \\ &= [\boldsymbol{C}^{(b1)}(i-1)^T,\ \ldots,\ \boldsymbol{C}^{(bJ)}(i-1)^T,\ \boldsymbol{C}^{(b1)}(i)^T,\ \ldots,\ \boldsymbol{C}^{(bJ)}(i)^T]^T, \\ \boldsymbol{\xi}_1 &= [\boldsymbol{\xi}(i-1)^T,\ \boldsymbol{\xi}(i)^T]^T \\ &= [\boldsymbol{\xi}^{(b1)}(i-1)^T,\ \ldots,\ \boldsymbol{\xi}^{(bJ)}(i-1)^T,\ \boldsymbol{\xi}^{(b1)}(i)^T,\ \ldots,\ \boldsymbol{\xi}^{(bJ)}(i)^T]^T. \end{aligned}$$

The covariance matrix of $\boldsymbol{y}$ is

$$\begin{aligned} \boldsymbol{R}_y &= E\{\boldsymbol{y}\boldsymbol{y}^H\} \\ &= a_1\boldsymbol{B}_1\mathcal{E}_1\boldsymbol{R}_{c_1}\mathcal{E}_1^H\boldsymbol{B}_1^H + \boldsymbol{R}_{\xi_1} \\ &= a_1\boldsymbol{B}_1\mathcal{E}_1\boldsymbol{R}_{c_1}\mathcal{E}_1\boldsymbol{B}_1 + \boldsymbol{R}_{\xi_1}, \end{aligned} \tag{6.2}$$

where we used the fact that $\mathcal{E}_1$ and $\boldsymbol{B}_1$ are Hermitian. The covariance matrix of the channel vector over two adjacent bit intervals $\boldsymbol{C}_1$ is

$$\boldsymbol{R}_{c_1} = E\left[\boldsymbol{C}_1\boldsymbol{C}_1^H\right], \tag{6.3}$$

and the noise covariance matrix is

$$\boldsymbol{R}_{\xi_1} = E\left[\boldsymbol{\xi}_1 \boldsymbol{\xi}_1^H\right] = \begin{bmatrix} \boldsymbol{R}_\xi & 0 \\ 0 & \boldsymbol{R}_\xi \end{bmatrix}, \tag{6.4}$$

where $\boldsymbol{R}_\xi$ is defined in (3.19). $\boldsymbol{R}_{\xi_1}$ represents the additive noise covariance matrix at the fractionally spaced decorrelator output for user 1.

Once $\boldsymbol{y}$ (the multiuser interference-free, discrete time formulation of the DPSK received signal over a two symbol period) is obtained, the detection approach similar to the one derived in [7] can be applied. The $2JL \times 1$ decorrelator output vector $\boldsymbol{y}$, being the sum of two independent complex Gaussian random vectors (due to the Rayleigh type of fading), has a $2JL$-variate complex Gaussian distribution [55]

$$p(\boldsymbol{y}) = \frac{1}{\pi^{2JL}|\boldsymbol{R}_y|} e^{-\boldsymbol{y}^H \boldsymbol{R}_y^{-1} \boldsymbol{y}}, \tag{6.5}$$

where $|\boldsymbol{R}_y|$ is the determinant of $\boldsymbol{R}_y$.

The rest of the detection follows exactly the same procedure as presented in Chapter 4 for the frequency nonselective channel. Let hypothesis "H_1" correspond to transmitting the information bit 1, i.e., pairs of differentially encoded symbols $(-1, -1)$ or $(1, 1)$ over two consecutive symbol intervals, and let hypothesis "H_0" correspond to transmitting the information bit -1. The likelihood ratio can be written as

$$\Lambda(\boldsymbol{y}) = \frac{p(\boldsymbol{y}|H_1)}{p(\boldsymbol{y}|H_0)} = \frac{\frac{1}{\pi^{2JL}|\boldsymbol{R}_{y(1)}|} e^{-\boldsymbol{y}^H \boldsymbol{R}_{y(1)}^{-1} \boldsymbol{y}}}{\frac{1}{\pi^{2JL}|\boldsymbol{R}_{y(-1)}|} e^{-\boldsymbol{y}^H \boldsymbol{R}_{y(-1)}^{-1} \boldsymbol{y}}}, \tag{6.6}$$

where $\boldsymbol{R}_{y(1)}$ and $\boldsymbol{R}_{y(-1)}$ are the covariance matrices of $\boldsymbol{y}$ corresponding to transmitted information bits 1 and -1, respectively. These covariance matrices can be written as

$$\boldsymbol{R}_{y(1)} = a_1 \mathcal{E}_1 \boldsymbol{R}_{c_1} \mathcal{E}_1 + \boldsymbol{R}_{\xi_1} = \boldsymbol{R} \tag{6.7}$$

$$\begin{aligned} \boldsymbol{R}_{y(-1)} &= (a_1 \mathcal{E}_1 \boldsymbol{R}_{c_1} \mathcal{E}_1 + \boldsymbol{R}_{\xi_1}) \bigotimes \begin{bmatrix} 1 & -1 \\ -1 & 1 \end{bmatrix} \\ &= \boldsymbol{R} \bigotimes \begin{bmatrix} 1 & -1 \\ -1 & 1 \end{bmatrix}. \end{aligned} \tag{6.8}$$

In equation (6.8), $\mathbf{1}$ is a $JL \times JL$ square matrix with all elements equal to 1, and $\otimes$ stands for the Hadamard product, giving element by element multiplication.

The maximum *a posteriori* (MAP) decision rule and the decision statistics (with equally likely information bits assumed) for the i^{th} information bit of user 1 can be expressed exactly the same as in (4.8) and (4.9), which are replicated here for convenience

$$\Lambda(\boldsymbol{y}) \underset{H_0}{\overset{H_1}{\gtrless}} \frac{\Pr(H_0)}{\Pr(H_1)}, \tag{6.9}$$

$$\lambda_i = \boldsymbol{y}^H(\boldsymbol{R}_{y(-1)}^{-1} - \boldsymbol{R}_{y(1)}^{-1})\boldsymbol{y} = \boldsymbol{y}^H\boldsymbol{Q}\boldsymbol{y}. \tag{6.10}$$

6.2.2 Error Performance Analysis

Giving the ML decision variable in (6.10), error performance can be carried out in a way similar to what was presented in Chapter 4. The difference between this detector and the one in Chapter 4 is that the vector that is used for performing information decision is different: In Chapter 4, $\boldsymbol{y}$ is a $K \times 1$ vector obtained from K samples over one bit interval of the desired user; here for the frequency selective channel, $\boldsymbol{y}$ is obtained from blocks over one bit interval, and the signal in each block consists of information obtained from the L resolvable paths. The MAP detection here combines all paths of user 1 to yield the decision variable in (6.10) which is a quadratic function. Let γ_k, $k = 1, \ldots, 2JL$ be the eigenvalues of matrix $\boldsymbol{RQ}$, and define

$$\beta_u = \prod_{\substack{v=1 \\ v \neq u}}^{2JL} \frac{\gamma_u}{\gamma_u - \gamma_v}.$$

Then, in the case of distinct eigenvalues, the probability of error is given by

$$P_e = \sum_{\gamma_u < 0} \beta_u = \sum_{\gamma_u < 0} \prod_{\substack{v=1 \\ v \neq u}}^{2JL} \frac{\gamma_u}{\gamma_u - \gamma_v}. \tag{6.11}$$

6.3 Numerical Examples and Discussion

For a typical mobile radio channel, the average delay spread is $0.5\mu s$ in a suburban area and $3\mu s$ in an urban area [39]. Hence for a CDMA system with data rate 9.6 bps and spreading gain 128, approximately $L = 2$ and $L = 5$ resolvable paths can be resolved, respectively. We will focus on the low delay spread case ($L = 2$) case for our numerical examples, so the suburban environment with a total number of resolvable paths of $L = 2$ is considered. There are two major reasons for this: first, when there are more than three resolvable paths, fractional sampling gain will be relatively small; second, as the number of resolvable paths and the number of active users increase, it will be harder to realize the bit-by-bit decorrelator due to the matrix singularity problem.

The usual way to combine all L fingers for DPSK in a multipath fading channel is to use equal gain combining. For the proposed detector we have multiple samples per bit for every path and the decision variable is derived according to the ML decision rule. The performance of this detector depends on the parameters such as the number of users K, the number of samples per bit J and the fading rate f_dT. We will evaluate the effect of these parameters on the detector performance under the assumption that all paths are of equal strength and independent of each other, with the Jakes' model used to model the spaced-time correlation of the fading process. Comparison will be made between the ideal RAKE (assume zero path cross-correlation and no ISI) with equal gain combining of all resolvable fading paths in a single user environment, and the proposed detector in a multiuser environment. Gold sequences of length 127 are assigned to each user. Figs. 6.1 and 6.2 show the performance for $J = 2$, $f_dT = 0.01$ versus the number of samples. Observing that the single user ideal RAKE error floor occurs at approximately 35 dB, the performance of the proposed detector operating in a $K = 6$ and $K = 12$ user environment is

therefore very close to that of the single user ideal RAKE performance and didn't exhibit an error for the range of the SNRs considered.

Figs. 6.3 and 6.4 give the performance for normalized Doppler shift $f_dT = 0.04$, and Figs. 6.5 and 6.6 show the performance for a normalized Doppler shift $f_dT = 0.08$ with $J = 2$ and $J = 3$ samples per bit. Obviously, the error floor for the ideal RAKE in a single user environment for a relative high fading rate such as $f_dT = 0.08$ increased a lot compared to a slower fading of $f_dT = 0.01$, however, the proposed detector, even operating in a multiuser environment, demonstrated its superiority at higher fading rates. Its performance becomes better as the fading rate increases and no error was observed for the SNR range analyzed. In the region of small signal to noise ratio, the proposed detector performance is slightly worse than that of the ideal RAKE performance in a single user environment.

Through all these examples, we observed that for the same communication scenario the performance with $J = 2$ samples per bit is somewhat better than that for $J = 3$ samples per bit case. The reason for this is that with the increased number of samples per bit, the fractionally-spaced decorrelator performs worse and the incremental oversampling gain from $J = 2$ to $J = 3$ is too small to compensate for the performance loss due to decorrelation. The performance improvement due to oversampling, however, increases dramatically from one to two samples per bit, beyond that, it will be marginal. So in practice, $J = 2$ is usually enough for this detector structure in the frequency selective fading channel and the sampling points over one bit interval do not necessarily need to be uniform in time, although we can make it as uniform as possible.

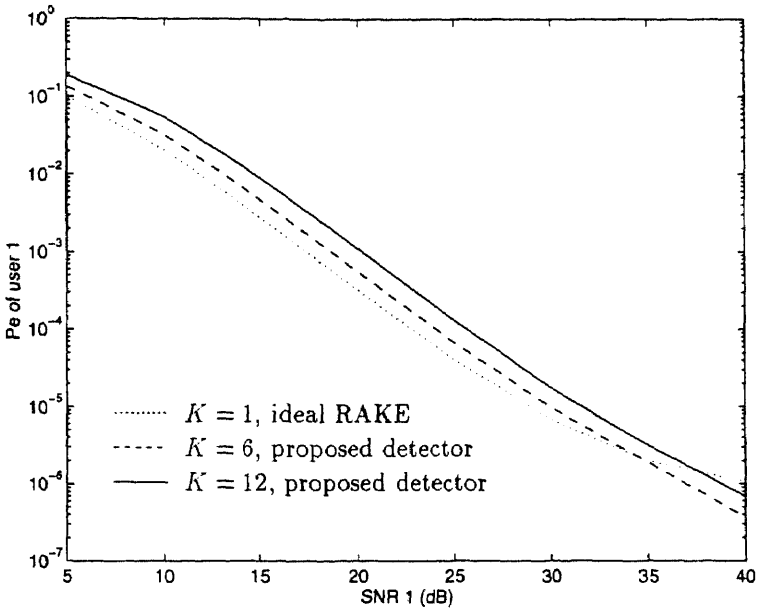

Figure 6.1 Performance comparison, $J = 2$, $f_d T = 0.01$

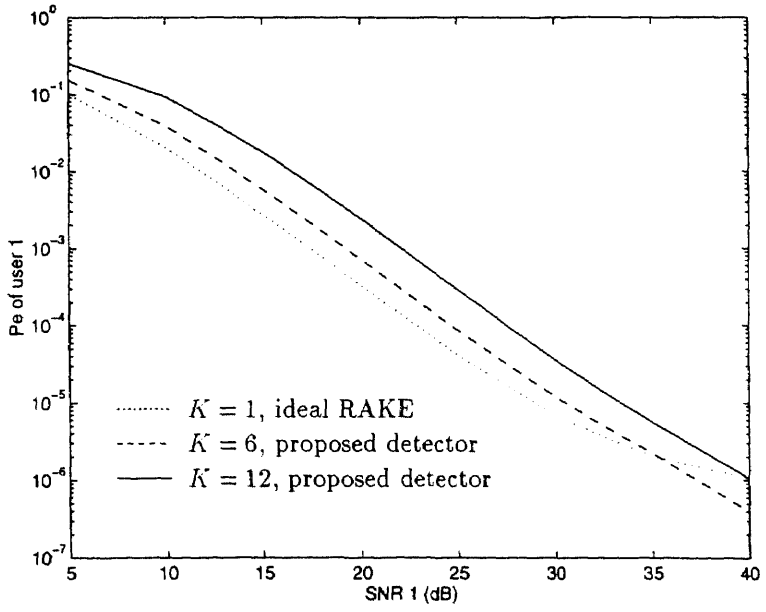

Figure 6.2 Performance comparison, $J = 3$, $f_d T = 0.01$

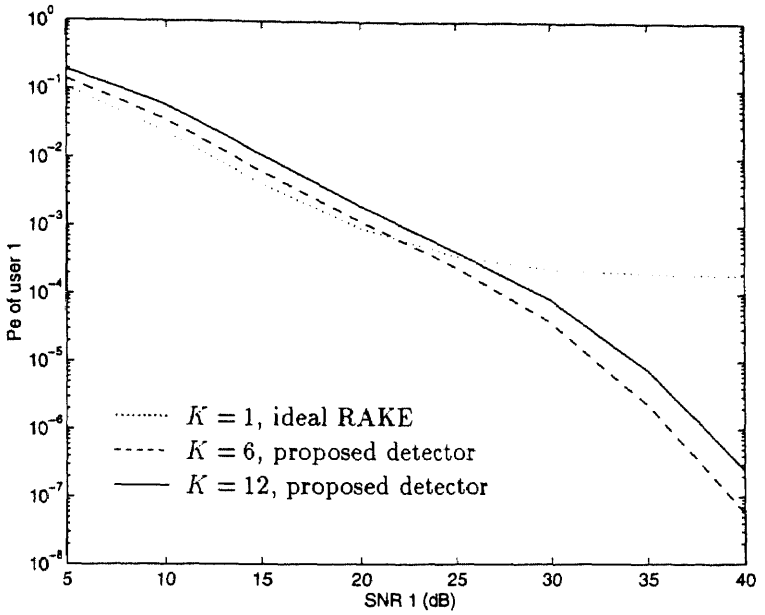

Figure 6.3 Performance comparison, $J = 2$, $f_dT = 0.04$

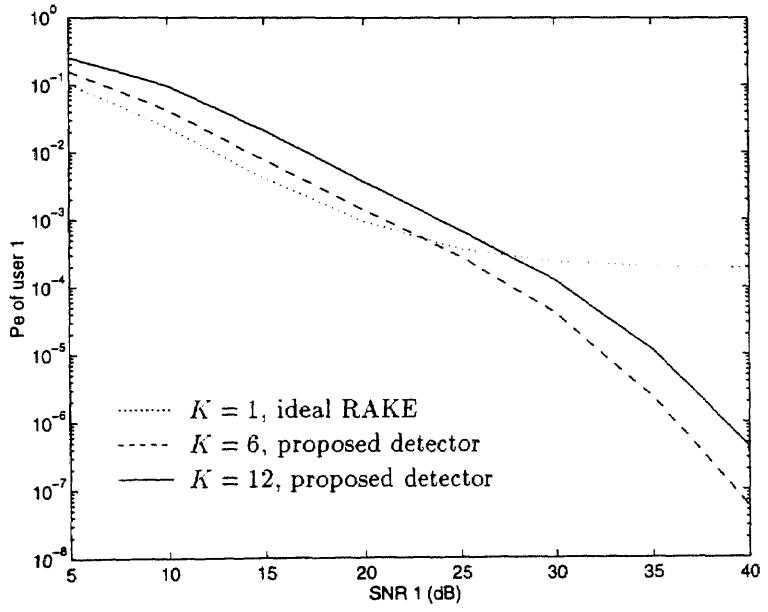

Figure 6.4 Performance comparison, $J = 3$, $f_dT = 0.04$

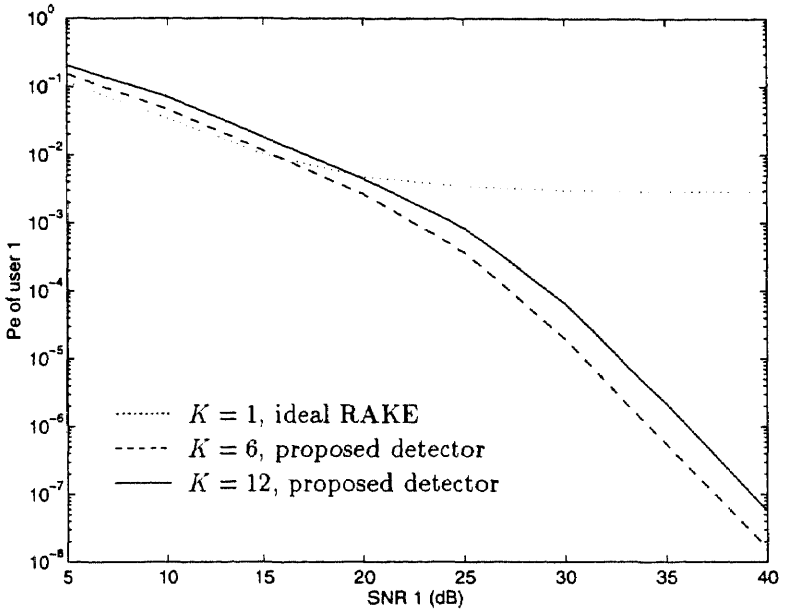

Figure 6.5 Performance comparison, $J = 2$, $f_dT = 0.08$

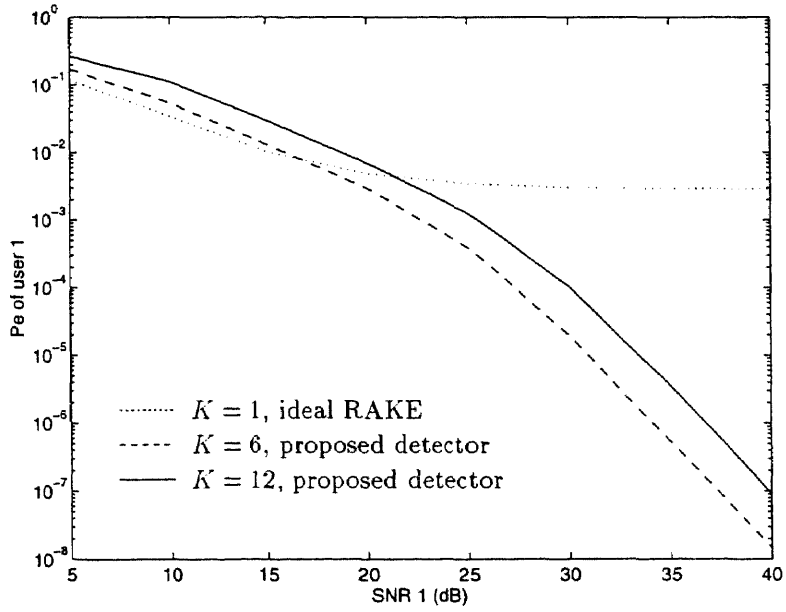

Figure 6.6 Performance comparison, $J = 3$, $f_dT = 0.08$

CHAPTER 7

COHERENT DETECTION FOR TIME-VARYING FREQUENCY SELECTIVE RAYLEIGH FADING CHANNELS

7.1 Introduction

In Chapter 6, we proposed a fractionally-spaced bit-by-bit decorrelating detector employing differentially coherent detection for a time-varying multipath channel fading channel. We demonstrated the performance improvement due to fractional sampling.

In this chapter, we consider coherent detection for the same environment as described in Chapter 6. The detection procedure following this decorrelator will exploit the following forms of diversity: first the effective time diversity achieved by fractional sampling over one bit interval in the time-varying fading channel; second, the time diversity achieved by the ability of the RAKE type of receiver to capture the energy contained in all resolvable multipaths in a frequency selective channel. Essentially, MRC is applied to the output at the bit-by-bit multipath decorrelator proposed in Section 3.4 to combine the energy for the same information contained in all blocks and all resolvable paths.

Channel estimation is, of course, needed for the maximum ratio combining. The DF MAP channel estimation structure and principle proposed in Section 5.3, although considered for a different channel situation, can be applied here by performing joint estimation at the decorrelator output on all paths and all blocks that correspond to the same information bit, simultaneously.

Chapter 7 is organized as follows: in Section 7.2, perfect channel estimates are assumed, and the corresponding error performance of this coherent detector represents the ultimate error lower bound that we can achieve for this type of structure. The adaptive channel estimates obtained by using the DF MAP channel estimator applied to the multipath decorrelator output are then used to perform

coherent detection in Section 7.3. Numerical examples are provided in Section 7.4 followed by a performance comparison between the detector of Chapter 6 and that of this coherent detector in the same environment.

7.2 Coherent Detection with Perfect Channel Estimates

The received baseband signal $r(t)$ was given in (3.2) for a K-user asynchronous CDMA time-varying frequency selective Rayleigh fading channel and all the definitions presented there apply here. The channel spaced-time correlation function is described in (3.3) and the fading channel model is given in (3.5).

Following the fractionally-spaced decorrelator structure in Section 3.4, the decorrelated output for user 1 is given in (3.11), and is shown here for convenience, i.e.,

$$\boldsymbol{z}(i) = \begin{bmatrix} \boldsymbol{z}^{(b1)}(i) \\ \vdots \\ \boldsymbol{z}^{(bJ)}(i) \end{bmatrix} = b_1(i)\sqrt{a_1}\mathcal{E}\boldsymbol{C}(i) + \boldsymbol{\xi}(i).$$

This vector of JL elements corresponds to the same information bit, therefore, coherent detection for bit i of user 1 can be carried out by optimally combining all JL elements. Notice that the noise components of $\boldsymbol{z}(i)$ are correlated, with the covariance matrix $\boldsymbol{R}_\xi$ defined in (3.19). So before the combining, a noise whitening filter $(\boldsymbol{T}^H)^{-1}$ should be applied to $\boldsymbol{z}(i)$ where $\boldsymbol{T}$ can be obtained by the Cholesky decomposition

$$\boldsymbol{R}_\xi = \boldsymbol{T}^H\boldsymbol{T}, \tag{7.1}$$

in which $\boldsymbol{R}_\xi$ is Hermitian and positive definite for practical situations. The whitening filter output for user 1 can be expressed as a $JL \times 1$ vector

$$\begin{aligned} \boldsymbol{y} &= (\boldsymbol{T}^H)^{-1}\boldsymbol{z}(i) \\ &= b_1(i)\sqrt{a_1}(\boldsymbol{T}^H)^{-1}\mathcal{E}\boldsymbol{C}(i) + \sqrt{a_1}(\boldsymbol{T}^H)^{-1}\boldsymbol{\xi}(i) \\ &= \sqrt{a_1}\boldsymbol{w}b_1 + \boldsymbol{\zeta}, \end{aligned} \tag{7.2}$$

where

$$\boldsymbol{w} = (\boldsymbol{T}^H)^{-1}\,\mathcal{E}\boldsymbol{C}(i), \tag{7.3}$$

$$\boldsymbol{\zeta} = (\boldsymbol{T}^H)^{-1}\,\boldsymbol{\xi}(i). \tag{7.4}$$

Equation (7.3) represents the equivalent channel vector, which can be obtained from the actual channel vector adjusted by the whitening matrix $(\boldsymbol{T}^H)^{-1}$ and the energy in each block $\mathcal{E}$. The channel covariance matrix can be expressed as

$$\boldsymbol{R}_w = (\boldsymbol{T}^H)^{-1}\,\mathcal{E}\boldsymbol{R}_c\mathcal{E}\,(\boldsymbol{T}^H)\,, \tag{7.5}$$

where $\boldsymbol{R}_c$ is defined in (3.16), and it is easy to show that

$$E\left[\boldsymbol{\zeta}\boldsymbol{\zeta}^H\right] = N_0\boldsymbol{I}. \tag{7.6}$$

The covariance matrix of $\boldsymbol{y}$ can then be expressed as

$$\boldsymbol{R}_y = a_1\boldsymbol{R}_w + N_0\boldsymbol{I}.$$

Assuming the availability of the perfect channel vector $\boldsymbol{w}$ in (7.3), the decision variable for the coherent detection at the noise whitened decorrelator output in (7.2) can be written as

$$\lambda_i = \Re\{\boldsymbol{w}^H\boldsymbol{y}\}. \tag{7.7}$$

Let

$$\boldsymbol{v} = \begin{bmatrix} \boldsymbol{w} \\ \boldsymbol{y} \end{bmatrix},$$

so the coherent decision variable in (7.7) can be written as

$$\begin{aligned} \lambda_i &= \begin{bmatrix} \boldsymbol{w} \\ \boldsymbol{y} \end{bmatrix}^H \begin{bmatrix} \mathbf{o} & 0.5\boldsymbol{I} \\ 0.5\boldsymbol{I} & \mathbf{o} \end{bmatrix} \begin{bmatrix} \boldsymbol{w} \\ \boldsymbol{y} \end{bmatrix} \\ &= \boldsymbol{v}^H\boldsymbol{Q}\boldsymbol{v}, \end{aligned} \tag{7.8}$$

where $\mathbf{o}$ is a $JL \times JL$ matrix with all elements equal to zero. Introduce matrix

$$\boldsymbol{V} = E[\boldsymbol{v}\boldsymbol{v}^H] = E\left\{\begin{bmatrix} \boldsymbol{w} \\ \boldsymbol{y} \end{bmatrix}[\boldsymbol{w}^H\boldsymbol{y}^H]\right\}.$$

The $2JL \times 2JL$ matrix $\boldsymbol{VQ}$ can be written as

$$\boldsymbol{VQ} = 0.5 \begin{bmatrix} \sqrt{a_1}\boldsymbol{R}_w & \boldsymbol{R}_w \\ a_1\boldsymbol{R}_w + N_0\boldsymbol{I} & \sqrt{a_1}\boldsymbol{R}_w \end{bmatrix},$$

The error performance for the quadratic function in (7.8) is

$$P_e = P\{\lambda_i < 0\} = \sum_{\gamma_l<0} \prod_{\substack{m=1 \\ m\neq l}}^{2JL} \frac{\gamma_l}{\gamma_l - \gamma_m}, \tag{7.9}$$

in which $\gamma_1, \ldots, \gamma_{2K}$ are the eigenvalues of the matrix $\boldsymbol{VQ}$.

This error performance in (7.9) represents the ultimate error lower bound that can be achieved for this coherent multiuser structure.

7.3 Coherent Detection with Adaptive Channel Estimates

The estimation of the equivalent channel in (7.3) can be obtained by applying the principle of the decision feedback MAP channel estimator proposed in Section 5.3 on the equivalent channel vector $\boldsymbol{w}$. Given the desired user's signal vector $\boldsymbol{y}$ from bit $(i-M)$ to $(i-1)$, and the information bit decisions for the same bit indices, we want to estimate $\boldsymbol{w}$, the $JL \times 1$ channel vector in the i^{th} bit interval. The DF MAP channel estimates are

$$\widehat{\boldsymbol{w}}(i) = \boldsymbol{R}_{y21}\boldsymbol{R}_{y11}^{-1}\mathcal{Y}_{i-1}, \tag{7.10}$$

where $\mathcal{Y}_{i-1}$, $\boldsymbol{R}_{y11}$ and $\boldsymbol{R}_{y21}$ are defined in (5.14), (5.17) and (5.19), respectively.

Without loss of generality, we will assume that the transmitted bit is 1 when deriving the error probability of the detector for coherent detection. The coherent decision variable under the adaptive channel estimates can be written as

$$\begin{aligned} \lambda_i &= \Re\{\widehat{\boldsymbol{w}}^H\boldsymbol{y}\} \\ &= \begin{bmatrix} \widehat{\boldsymbol{w}} \\ \boldsymbol{y} \end{bmatrix}^H \begin{bmatrix} \mathbf{0} & 0.5\boldsymbol{I} \\ 0.5\boldsymbol{I} & \mathbf{0} \end{bmatrix} \begin{bmatrix} \widehat{\boldsymbol{w}} \\ \boldsymbol{y} \end{bmatrix} \\ &= \boldsymbol{v}^H\boldsymbol{Q}\boldsymbol{v}, \end{aligned} \tag{7.11}$$

where o is a $JL \times JL$ matrix with all elements equal to zero, and

$$\boldsymbol{v} = \begin{bmatrix} \widehat{\boldsymbol{w}} \\ \boldsymbol{y} \end{bmatrix},$$

with the covariance matrix

$$\boldsymbol{V} = E\{\boldsymbol{v}\boldsymbol{v}^H\} = E\left\{\begin{bmatrix} \widehat{\boldsymbol{w}} \\ \boldsymbol{y} \end{bmatrix}[\widehat{\boldsymbol{w}}^H \boldsymbol{y}^H]\right\}.$$

Matrix $\boldsymbol{VQ}$ is expressed as

$$\boldsymbol{VQ} = 0.5\begin{bmatrix} \sqrt{a_1}\boldsymbol{R}_{y21}\boldsymbol{R}_{y11}^{-1}\boldsymbol{R}_{y12} & \boldsymbol{R}_{y21}\boldsymbol{R}_{y11}^{-1}\boldsymbol{R}_{y12} \\ a_1\boldsymbol{R}_{y22} + N_0\boldsymbol{I} & \sqrt{a_1}\boldsymbol{R}_{y21}\boldsymbol{R}_{y11}^{-1}\boldsymbol{R}_{y12} \end{bmatrix}.$$

As described in Chapter 5, in the case of distinct eigenvalues the probability of error of the quadratic decision variable is

$$P_e = P\{\lambda_i < 0\} = \sum_{\gamma_l<0} \prod_{\substack{m=1 \\ m\neq l}}^{2JL} \frac{\gamma_l}{\gamma_l - \gamma_m}, \tag{7.12}$$

in which $\gamma_1, \ldots, \gamma_{2JL}$ are the eigenvalues of the matrix $\boldsymbol{VQ}$.

7.4 Numerical Examples and Discussion

Several examples will be presented in this section to evaluate the performance of this detector and its dependence on various parameters such as number of samples per bit J, fading rate f_dT and number of users K. Jakes' model is used and Gold sequences of length 127 are assigned to each user. We assume the availability of perfect channel estimates first and the performance comparison for this case is made between the bit-spaced ideal RAKE receiver in a single user scenario and the proposed detector in a multiuser scenario. In Figs. 7.1 and 7.2, $f_dT = 0.01$ was chosen for $J = 2$ and $J = 3$ samples per bit. Under this fading rate, performance for the $J = 3$ case is a little bit worse than that of $J = 2$ since the decorrelator performs a little bit worse for the latter due to the increased condition number of its correlation matrix. Figs. 7.3-7.6 show the performance for $f_dT = 0.04$ and $f_dT = 0.08$. In the case of

a relatively fast fading of $f_dT = 0.08$, performance for the case of $J = 3$ is better than that of $J = 2$, and as the signal to noise ratio increases the multiuser detector in a multiuser scenario of $K = 6$ and $K = 12$ outperforms the ideal RAKE (single sample per bit) that operates in a single user transmission scenario.

Error performance lower bounds of the proposed receiver using the DF MAP channel estimates are given in Figs. 7.7-7.12 for different f_dT, K and J values. Again, as described in Chapter 5, this error rate lower bound is obtained by assuming correct previous bit decisions in performing the decision feedback MAP channel estimation with the memory depth of $M = 4$. Since we do not have an appropriate existing channel estimator [1] for the channel fading process modeled by Jakes' model, the performance of single user transmission is not shown here. We observe that only for a relative fast fading ($f_dT = 0.08$), performance of $J = 3$ is better than that of $J = 2$. For the proposed multiuser detector with the fractionally spaced DF MAP, error floor was not observed even for an SNR up to $40dB$ and a fading rate as high as $f_dT = 0.08$.

Performance comparisons between the differentially coherent multiuser proposed in Chapter 6 and the coherent multiuser detector with the DF MAP channel estimates for the same frequency selective environment are shown in Fig. 7.13 and 7.14 for $J = 2$ and $J = 3$, respectively, wherein the curves for the coherent detector are the error lower bounds obtained by assuming correct previous decisions in performing channel estimation. From these two figures, we see that the performance lower bound of the coherent detector is a little bit worse than that of the DPSK detector in the signal to noise ratio range of $5 - 40$ dB.

[1] In [80], Jakes' model is approximated by using the second order AR model and a Kalman filter is then applied for channel estimation.

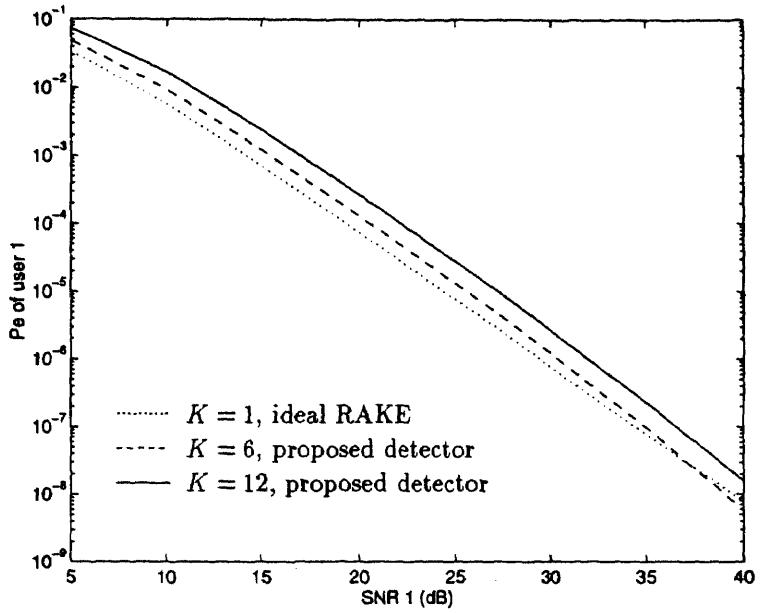

Figure 7.1 Performance with perfect channel estimates, $J = 2$, $f_d T = 0.01$

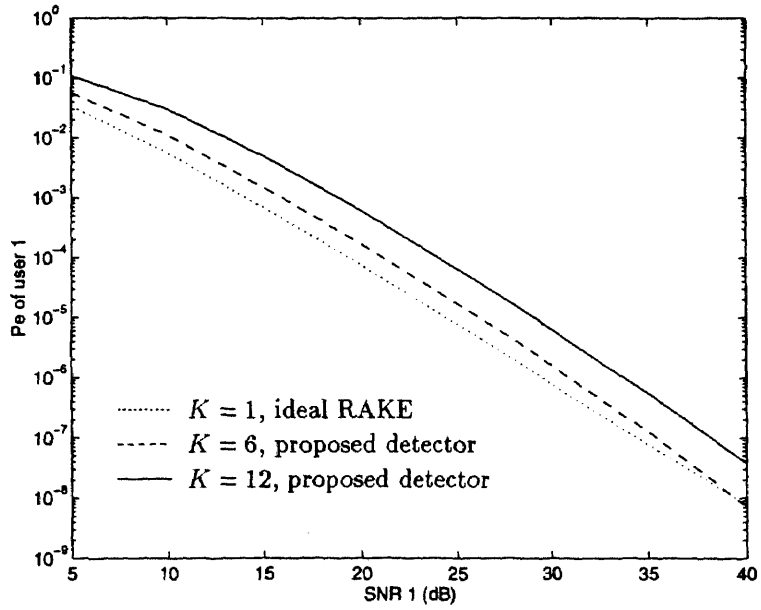

Figure 7.2 Performance with perfect channel estimates, $J = 3$, $f_d T = 0.01$

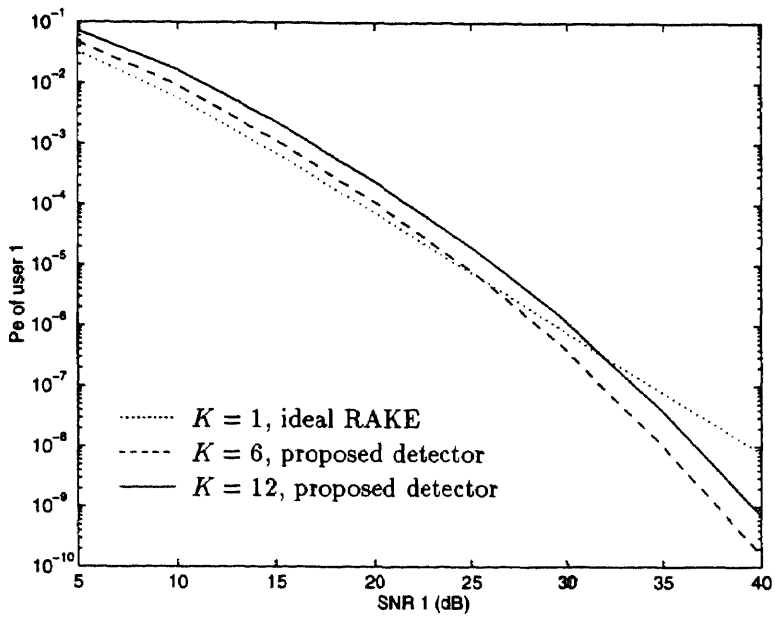

Figure 7.3 Performance with perfect channel estimates, $J = 2$, $f_dT = 0.04$

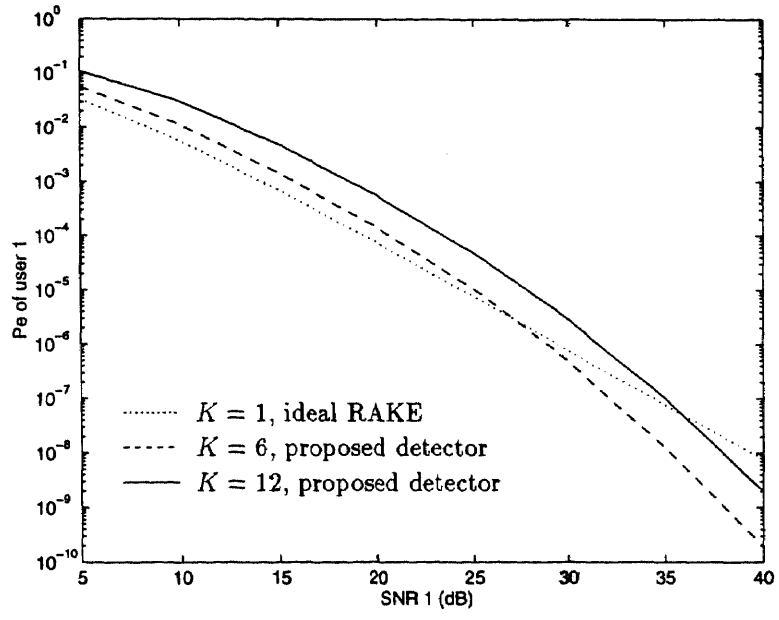

Figure 7.4 Performance with perfect channel estimates, $J = 3$, $f_dT = 0.04$

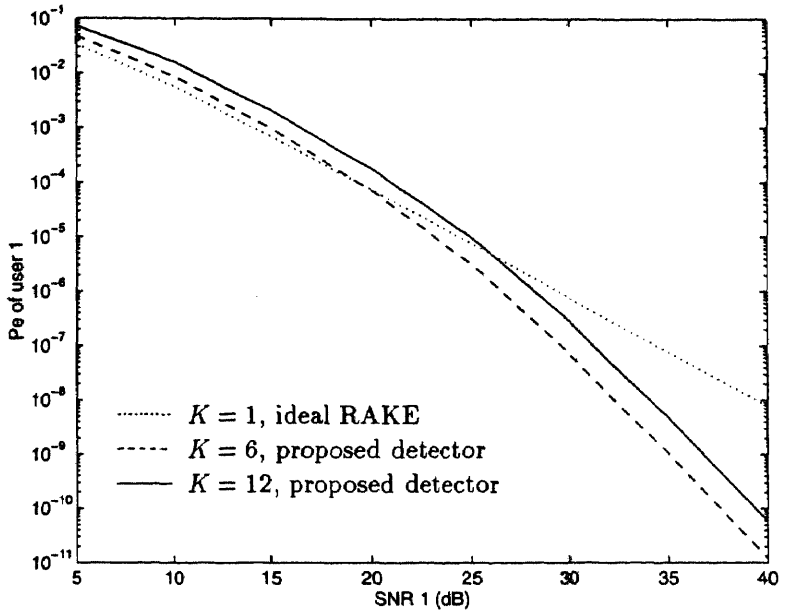

Figure 7.5 Performance with perfect channel estimates, $J = 2$, $f_dT = 0.08$

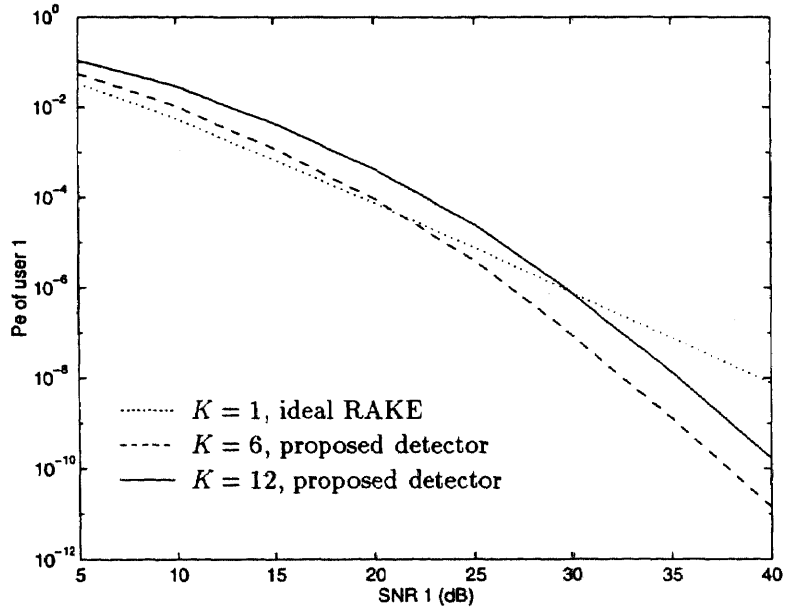

Figure 7.6 Performance with perfect channel estimates, $J = 3$, $f_dT = 0.08$

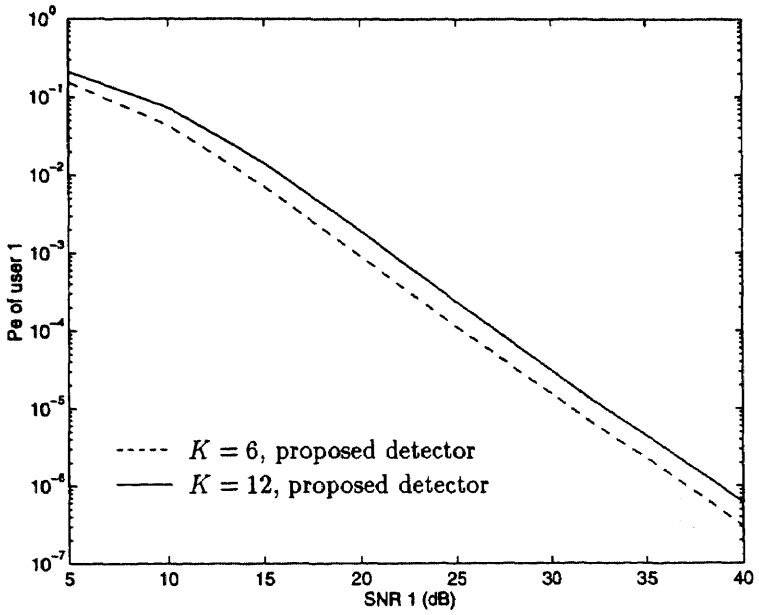

Figure 7.7 Performance lower bound with the DF MAP channel estimates, $J = 2$, $f_dT = 0.01$

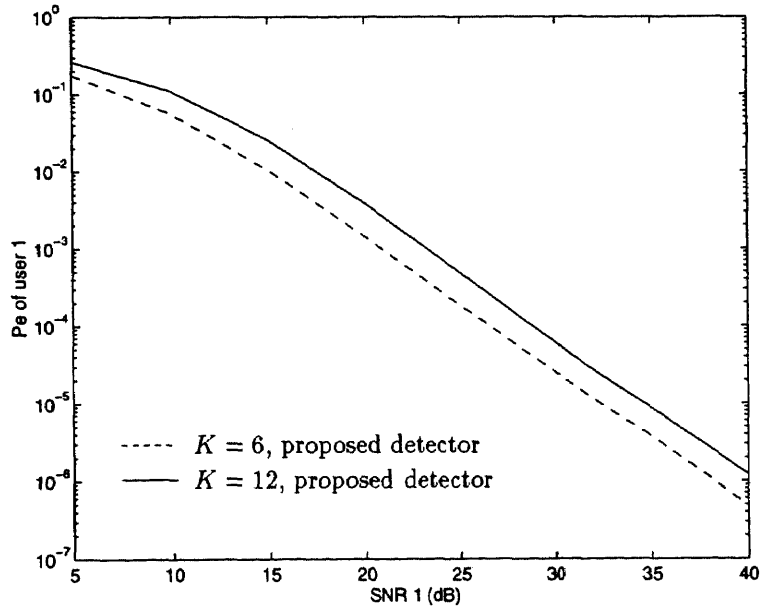

Figure 7.8 Performance lower bound with the DF MAP channel estimates, $J = 3$, $f_dT = 0.01$

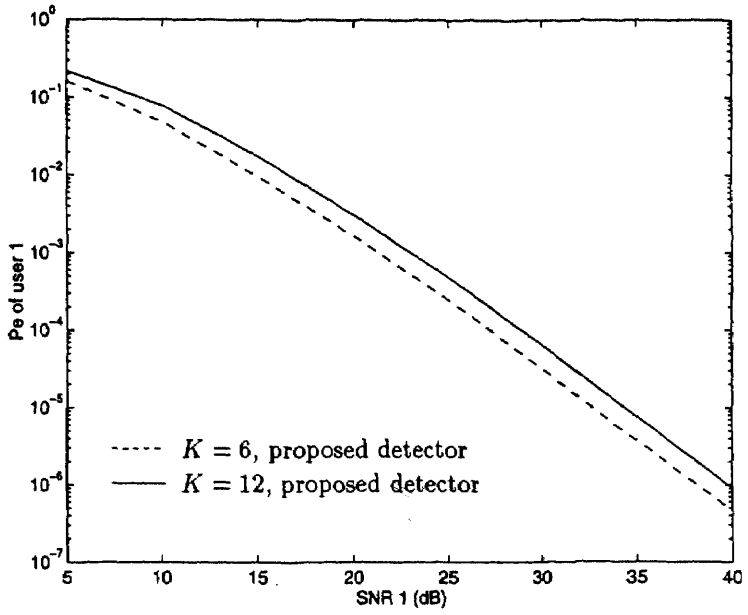

Figure 7.9 Performance lower bound with the DF MAP channel estimates, $J = 2$, $f_dT = 0.04$

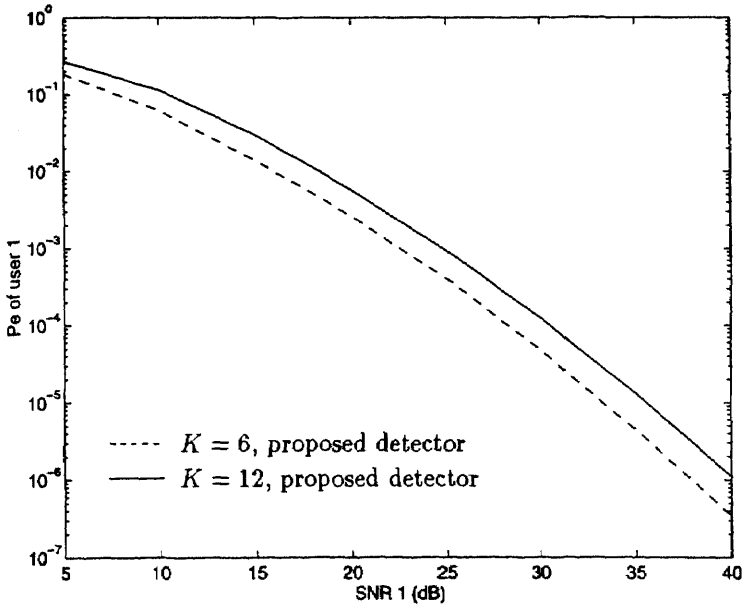

Figure 7.10 Performance lower bound with the DF MAP channel estimates, $J = 3$, $f_dT = 0.04$

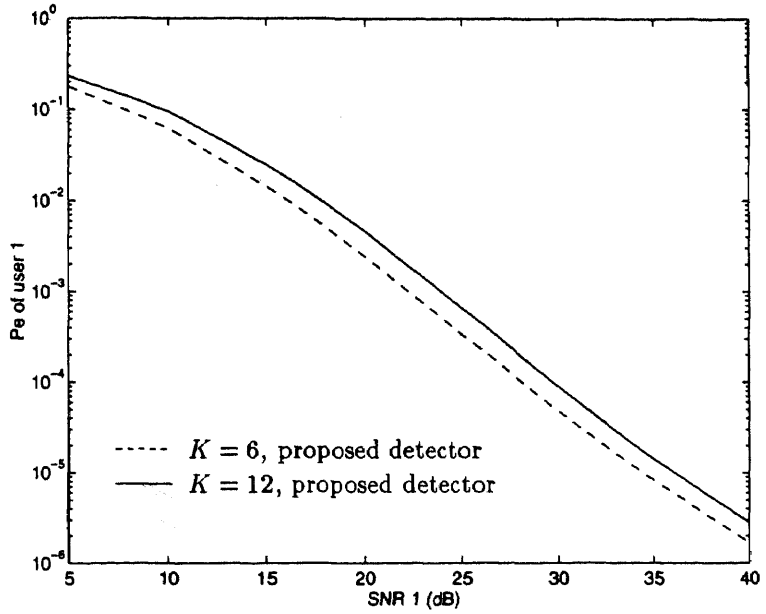

Figure 7.11 Performance lower bound with the DF MAP channel estimates, $J = 2$, $f_dT = 0.08$

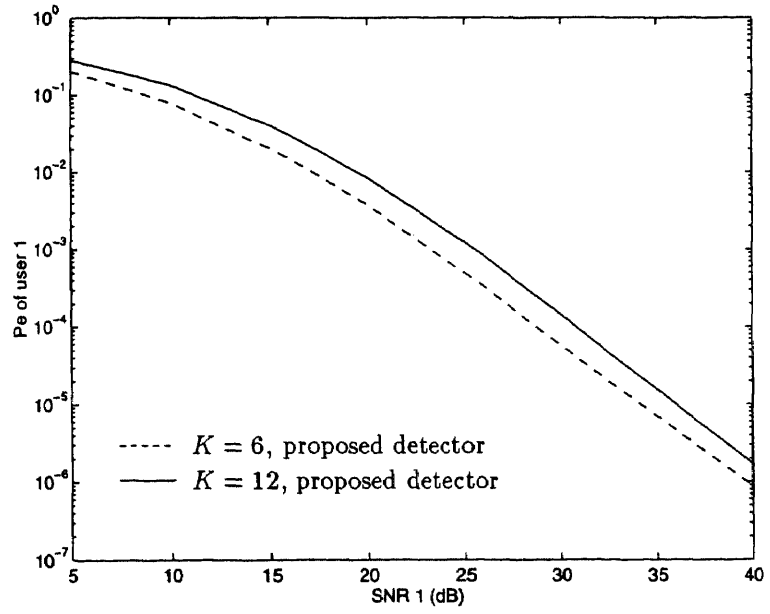

Figure 7.12 Performance lower bound with the DF MAP channel estimates, $J = 3$, $f_dT = 0.08$

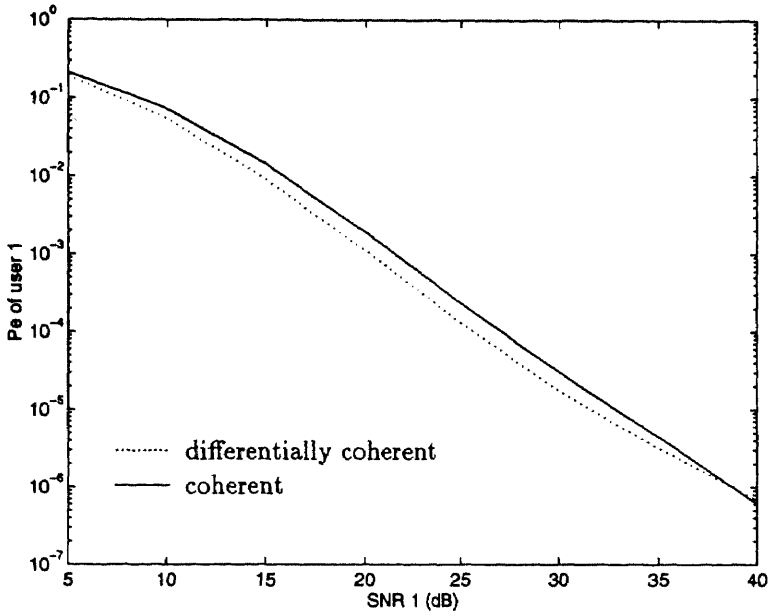

Figure 7.13 Performance comparison of the coherent and differentially coherent detector, $J = 2$, $f_dT = 0.01$, $K = 12$ and $L = 2$

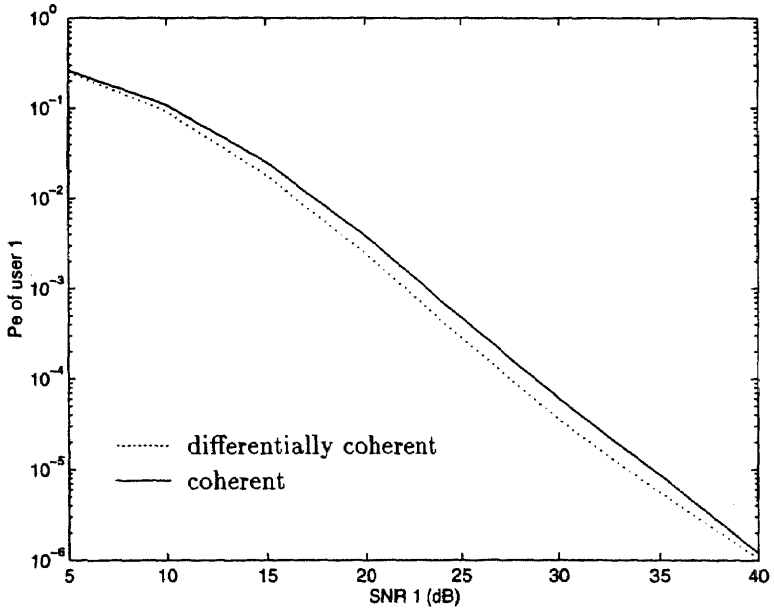

Figure 7.14 Performance comparison of the coherent and differentially coherent detector, $J = 3$, $f_dT = 0.01$, $K = 12$ and $L = 2$

CHAPTER 8

CONCLUSIONS

In this dissertation, we proposed novel low complexity decorrelating multiuser detectors in DS-CDMA time-varying frequency nonselective and frequency selective fading channel and analyzed their performance. We addressed two important problems of existing multiuser detectors in the time-varying fading environment: the error floor associated with coherent or differentially coherent signaling in a time-varying fading channels, and the decorrelator complexity. Throughout the dissertation, an analytical approach is employed and Monte Carlo simulation is used to confirm our theoretical results.

We started with looking at the impact of the reverse link power control imperfection on the multiple access interference in the IS-95 system. The multiple access interference versus power control imperfection analysis is performed based on solving the simultaneous linear equations for the mobiles' required transmitted power wherein each mobile's transmitted power represents the interference of the other mobiles in the system. Large standard deviation of received signal to interference plus noise density ratio of each user was shown to affect system average interference appreciably.

Then we considered the issue of multiuser detection in a mobile environment. In the frequency nonselective fading channels, both differentially coherent and coherent detection methods were employed in conjunction with the decorrelating type of multiuser detectors. The underlying approach in the design of the proposed detectors is based on employing fractional sampling. Beside providing the basis of the realization of a low complexity bit-by-bit decorrelator in the asynchronous CDMA channel, fractional sampling also provides the basis of the exploitation of a form of time-diversity in the time-varying fading channel. For the differentially coherent

detection, a maximum likelihood detection is applied at the fractionally-spaced decorrelator output resulting in a DPSK multiuser detector with a significantly lowered error floor. For the coherent detection, we proposed a fractionally-spaced single-stage and a two-stage decision feedback maximum *a posteriori* channel estimator to obtain the complex channel state of a Rayleigh fading channel. The single-stage channel estimator is then applied at the fractionally-spaced decorrelator output to estimate the complex Rayleigh fading channel for the coherent detection. Through numerous numerical examples, we found that this multiuser detector works very well even for a relatively fast fading of $f_dT = 0.08$ when Jakes' channel model is adopted. Another important feature of the proposed channel estimator is that it can be applied to a Rayleigh fading channel with an arbitrary spaced-time correlation function. Performance comparisons are made between the proposed multiuser detector operating in a multiuser environment and that of the conventional single sample per bit DPSK, or coherent receiver operating in a single user environment. Clear error performance superiority of the proposed detectors was observed in the time-varying frequency nonselective fading channels.

The fractionally-sampled multiuser detector structure was also extended to the time-varying frequency selective fading channels. The fractionally-spaced decorrelator is applied to eliminate MAI, ISI, and path cross-correlation interference. Maximum likelihood detection is then applied to the signal vector over two consecutive bit intervals for DPSK, and by a maximum ratio combiner on the signal vector over one bit interval for coherent detection. For the differentially coherent detection, the proposed multiuser detector did not exhibit an error floor for a fading rate of $f_dT = 0.08$ at SNR as high as 40 dB in the presence of MAI, while the symbol-spaced ideal RAKE receiver exhibited an error floor for all fading rates considered ($f_dT = 0.01,\ 0.04,\ 0.08$) even in the absence of MAI. For coherent detection, the channel estimates are obtained using the proposed single-stage DF

MAP channel estimator at the decorrelator output devoid of MAI, ISI, and path cross-correlation interference for each path of each user. Perfect channel estimates are assumed first, and numerical examples for this case show that the performance of the proposed detector in a multiuser environment rivals that of the ideal RAKE receiver in a single user environment for a relatively slow fading ($f_dT = 0.01$). As the fading rate and the SNR increase, the proposed detector with the MAI present demonstrated superior performance to that of the ideal RAKE receiver in a single user environment. When the proposed DF MAP channel estimates are employed for coherent detection, we were unable to make a comparison with the conventional RAKE receiver because there are no existing channel estimators in the literature for a Rayleigh fading channel whose spaced-time correlation function is given by Jakes' model. But the proposed detector did not exhibit an error floor even for a relatively fast fading of $f_dT = 0.08$ at SNR as high as 40 dB. Although in our numerical examples we considered the low number of resolvable multipaths ($L = 2$), and a low number of samples per bit ($J = 2$ and $J = 3$), the general structure is applicable for any values of L and J.

Throughout the dissertation, we assumed the availability of the channel second order statistics (spaced-time correlation) and users' relative delays. In order to perform decorrelation, we have to invert the correlation matrices. Although we addressed the matrix singularity problem and suggested solutions to this problem with limitted simulations, we did not perform any analytical analysis for this problem. The future research based on the achievements in this dissertation may include

- algorithms of adaptive or non-adaptive type for estimation of the spaced-time correlation of a time-varying fading channel and the detector performance analysis by applying the proposed algorithms to a time-varying multiuser environment.

- sensitivity analysis of the proposed detector performance when the channel spaced-time correlation exhibits mismatch.

- further research regarding the singularity problem of the correlation matrices for the fractionally-sampled decorrelator for either un-filtered or filtered signature waveforms and their impact on the error performance of the proposed detectors.

- performance of the receiver with antenna diversity for frequency nonselective or selective channels.

- examination the use of the single and two-stage DF MAP channel estimators for adaptive multiuser detection in a time-varying fading channel and comparison with the performance of the MMSE type of adaptive multiuser detectors in the same environment.

- extension of the proposed detector structure to wideband and multi-rate CDMA for a similar communications environment.

APPENDIX A

LINEAR TRANSFORMATION USED IN DERIVING (4.10)

Considering the differentially encoded symbols $b_1(i-1)$ and $b_1(i)$ in the intervals $(i-1)$ and i, respectively, define

$$\boldsymbol{S} = \begin{bmatrix} \boldsymbol{S}(i-1) \\ \boldsymbol{S}(i) \end{bmatrix} = \begin{bmatrix} \sqrt{a_1}\mathcal{E}_1(i)\boldsymbol{C}_1(i-1) + \boldsymbol{\xi}_1(i-1) \\ \sqrt{a_1}\mathcal{E}_1(i)\boldsymbol{C}_1(i) + \boldsymbol{\xi}_1(i) \end{bmatrix},$$

which corresponds to the received signals of user 1 over the $(i-1)^{th}$ and the i^{th} bit intervals with transmitted differentially encoded bits $b_1(i-1)$ and $b_1(i)$ removed. Also defining

$$\boldsymbol{U} = E\{\boldsymbol{S}(i)\boldsymbol{S}(i)^H\},$$

a $K \times K$ matrix representing the correlation matrix over one symbol interval, and

$$\boldsymbol{V} = E\{\boldsymbol{S}(i-1)\boldsymbol{S}(i)^H\},$$

a $K \times K$ matrix representing the cross-correlation matrix over adjacent bit intervals, matrix $\boldsymbol{R}$ can be partitioned as

$$\begin{aligned} \boldsymbol{R} &= E\{\boldsymbol{S}\boldsymbol{S}^H\}, \\ &= \begin{bmatrix} \boldsymbol{U} & \boldsymbol{V} \\ \boldsymbol{V}^H & \boldsymbol{U} \end{bmatrix}. \end{aligned}$$

The inverse of $\boldsymbol{R}$ in (4.5) can be obtained by using a matrix inversion lemma as in [7].

Matrix $\boldsymbol{Q}$ can be transformed into

$$\boldsymbol{Q} = \begin{bmatrix} \mathbf{o} & \boldsymbol{\Delta} \\ \boldsymbol{\Delta}^H & \mathbf{o} \end{bmatrix},$$

where $\mathbf{o}$ is a $K \times K$ matrix with all elements equal to zero,

$$\boldsymbol{\Delta} = 2\boldsymbol{U}^{-1}\boldsymbol{V}\boldsymbol{\Theta}^{-1},$$

and

$$\boldsymbol{\Theta} = \boldsymbol{U} - \boldsymbol{V}^H \boldsymbol{U}^{-1} \boldsymbol{V}.$$

It is easy to show that the decision variable in (4.9) is equivalent to

$$\begin{aligned} \lambda_i &= \boldsymbol{S}^H \begin{bmatrix} \mathbf{0} & \boldsymbol{B}_1(i-1)\boldsymbol{B}_1(i)\boldsymbol{\Delta} \\ \boldsymbol{B}_1(i-1)\boldsymbol{B}_1(i)\boldsymbol{\Delta}^H & \mathbf{0} \end{bmatrix} \boldsymbol{S} \\ &= d_1(i)\boldsymbol{S}^H \begin{bmatrix} \mathbf{0} & \boldsymbol{\Delta} \\ \boldsymbol{\Delta}^H & \mathbf{0} \end{bmatrix} \boldsymbol{S}, \end{aligned} \tag{A.1}$$

where $d_1(i) = b_1(i-1)b_1(i) \in [-1, 1]$ is the i^{th} information bit before differential encoding.

We can then transform $\boldsymbol{S}$, whose elements of the signal part are correlated with each other, into another complex Gaussian random vector with unit variance and independent elements using a linear transformation.

APPENDIX B

DERIVATION OF EQUATION (5.35)

$$\begin{aligned} p\{\boldsymbol{w}(i)|\mathcal{Y}_{i-1},\ \tilde{\boldsymbol{y}}(i)\} &= \frac{p\{\boldsymbol{w}(i),\ \mathcal{Y}_{i-1},\ \tilde{\boldsymbol{y}}(i)\}}{p\{\mathcal{Y}_{i-1},\ \tilde{\boldsymbol{y}}(i)\}} \\ &= \frac{p\{\tilde{\boldsymbol{y}}(i)|\mathcal{Y}_{i-1},\ \boldsymbol{w}(i)\}p\{\mathcal{Y}_{i-1},\ \boldsymbol{w}(i)\}}{p\{\mathcal{Y}_{i-1},\ \tilde{\boldsymbol{y}}(i)\}}. \end{aligned} \tag{B.1}$$

The received signal vector in the i^{th} bit interval with the data removed (by using tentative decisions) can be expressed as

$$\tilde{\boldsymbol{y}}(i) = \sqrt{a}[\tilde{b}(i)b(i)]\boldsymbol{w}(i) + \boldsymbol{\xi}(i).$$

It can be concluded from the above equation that the appearance of the previous received signal vector $\mathcal{Y}_{i-1}$ does not remove the uncertainty of $\tilde{\boldsymbol{y}}(i)$ if we have $\boldsymbol{w}(i)$, so the following equation is valid

$$p\{\tilde{\boldsymbol{y}}(i)|\mathcal{Y}_{i-1},\ \boldsymbol{w}(i)\} = p\{\tilde{\boldsymbol{y}}(i)|\boldsymbol{w}(i)\}. \tag{B.2}$$

Hence (B.1) can be written as

$$\begin{aligned} p\{\boldsymbol{w}(i)|\mathcal{Y}_{i-1},\ \tilde{\boldsymbol{y}}(i)\} &= \frac{p\{\tilde{\boldsymbol{y}}(i)|\boldsymbol{w}(i)\}p\{\mathcal{Y}_{i-1},\ \boldsymbol{w}(i)\}}{p\{\mathcal{Y}_{i-1},\ \tilde{\boldsymbol{y}}(i)\}} \\ &= \frac{p\{\mathcal{Y}_{i-1},\ \boldsymbol{w}(i)\}p\{\tilde{\boldsymbol{y}}(i),\ \boldsymbol{w}(i)\}}{p\{\mathcal{Y}_{i-1},\ \tilde{\boldsymbol{y}}(i)\}p\{\boldsymbol{w}(i)\}}, \end{aligned} \tag{B.3}$$

which gives (5.35).

APPENDIX C

DERIVATION OF EQUATION (5.47)

Recall the definition of

$$\mathcal{Y} = [\mathcal{Y}_{i-1}^T,\ \boldsymbol{w}(i)^T]^T,$$

in (5.15), and

$$\mathcal{Z} = [\tilde{\boldsymbol{y}}(i)^T,\ \boldsymbol{w}(i)^T]^T,$$

in (5.36). Since $\mathcal{Y}_{i-1}$, $\boldsymbol{w}(i)$ and $\tilde{\boldsymbol{y}}(i)$ are complex Gaussian random vectors, so are $\mathcal{Y}$ and $\mathcal{Z}$. Hence both $\mathcal{Y}$ and $\mathcal{Z}$ have complex Gaussian distribution. Because $p\{\mathcal{Y}_{i-1},\ \tilde{\boldsymbol{y}}(i)\}$ in (5.35) is independent of the channel vector $\boldsymbol{w}(i)$, (5.35) can be simplified as

$$p\{\boldsymbol{w}(i)|\mathcal{Y}_{i-1},\ \tilde{\boldsymbol{y}}(i)\} = \mathcal{C}\ exp\{-\mathcal{Y}^H \boldsymbol{R}_{\mathcal{Y}}^{-1}\mathcal{Y} - \mathcal{Z}^H \boldsymbol{R}_{\mathcal{Z}}^{-1}\mathcal{Z} + \boldsymbol{w}(i)^H \boldsymbol{R}_w^{-1}\boldsymbol{w}(i)\}, \quad \text{(C.1)}$$

where $\mathcal{C}$ is a constant. Maximizing the above probability density function is equivalent to minimizing the following quadratic function

$$l = \mathcal{Y}^H \boldsymbol{R}_{\mathcal{Y}}^{-1}\mathcal{Y} + \mathcal{Z}^H \boldsymbol{R}_{\mathcal{Z}}^{-1}\mathcal{Z} - \boldsymbol{w}(i)^H \boldsymbol{R}_w^{-1}\boldsymbol{w}(i). \quad \text{(C.2)}$$

Substitution of (5.23) and (5.42) into the above equation gives

$$\begin{aligned} l \ = \ & \left[\mathcal{Y}_{i-1}^H\ \boldsymbol{w}(i)^H\right] \begin{bmatrix} \boldsymbol{R}_{\mathcal{Y}i11} & \boldsymbol{R}_{\mathcal{Y}i12} \\ \boldsymbol{R}_{\mathcal{Y}i21} & \boldsymbol{R}_{\mathcal{Y}i22} \end{bmatrix} \begin{bmatrix} \mathcal{Y}_{i-1} \\ \boldsymbol{w}(i) \end{bmatrix} + \\ & \left[\tilde{\boldsymbol{y}}(i)^H\ \boldsymbol{w}(i)^H\right] \begin{bmatrix} \boldsymbol{R}_{\mathcal{Z}i11} & \boldsymbol{R}_{\mathcal{Z}i12} \\ \boldsymbol{R}_{\mathcal{Z}i21} & \boldsymbol{R}_{\mathcal{Z}i22} \end{bmatrix} \begin{bmatrix} \tilde{\boldsymbol{y}}(i) \\ \boldsymbol{w}(i) \end{bmatrix} - \\ & \boldsymbol{w}(i)^H \boldsymbol{R}_w^{-1}\boldsymbol{w}(i). \end{aligned} \quad \text{(C.3)}$$

Taking the derivative of the right hand side of (C.3) with respect to $\boldsymbol{w}(i)^H$ yields

$$\begin{aligned} \frac{\partial l}{\partial \boldsymbol{w}(i)^H} \ = \ & (\boldsymbol{R}_{\mathcal{Y}i21}\mathcal{Y}_{i-1} + \boldsymbol{R}_{\mathcal{Y}i22}\boldsymbol{w}(i)) + \\ & (\boldsymbol{R}_{\mathcal{Z}i21}\tilde{\boldsymbol{y}}(i) + \boldsymbol{R}_{\mathcal{Z}i22}\boldsymbol{w}(i)) - \boldsymbol{R}_w^{-1}\boldsymbol{w}(i) \end{aligned} \quad \text{(C.4)}$$

By letting

$$\frac{\partial l}{\partial \boldsymbol{w}(i)^H} = \begin{bmatrix} 0 \\ \vdots \\ 0 \end{bmatrix}_{K\times 1},$$

we obtain (5.47).

REFERENCES

1. A. D. A. D'Andrea and U. Mengali, "Symbol-aided channel estimation with nonselective Rayleigh fading channels," *IEEE Trans. on Vehicular Technology*, vol. 44, no. 1, pp. 41–48, Feb. 1995.

2. W. Al-Qaq and J. K. Townsend, "Importance sampling for the efficient simulation of adaptive systems in frequency nonselective slow Rayleigh fading," *Proc. of Communications Theory Mini-conference at Globecom'94*, pp. 1435–1440, San Francisco, CA, Nov. 1994.

3. M. Barrett, "Error probability for optimal and suboptimal quadratic receivers in rapid Rayleigh fading channels," *IEEE Journal on Selected Areas in Communications*, vol. SAC-5, no. 2, pp. 302–304, Feb. 1987.

4. J. K. Cavers, "An analysis of pilot symbol assisted modulation for Rayleigh fading channels," *IEEE Trans. on Vehicular Technology*, vol. 40, no. 4, pp. 686–693, Nov. 1991.

5. D. S. Chen and S. Roy, "An adaptive multiuser receiver for CDMA systems," *IEEE Journal on Selected Areas in Communications*, vol. 12, no. 5, pp. 808–816, June 1994.

6. J. C.-I. Chuang, "The effect of time delay spread on portable radio communications channels with digital modulation," *IEEE Journal on Selected Areas in Communications*, vol. SAC-5, no. 5, pp. 879–889, June 1987.

7. W. Dam and D. Taylor, "An adaptive maximum likelihood receiver for correlated Rayleigh-fading channels," *IEEE Trans. on Communications*, vol. 42, no. 9, pp. 2684–2692, Sep. 1994.

8. F. Davarian, "Mobile digital communications via tone calibration," *IEEE Trans. on Vehicular Technology*, vol. VT-36, no. 1, pp. 55–62, May 1987.

9. D. Divsalar and M. K. Simon, "Multiple-symbol differential detection of MPSK," *IEEE Trans. on Communications*, vol. 38, no. 3, pp. 300–308, Mar. 1990.

10. A. Duel-Hallen, "On suboptimal detection for asynchronous code-division multiple access channels," *Proc. of the 26th Annual Conference on Information Sciences and Systems*, pp. 838–843, Princeton, NJ, Mar. 1992.

11. A. Duel-Hallen, "Decorrelating decision-feedback multiuser detector for synchronous code-division multiple-access channels," *IEEE Trans. on Communications*, vol. 41, no. 2, pp. 285–290, Feb. 1993.

12. A. Duel-Hallen, "A family of multiuser decision-feedback detectors for asynchronous code-division multiple access channel," *IEEE Trans. on Communications*, vol. 43, no. 2, Feb. 1995.

13. A. Duel-Hallen, J. Holtzman, and Z. Zvonar, "Multiuser detection for CDMA systems," *IEEE Personal Communications*, vol. 2, no. 2, pp. 46–58, Apr. 1995.

14. K. I. Pedersen *et al*, "DS/CDMA successive interference," *Rutgers Wireless Information Network Laboratory Technical Report*, July 1996.

15. K. S. Gilhousen, I. M. Jacobs, R. Padovani, A. J. Viterbi, J. L. A. Weaver, Jr. and C. E. Wheatley III, "On the capacity of a cellular CDMA system," *IEEE Trans. on Vehicular Technology*, vol. 40, no. 2, pp. 303–311, May 1991.

16. R. Haeb and H. Meyr, "A systematic approach to carrier recovery and detection of digitally phase modulated signals on fading channels," *IEEE Trans. on Communications*, vol. 37, no. 7, pp. 748–754, July 1989.

17. H. Hashemi, "The indoor radio propagation channel," *Proc. of the IEEE*, vol. 81, no. 7, pp. 943–967, July 1993.

18. S. Haykin, *Adaptive Filters*, John Wiley and Sons, Inc., New York, NY, 3rd ed., 1994.

19. F. V. Heeswyk, D. D. Falconer, and A. U. H. Sheikh, "Decorrelating detector for quasi-synchronous CDMA," *Wireless Personal Communications*, vol. 3, no. 1-2, pp. 129–147, Kluwer Academic Publishers, Dordrecht, The Netherlands, 1996.

20. P. Ho and D. Fung, "Error performance of multiple-symbol differential detection of PSK signals transmitted over correlated Rayleigh fading channels," *IEEE Trans. on Communications*, vol. 40, no. 10, pp. 1566–1568, Oct. 1992.

21. M. L. Honig, U. Madhow, and S. Verdú, "Blind adaptive multiuser detection," *IEEE Trans. on Information Theory*, vol. 41, no. 4, pp. 944–960, July 1995.

22. H. C. Huang and S. C. Schwartz, "A comparative analysis of linear multiuser detectors for fading multipath channels," *Proc. of the 1994 IEEE Globecom Conference*, pp. 11–15, San Francisco, CA, Nov. 1994.

23. G. T. Irvine and P. J. McLane, "Symbol-aided plus decision-directed reception for PSK/TCM modulation on shadowed mobile satellite fading channels," *IEEE Journal on Selected Areas in Communications*, vol. 10, no. 8, pp. 1289–1299, Oct. 1992.

24. W. C. Jakes, *Microwave Mobile Communications*, John Wiley and Sons, Inc., New York, NY, 1974.

25. P. Jung, P. Walter, and A. Steil, "Advantages of CDMA and spread spectrum techniques over FDMA and TDMA in cellular mobile radio applications," *IEEE Trans. on Vehicular Technology*, vol. 42, no. 3, pp. 357–364, Aug. 1993.

26. M. J. Juntti and B. Aazhang, "Finite memory-length linear multiuser detection for asynchronous CDMA communications," *IEEE Trans. on Communications*, vol. 45, no. 5, pp. 611–622, May 1997.

27. J. K. M. Mackenthun, "A fast algorithm for multiple-symbol differential detection of MPSK," *IEEE Trans. on Communications*, vol. 42, no. 2/3/4, pp. 1471–1474, Feb./Mar./Apr. 1994.

28. A. Kajiwara and M. Nakagawa, "Microcellular CDMA system with a linear multiuser interference canceler," *IEEE Journal on Selected Areas in Communications*, vol. 12, no. 4, pp. 605–611, April 1994.

29. P. K. Kam, "Maximum likelihood carrier phase recovery for linear suppressed-carrier digital data modulations," *IEEE Trans. on Communications*, vol. COM-34, no. 6, pp. 522–527, June 1986.

30. P. K. Kam, "Adaptive diversity reception over a slow nonselective fading channel," *IEEE Trans. on Communications*, vol. COM-35, no. 5, pp. 572–574, May 1987.

31. P. K. Kam, "Bit error probabilities of MDPSK over the nonselective Rayleigh fading channel with diversity reception," *IEEE Trans. on Communications*, vol. 39, no. 2, pp. 220–224, Feb. 1991.

32. P. K. Kam, "Optimal detection of digital data over the nonselective Rayleigh fading channel with diversity reception," *IEEE Trans. on Communications*, vol. 39, no. 2, pp. 214–219, Feb. 1991.

33. P. K. Kam and H. M. Ching, "Sequence estimation over the slow nonselective Rayleigh fading channel with diversity reception and its application to Viterbi decoding," *IEEE Journal on Selected Areas in Communications*, vol. 10, no. 3, pp. 562–569, Apr. 1992.

34. P. K. Kam and C. H. Teh, "Reception of PSK signals over fading channels via quadrature amplitude estimation," *IEEE Trans. on Communications*, vol. COM-31, no. 8, pp. 1024–1027, Aug. 1983.

35. P. K. Kam and C. H. Teh, "An adaptive receiver with memory for slow fading channels," *IEEE Trans. on Communications*, vol. COM-32, no. 6, pp. 654–659, June 1984.

36. S. M. Kay, *Modern Spectral Estimation*, Prentice Hall, Englewood Cliffs, NJ, 1988.

37. A. Klein and P. W. Baier, "Linear unbiased data estimation in mobile radio systems applying CDMA," *IEEE Journal on Selected Areas in Communications*, vol. 11, no. 7, pp. 1058–1066, Sep. 1993.

38. M. A. Landolsi, V. V. Veeravalli, and N. Jain, "New results on the reverse link capacity of CDMA cellular networks," *Proc. of the 46th Vehicular Technology Conference*, pp. 1462–1466, Apr. 28 - May 1, Atlanta, GA 1996.

39. W. C. Lee, "Overview of cellular CDMA," *IEEE Trans. on Vehicular Technology*, vol. 40, no. 2, pp. 291–302, May 1991.

40. F. Ling, "Coherent detection with reference-symbol based channel estimation for direct sequence CDMA uplink communications," *Proc. of the 43th Vehicular Technology Conference*, pp. 400–403, Secaucus, NJ, May 1993.

41. H. Liu and Z. Siveski, "Differentially coherent CDMA multiuser detector for Rayleigh fading channels," *Proc. of the 30th Annual Conference on Information Sciences and Systems*, pp. 86–89, Princeton, NJ, Mar. 1996.

42. H. Liu and Z. Siveski, "Differentially coherent decorrelating detector for CDMA single-path time-varying Rayleigh fading channels," *under revision for publication in IEEE Trans. on Communications*, Aug. 1996.

43. H. Liu and Z. Siveski, "Fractionally sampled decorrelator for CDMA Rayleigh fading channels," *Electronics Letters*, vol. 33, no. 9, pp. 741–742, Apr. 1997.

44. H. Liu and Z. Siveski, "A method of calculating transmitted power of mobiles in sectored cellular CDMA reverse link with imperfect power control," *Proc. of the 31st Annual Conference on Information Sciences and Systems*, pp. 299–302, John Hopkins University, Baltimore, MD, Mar. 1997.

45. H. Liu, Z. Siveski, and N. Ansari, "Coherent decorrelating detector with imperfect channel estimates for CDMA Rayleigh fading channels," *Proc. of ICC'97*, pp. 600–604, Montreal, Canada, June 1997.

46. H. Liu, Z. Siveski, and N. Ansari, "Fractionally spaced coherent detection with df map estimation of statistically known time-varying Rayleigh fading channel," *Proc. of Globecom'97*, Nov. 1997.

47. R. Lupas and S. Verdú, "Linear multiuser detectors for synchronous code-division multiple-access channels," *IEEE Trans. Information Theory*, vol. IT-35, no. 1, pp. 123–136, Jan. 1989.

48. R. Lupas and S. Verdú, "Near-far resistance of multiuser detectors in asynchronous channels," *IEEE Trans. on Communications*, vol. 38, no. 4, pp. 496–508, Apr. 1990.

49. D. W. Matolak and S. G. Wilson, "Detection for a statistically known, time-varying dispersive channel," *IEEE Trans. on Communications*, vol. 44, no. 12, pp. 1673–1683, Dec. 1996.

50. J. P. McGeehan and A. J. Bateman, "Phase locked transparent tone-in-band(TTIB): A new spectrum configuration particularly suited to the transmission of data over SSB mobile radio networks," *IEEE Trans. on Communications*, vol. COM-32, no. 1, pp. 81–87, Jan. 1984.

51. S. Miller, "An adaptive direct-sequence code-division multiple-access receiver for multiuser interference," *IEEE Trans. on Communications*, vol. 43, no. 2/3/4, pp. 1746–1755, Feb./Mar./Apr. 1995.

52. M. Mydlow, S. Basavaraju, and A. Duel-Hallen, "Decorrelating detector with diversity combining for single user frequency-selective Rayleigh fading multipath channels," *Wireless Personal Communications*, vol. 3, no. 1-2, pp. 175–193, Kluwer Academic Publishers, Dordrecht, The Netherlands, 1996.

53. R. Pickholtz, D. Schilling, and L. Milstein, "Theory of spread-spectrum communications — a tutorial," *IEEE Trans. on Communications*, vol. COM-30, no. 5, pp. 855–884, May 1982.

54. J. N. Pierce and S. Stein, "Multiple diversity with nonindependent fading," *Proc. of the IRE*, vol. 48, no. 1, pp. 89–104, Jan. 1960.

55. J. G. Proakis, *Digital Communications*, McGraw-Hill, New York, NY, 3rd ed., 1995.

56. M. Schwartz, W. R. Bennett, and S. Stein, *Communication Systems and Techniques, Chapter 10*, McGraw-Hill, New York, NY, 1966.

57. Z. Siveski, Y. Bar-Ness, and D. W. Chen, "Error performance of synchronous multiuser code division multiple access detector with multidimensional adaptive canceler," *European Trans. on Telecommunications and Related Technologies*, vol. 5, no. 6, pp. 719–724, Dec. 1994.

58. Z. Siveski, L. Zhong, and Y. Bar-Ness, "Adaptive multiuser CDMA detector for asynchronous AWGN channels," *Proc. of the 5th IEEE International Symposium on Personal, Indoor and Mobile Radio Communications*, The Hague, The Netherlands, Sep. 1994.

59. S. Stein, "Fading channel issues in system engineering," *IEEE Journal on Selected Areas in Communications*, vol. SAC-5, no. 2, pp. 68–88, Feb. 1987.

60. E. G. Strom, S. Parkvall, S. L. Miller, and B. E. Ottersten, "Sensitivity analysis of near-far resistant DS-CDMA receivers to propagation delay estimation errors," *Proc. of the 44th Vehicular Technology Conference*, vol. 2, pp. 757–761, June 1994.

61. M. K. Varanasi, "Noncoherent detection in asynchronous multiuser channels," *IEEE Trans. Information Theory*, vol. 39, no. 1, pp. 157–176, Jan. 1993.

62. M. K. Varanasi and B. Aazhang, "Multistage detection in asynchronous code-division multiple-access communications," *IEEE Trans. Communications*, vol. 38, no. 4, pp. 509–519, Apr. 1990.

63. M. K. Varanasi and B. Aazhang, "Near-optimal detection in synchronous code-division multiple-access systems," *IEEE Trans. Communications*, vol. 39, no. 5, pp. 725–736, May 1991.

64. P. K. Varshney and A. H. Haddad, "A receiver with memory for fading channels," *IEEE Trans. on Communications*, vol. COM-32, no. 2, pp. 278–283, Feb. 1978.

65. S. Vasudevan and M. K. Varanasi, "Receivers for CDMA communication over time-varying Rayleigh fading channels," *Proc. of Communication Theory Mini-Conference, Globecom 1993*, pp. 60–64, Houston, TX, Nov. 1993.

66. S. Vembu and A. J. Viterbi, "Two different philosophies in CDMA - a comparison," *Proc. of the 46th Vehicular Technology Conference*, pp. 869–873, Apr. 28 - May 1, Atlanta, GA 1996.

67. S. Verdú, "Minimum probability of error for asynchronous Gaussian multiple-access channels," *IEEE Trans. on Information Theory*, vol. IT-32, no. 1, pp. 85–96, Jan. 1986.

68. S. Verdú, "Recent progress in multiuser detection," *Advances in Communications and Signal Processing*, pp. 27–38, Springer-Verlag 1989.

69. S. Verdú, "Adaptive multiuser detection," *in Code Division Multiple Access Communications*, pp. 97–115, Kluwer Academic Publishers, Dordrecht, The Netherlands, 1995.

70. A. J. Viterbi, *CDMA-Principles of Spread Spectrum Communication*, Addison-Wesley, Reading, MA, 1995.

71. A. J. Viterbi, A. M. Viterbi, and E. Zehavi, "Performance of power-controlled wideband terrestrial digital communication," *IEEE Trans. on Communications*, vol. 41, no. 4, pp. 559–569, Apr. 1993.

72. A. J. Viterbi, A. M. Viterbi, and E. Zehavi, "Other-cell interference in cellular power-controlled CDMA," *IEEE Trans. on Communications*, vol. 42, no. 2/3/4, pp. 1501–1504, Feb./Mar./Apr. 1994.

73. A. M. Viterbi and A. J. Viterbi, "Erlang capacity of a power controlled CDMA system," *IEEE Journal on Selected Areas in Communications*, vol. 11, no. 6, pp. 892–899, Aug. 1993.

74. G. M. Vitetta and D. P. Taylor, "Maximum likelihood decoding of uncoded and coded PSK signal sequences transmitted over Rayleigh flat-fading channels," *IEEE Trans. on Communications*, vol. 43, no. 11, pp. 2750–2758, Nov. 1995.

75. G. M. Vitetta and D. P. Taylor, "Multisampling receivers for uncoded and coded PSK signal sequences transmitted over Rayleigh frequency-flat fading channels," *IEEE Trans. on Communications*, vol. 44, no. 2, pp. 130–133, Feb. 1996.

76. S. S. H. Wijayasuriya, G. H. Norton, and J. P. McGeehan, "A sliding window decorrelating receiver for multiuser DS-CDMA mobile radio networks," *IEEE Trans. on Vehicular Technology*, vol. 45, no. 3, pp. 503–521, Aug. 1996.

77. H. Y. Wu and A. Duel-Hallen, "Channel estimation and multiuser detection for frequency-nonselective fading synchronous CDMA channels," *Proc. 32nd Annual Allerton Conference on Communication, Computing and Control*, pp. 335–344, Monticello, IL, Sep. 1994.

78. H. Y. Wu and A. Duel-Hallen, "Performance of multiuser decision-feedback detectors for flat Rayleigh fading synchronous CDMA channels," *CISS'94*, pp. 133–138, Mar. 1994.

79. H. Y. Wu and A. Duel-Hallen, "Multiuser detection with differentially encoded data for mismatched flat Rayleigh fading CDMA channels," *Proc. 1996 Conference on Information Sciences and Systems*, pp. 332–337, Princeton, NJ, Mar. 1996.

80. H. Y. Wu and A. Duel-Hallen, "On the performance of coherent and noncoherent multiuser detectors for radio CDMA channels," *Proc. of the 5th International Conference on Universal Personal Communications*, vol. 1, pp. 76–80, Sep. 29-Oct. 2, Boston, MA 1996.

81. F.-C. Zheng and S. K. Barton, "Near-far resistant detection of CDMA signals via isolation bit insertion," *IEEE Trans. on Communications*, vol. 43, no. 2/3/4, pp. 1313–1317, Feb./Mar./Apr. 1995.

82. L. Zhong and Z. Siveski, "A parallel one-shot decorrelator structure for asynchronous multiuser AWGN channel," *Proc. 1995 Conference on Information Sciences and Systems*, pp. 205–208, Baltimore, MD, Mar. 1995.

83. Z. Zvonar, "Combined multiuser detection and diversity reception for wireless CDMA systems," *IEEE Trans. on Vehicular Technology*, vol. 45, no. 1, pp. 205–211, Feb. 1996.

84. Z. Zvonar, "Multiuser detection in asynchronous CDMA frequency-selective fading channels," *Wireless Personal Communications*, vol. 2, pp. 373–392, Kluwer Academic Publishers, Dordrecht, The Netherlands, 1996.

85. Z. Zvonar and D. Brady, "Optimum detection in asynchronous multiple-access multipath Rayleigh fading channels," *Proc. 1992 Conference on Information Sciences and Systems*, Princeton, NJ, Mar. 1992.

86. Z. Zvonar and D. Brady, "Adaptive multiuser receiver for fading CDMA channels with severe ISI," *Proc. of Conference on Information Sciences and Systems*, Mar. 1993.

87. Z. Zvonar and D. Brady, "Adaptive multiuser receivers with diversity reception for nonselective Rayleigh fading asynchronous CDMA channels," *Proc. IEEE Military Communications Conference*, pp. 982–986, Fort Monmouth, NJ, Oct. 1994.

88. Z. Zvonar and D. Brady, "Multiuser detection in single-path fading channels," *IEEE Trans. on Communications*, vol. 42, no. 2/3/4, pp. 1729–1739, Feb./Mar./Apr. 1994.

89. Z. Zvonar and D. Brady, "Differentially coherent multiuser detection in asynchronous CDMA flat Rayleigh fading channels," *IEEE Trans. on Communications*, vol. 43, no. 2/3/4, pp. 1252–1255, Feb./Mar./Apr. 1995.

90. Z. Zvonar and D. Brady, "Suboptimal multiuser detection for frequency-selective Rayleigh fading synchronous CDMA channels," *IEEE Trans. on Communications*, vol. 43, no. 2/3/4, pp. 154–157, Feb./Mar./Apr. 1995.

91. Z. Zvonar and M. Stojanovic, "Performance of antenna diversity multiuser receivers in CDMA channels with imperfect fading estimation," *Wireless Personal Communications*, vol. 3, no. 1-2, pp. 91–110, Kluwer Academic Publishers, Dordrecht, The Netherlands, 1996.

92. Z. Zvonar, "Multiuser detection for Rayleigh fading channels," *Ph.D. Dissertation, Northeastern University*, Boston, MA, 1993.

93. Z. Zvonar and M. Stojanovic, "Performance of multiuser diversity reception in nonselective Rayleigh fading CDMA channels," *Proc. Third Communication Theory Mini-Conf. (CTMC'94)*, pp. 171–175, San Francisco, CA, Nov. 1994.